MASTER THESIS REPORT

CHANGING PHASE

Design of a Shading and Latent Heat Energy Storage System for Lightweight Dwellings

OSKAR ERIK GÖSTA FRICK
5625947

2023

CHANGING PHASE

Design of a Shading and Latent Heat Energy Storage System for Lightweight Dwellings

Oskar Erik Gösta Frick | Student number: 5625947
MSc Architure, Urbanism and Building Sciences
Track: Building Technology
Graduation Master Thesis 2023

First supervisor

Dr. ir. M.J. Tenpierik

(Building Physics)

Second supervisor

Dipl.-Ing. M. Bilow

(Façade product design)

Delegate of the Board of Examiners

Dr. AJ Oxenaar

(Architecture and the Built Environment)

Delft University of Technology
Faculty of Architecture and the Built Environment
Julianalaan 134
2628 BL Delft
The Netherlands

Coverpage image: Linen texture from Freepik.com

Abstract

This report investigates the potential use of Phase Change Material (PCM) technology in poorly insulated lightweight homes in the Netherlands. The aim is to develop a cost-effective and easy-to-install PCM product that can decrease energy consumption through passive heating and cooling. The proposed design involves a multi-layer curtain system with small PET macroencapsulations containing salt hydrate attached to a sheer curtain. The system also includes a secondary insulation layer made of polyester with a reflective aluminum lining as a thermal barrier. MATLAB simulations indicate that this system, with 16 liters of PCM, can reduce heating loads by 7-9% when applied to a living room bay window measuring 4.46 m2 within a 28.8 m2 room. However, the insulation layer provides the most significant heat loss reduction. The simulation results also demonstrate a lower average summer temperature when the insulation curtain is not applied, suggesting effectiveness in both summer and winter. The estimated payback period for the system, based on the Dutch gas price cap of €1.45 per m³, is 5 - 8.5 years. The report concludes that while the proposed PCM system has the potential to reduce energy usage in lightweight homes, further research is necessary to determine its actual effectiveness.

Keywords:
Phase Change Material, Thermal energy storage, Interior shading, Curtain, Housing, The Netherlands, Cost-effectiveness, Energy savings.

ACKNOWLEDGMENT

I would like to express my gratitude to my thesis mentors, Dr. ir. Martin Tenpierik and Dipl.-Ing. Marcel Bilow, from the Faculty of Architecture and the Built Environment. Their expertise in building physics and product design was instrumental to the comprehensive and successful completion of my master thesis project.

I would also like to thank Dr. AJ Oxenaar, the delegate of the Board of Examiners from the same faculty, for his valuable feedback and enthusiasm during the presentations, which greatly boosted morale.

I am also appreciative of the access to the LAMA lab's tools and 3D printers, as well as the sewing machine provided by Dipl.-Ing. Marcel Bilow, which was of great help in the design process and final prototype.

I am grateful for the knowledge and guidance provided by the professors at the Faculty of Architecture at TU Delft throughout my master's degree.

Lastly, this achievement would not be doable without the unwavering support, encouragement, and inspiration from my parents, Lars and Lena, and my sister Olivia. I also want to give a shout-out to all my friends here in the Netherlands, which made my time here truly blissful. Cheers!

Oskar Frick

June 2023

Glossary

Q	stored heat	(J)
ρ	density of material	(kg/m3)
c	specific heat of material	(J/kg·K)
ΔT	temperature change	(K)
d	wall thickness	(m)
A	area	(m2)
dp	penetration depth	(m)
α	thermal diffusivity	(m2/s)
tp	time period	(s)
λ	heat conductivity	(W/mK)
m	mass	(kg)
Δh	phase change enthalpy	(J/kg)
λ_{max}	Wavelength at peak radiation intensity	(m)
K_w	Wien's constant ($2.89777 * 10^{-3}$)	(mK)
T	Temperature	(K)
E	Illuminance	(lux or lx)
lm	luminous flux	(lumen)
A	Area	(m2)
DF	Daylight factor	(%)
E_{inside}	Illuminance inside	(lx)
$E_{outside}$	Illuminance outside	(lx)

Nomenclature

BENG	Bijna Energieneutrale Gebouwen
CF	Convection factor
EPC	Energy performance coefficient
HALS	Hindered amine light stabilizers
HDPE	High density polyethylene
LDPE	Low density polyethylene
LLDPE	Linear low density polyethylene
MSVD	Magnetron sputtering vapor deposition
PC	Polycarbonate
PCM	Phase change material
PET	Polyethylene terephthalate
PMMA	Polymethyl methacrylate
PMV	Predicted mean vote
PPD	predicted percentage dissatisfied
PU	Polyurethane
PVC	Polyvinyl chloride
SC	Shading coefficient
SWOT	Strengths, weaknesses, opportunities, and threats
TES	Thermal energy storage
UV	Ultraviolet
VLT	Visible light transmittance

All figures not referenced are made by the author.

TABLE OF CONTENTS

1. INTRODUCTION

Before the innovation of modern mechanical systems, craftsmen relied on vernacular building techniques and locally found materials to build houses that could withstand the test of the natural elements. That often meant constructing buildings with high thermal inertia to passively control the indoor temperature and comfort. Materials with high thermal mass, such as rubble, rammed earth, adobe bricks, and stones, can store much heat energy before significantly changing temperature. (Zhai & Previtali, 2010) Although constructing buildings this way takes time and effort. Due to technological advancements and rapid urbanization during the 19th and 20th centuries, traditional construction techniques were left out of the equation in favor of active mechanical systems. (Britannica, 2022) According to Kalnæs & Jelle (2015), the building sector accounts for circa 40% of the energy consumption in the European Union, and a large portion of that energy is directly related to heating and cooling. As a result, the European Energy Performance of Buildings Directive (EPBD) set up a framework to decarbonize the European building stock by 2050. (European Commission, 2022)

To comply with the EPBDs framework, the Dutch Ministry of the Interior and Kingdom Relations put the nearly zero energy building (BENG) requirements into action on 1 January 2021, which replaced the old Energy Performance Coefficient (EPC). The new BENG requirements can help determine the energy performance of buildings in a more understandable way than the EPC. (Energiegids, 2019) According to Brom et al. (2018), between 1945 and 2000, 65% of the heated floor area in the Netherlands was built, and it was not until the late 1980s that the first thermal regulation was introduced. The lack of energy performance regulations, in combination with the massive demand for reconstruction after World War II, emphasized building quantity over quality, which is one of the main reasons for very poorly insulated dwellings. It was not until the 2000s that the energy regulations put real pressure on construction standards and quality. (van den Brom et al., 2018)

The goal that the Dutch government set for the year 2030 is to achieve a 49% CO_2 reduction, and by 2050 all building stocks in the Netherlands will follow the nearly zero energy standard. To achieve these goals, the plan is to ramp up major housing renovations to 200,000 units per year. However, one of the major obstacles is the renovation cost per dwelling unit, which is about 70,000-80000 Euro/dwelling. (van den Brom et al., 2018)

Problem statement:

In recent years, geopolitical, societal, environmental, and economic events have caused a spike in demand for sustainable stewardship from the construction industry and across all boards. The events caused gas and electricity prices to spike, significantly impacting the individual's wallet for the first time. (Ministerie van Algemene Zaken, 2022) Higher energy prices have led citizens to turn off the heating or only use it a few hours a day to save as much energy and money as possible. The situation is especially difficult for occupants living in the Dutch dwelling stock constructed before the 90s. Although, the Dutch government has implemented strategies to renovate all the buildings by 2050. (van den Brom et al., 2018) The goal is ambitious, and it does not get accomplished overnight. Therefore, a solution that can quickly be implemented to lower the energy bill and increase occupant comfort has excellent potential.

Focus & restrictions:

There are many ways to improve the thermal performance and comfort in a building passively. Such as adding thermal mass, more insulation, changing windows, sealing gaps, or installing shading devices. Although many of the mentioned strategies are expensive, technically demanding, or compromising the original aesthetics of the building. Therefore, this project is limited to cost- and energy-effective options that do not require government permits to be implemented. Sustainability is also essential; therefore, the embodied energy, durability, and end-of-life cycle determine the product's chosen materials. Modularity and the ability to replace or repair broken components are also part of a sustainable approach.

The building typology in focus is the existing Dutch lightweight dwelling stock. Therefore, the thermal energy storage medium needs to have a high heat capacity to weight ratio, so it does not compromise the structural integrity of the building. Phase change materials, or PCMs, are the chosen thermal storage medium. For the PCM to work correctly, the right type must be chosen for the specific building application and climate zone. According to the Köppen-Geiger classification, the Netherlands, is classified as a Cfb climate. (Peel et al., 2007) The primary application is interior window shading. This strategy increases the thermal inertia of the dwelling while also exposing the PCM to solar heat gain. A case study is used for thermal performance simulations. The case study is a small intermediate Dutch terraced house with poor thermal performance. The simulation will be restricted to only the living room with an area of 28.8 m2.

Objective:

The main objective of this graduation project is to design a PCM product that can be implemented into old lightweight dwellings in the Netherlands to improve annual thermal performance. The secondary objectives are to make the product user-friendly and straightforward enough so homeowners can install it independently without needing expertise. The ability to also be able to replace broken components is essential to maintain good thermal performance and longevity. Furthermore, the product must be lightweight enough to move aside when not desired. Finally, it must be aesthetically pleasing, durable, cost-effective, and marketable, so homeowners want to buy and showcase it in their homes.

Research question

Main research question

How can phase change material be incorporated into a cost-effective product to increase the thermal inertia of lightweight dwellings in a Cfb climate to enhance passive cooling and heating throughout the year?

Secondary research questions:

How do the summer and winter seasons affect the melting process of PCMs?

What would be the ideal behavior of the product during the different seasons?

How much PCM volume is required to make a sensible difference in an 28.8 m2 room?

What would be the ideal component size to balance flexibility with thermal performance?

Which is the ideal material and manufacturing method to make it a durable and cost-effective product?

Methodology:

This project follows research through design structure, meaning that the knowledge gained from simulations and trial and error will lead to further understanding, which could then be applied to improve the next design iteration. Figure 1 gives an overview of the complete research methodology.

The **literature review and research** will analyze the Dutch building stock and climate. Then establish a base knowledge of thermal performance, heat flow, sensible and latent heat, and phase change materials. Desirable characteristics, types, drawbacks, and typical building applications of PCMs. After that, extensive research into encapsulation methods, risks, and opportunities, performance aspects of interior applications. Finally, research into product design, material science, manufacturing methods, and end-of-life aspects.

The literature review and research are based on peer-reviewed literature published on ScienceDirect and technical data derived from Climate Consultant 6.0, Granta Edupack, and manufacturers' websites. In addition, professors and mentors from TU Delft provided supplemental knowledge and recommendation on scientific articles. The search terms used to find additional research papers specific to the subject are listed in Table 1.1.

Keywords		
Concept 1: Thermal energy storage	**Concept 2: Construction**	**Concept 3: Product**
Thermal mass	Dwelling	Modular
Phase change material	Lightweight	Component
PCM	Housing	Shell
Latent heat	Renovation	Microencapsulation
Sensible heat	Dutch	Macroencapsulation
	The Netherlands	Adjustable
		Shutter
		Curtain

Table 1.1: Keywords used for the literature search.

The **product design** phase follows an iterative process using Rhinoceros 7 and Grasshopper to generate various design options that will be 3D printed and sewn to test their functionality and relevance. Insight from the testing will inform the next design version. In addition, MATLAB and Ladybug are employed for thermal performance simulations to estimate the system's heat efficiency. The final design is developed once satisfactory results are achieved, including technical detailing, creating an assembly manual, and prototype construction. The components within the prototype will be moveable to illustrate how the system can be adjusted depending on the season. However, the prototype will not be filled with PCM due to potential leakage due to poor tolerances when 3D printing.

The **conclusion and discussion** assess whether the thermal performance and product functionality align with the objective and research question established at the start of the project. The conclusion also evaluates the product's cost-effectiveness compared to other alternatives. Additionally, the results and future potential of the system will be discussed at the end.

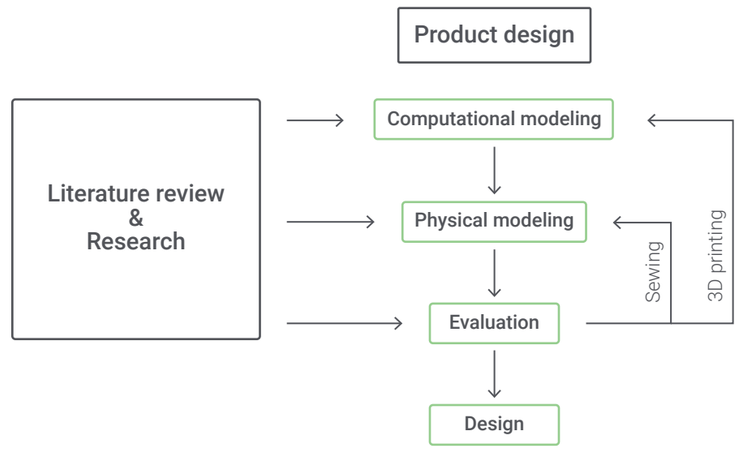

Figure 1.1: Design method.

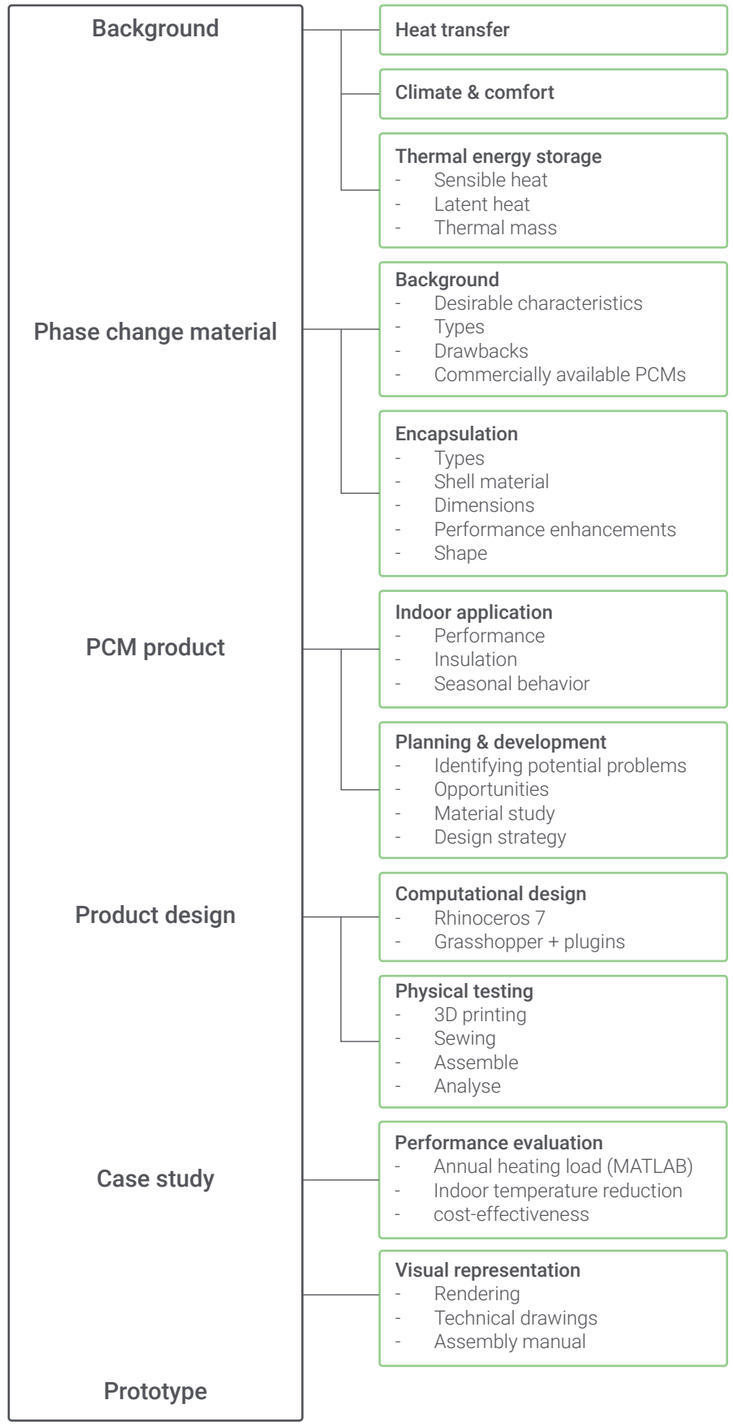

Figure 1.2:
Project framework.

2. LITERATURE STUDY

Building envelope

According to Sadineni et al. (2011), the building envelope is the physical barrier separating the outdoor and indoor environment of a building. It determines the indoor environmental conditions, such as air quality and thermal-, visual- and acoustic comfort, while also blocking out water. Each component of the building envelope can be classified based on its purpose. For example, structural support, flow and energy control, or aesthetical finish. Components such as walls, the roof, foundation, windows, insulation, and waterproofing are part of the building envelope. (van den Brom et al., 2018)

Heat transfer

Heat transfer occurs when there is a temperature difference between indoor and outdoor environments. The larger the temperature difference is, the greater the potential for heat transfer. Although, depending on the thermal property and dimension of the barrier separating the two environments, the heat transmittance or U-value (W/m2 K) may vary. Heat can transfer in three forms: conduction, convection, and radiation. (Rathakrishnan, 2012)

Conduction:

Conduction is direct heat transfer in solid mediums or fluids that are stationary. There needs to be a temperature difference within the body for conduction to occur so heat can flow from higher to lower temperatures. The heat conduction coefficient (λ) is a thermal property of a material that determines the intensity of heat that flows per unit area (W/mK). To calculate a material's heat resistance (r), the formula $r = d / \lambda$ can be used, where (d) is the thickness of the layer. The unit for heat resistance is m2K/W. (Bokel, 2021)

Convection:

Convection is heat transfer through the movement of fluids. The heat transfer rate depends on the flow speed of the heat transport medium and the temperature difference between the surface and moving fluid. The formula $q = \alpha (\Delta T)$ can be used to calculate the convective heat flow density between a solid and a fluid. α is the heat transfer coefficient for convection, and ΔT is the temperature difference between the two mediums. α is between 2 to 2.5 $W/m^2 \cdot K$ for typical indoor conditions in the Netherlands and 19 to 20 $W/m^2 \cdot K$ for average outdoor conditions. (Bokel, 2021)

Radiation

Any object with a temperature higher than 0 Kelvin radiates infrared heat. The amount of heat an object radiates can be determined by Stefan Boltzmann's law: $E = \varepsilon\sigma T^4$. E is heat flow density per wavelength (W/m2), ε is the emission constant of the radiating surface, σ is the Stefan-Boltzmann constant 5.67 10-8 ($W/m2 K^4$), and T is the surface temperature. (Bokel, 2021)

Heat loss

The U-value of the building envelope can be determined if the conduction, convection, and radiation heat flows are known for all the construction elements. The larger the U-value is, the faster the heat transmittance from one side to the other is. Based on Table 2.1, derived from Van den Brom et al. (2018), the most significant heat losses in the Dutch dwelling stock occur in the window system.

Solar heat gain

The most substantial part of the cooling load in residential buildings is from solar heat gain through windows. Solar heat gain is radiation from direct electromagnetic waves from the sun and diffused waves from the sky. Reflected radiation from the ground and surrounding surfaces can also significantly impact solar heat gain. The solar heat gain can be reduced depending on the physical properties (transmission, reflection, and absorption) of the glazing system. In most cases, some solar radiation will be directly transmitted to the interior space, and some radiation will be absorbed by the window and partially heat the space. The rest will be reflected away. (Bokel, 2021)

Table 2.1:
U-value of Dutch dwelling stock based on construction year and building part.
(Source: Modified from Van den Brom et al., 2018)

Building envelope U-Value (W/m² a)	Timeline							
	1920	1945	1960	1980	1990	2000	2010	2020
Single-dwelling								
Wall	1.21	1.20	1.09	0.78	0.41	0.27	0.22	0.20
Roof	1.02	1.02	0.83	0.53	0.35	0.21	0.17	0.15
Floor	1.65	1.65	1.51	1.38	0.51	0.22	0.13	0.13
Window	**2.18**	**2.21**	**2.23**	**2.20**	**2.21**	**2.04**	**1.81**	**1.43**
Multi-dwelling								
Wall	1.57	1.51	1.21	0.86	0.45	0.28	0.25	0.23
Roof	0.99	0.96	0.92	0.49	0.34	0.23	0.18	0.17
Floor	2.07	2.06	1.68	1.26	0.34	0.18	0.16	0.16
Window	**2.19**	**2.23**	**2.19**	**2.20**	**2.19**	**2.03**	**1.78**	**1.42**

Climate analysis

The Netherlands is classified as a temperate oceanic climate without dry season (Cfb) according to the Köppen-Geiger classification. (Peel et al., 2007) The average annual temperature is 11°C degrees, the mean temperature of the coldest month, February, is 3°C, and the warmest month, August, is 17°C. The average high during the summer is 20°C, and the average low is around 13°C. The average diurnal temperature swing in February is between 6°C and 2°C. Therefore, the Netherlands is a heating-dominated climate. In terms of sunlight. The daily mean direct normal radiation on a south-facing vertical surface fluctuates between 3295 Wh/m2 in July to around 493 Wh/m2 in December. See Figure 2.1, for average monthly direct normal radiation and temperature fluctuations. (Climate Consultant 6.0, 2021)

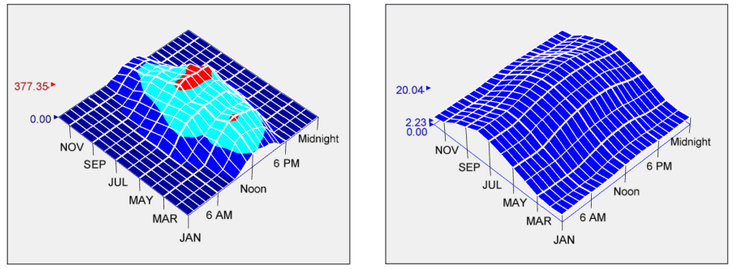

Direct normal radiation (Wh/m²)

54%		Night time
22%		4 - 158
22%		158 - 316
2%		316 - 474
0%		>474

Dry bulb temperature (°C)

0%		<0
100%		0 - 21
0%		21 - 27
0%		27 - 38
0%		>38

Figure 2.1:
Average monthly fluctuations of direct normal radiation (left) and dry bulb temperature (right). (Source: modified from Climate Consultant 6.0, 2021)

Thermal comfort

The indoor comfort is subjective to age, gender, and country of origin, and the outcome will alter depending on who is asked. A consensus of good thermal comfort is when the occupant has no desire to feel warmer or colder. Although, that does not work when multiple occupants are within the same space. The predicted mean vote (PMV) and predicted percentage dissatisfied (PPD) was introduced to determine what is good enough for a group of occupants. The standards are based on air temperature, mean radiant temperature, relative air velocity, air humidity, occupant activity level, and clothing. In addition, there cannot be any local discomfort, such as local draught or radiant temperature asymmetry. Although, an adaptable model has become common practice in buildings that do not have a cooling system but instead can utilize natural ventilation through operable windows. This model assumes that the occupants can affect their thermal comfort by wearing multiple layers. As a result, the adaptable model allows for a broader range of temperatures compared to the PMV and PPD models. (Frontczak & Wargocki, 2011) According to the ASHRAE standard 55, a comfortable indoor temperature during summer and winter is between 22.7-26 °C and 20-23.5 °C, respectively. This temperature range is expected to be acceptable to at least 80% of the occupants. (Dusseldorp et al., 2007)

Visual comfort:

Regarding visual comfort, the factors of daylight, glare, light color, and the distribution and uniformity of luminance and illuminance affect the overall result. (Frontczak & Wargocki, 2011) Visual comfort is also a relationship between how much light the occupant needs versus how much light is provided. Depending on the task, the amount of light provided will impact the psychological comfort and the ability to concentrate. (Giovannini et al., 2018)

Thermal energy storage

A thermal energy storage (TES) system can store heat energy for later use. The philosophy behind a TES system is to balance the gap between heat generation and heat usage. In architecture, thick concrete walls can be used as a thermal energy storage system because it heats up during a warm day and then discharges some of the heat during the night. According to Baggs & Mortensen (2022), the time it takes between peak external and peak indoor temperature is called time lag which is determined mainly by wall thickness and rate of heat transfer. As the heat wave travels through the massive concrete wall, a reduction in the amplitude and size of the heat wave occurs, leading to an overall temperature reduction, see Figure 2.2.

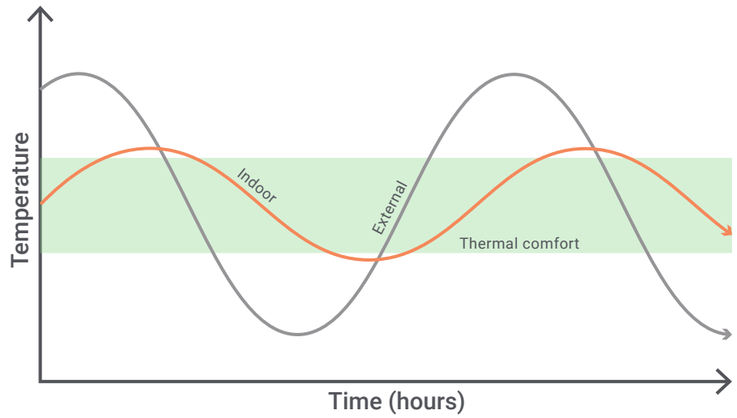

Figure 2.2:
Thermal energy storage systems can be used as a thermal buffer in a building to reduce peak indoor temperatures and sharp temperature swings.
(Source: modified from Baggs & Mortensen, 2022)

A thermal energy storage system involves three steps: charge, store, and discharge, and there are three different heat storage systems: sensible heat, latent heat, and thermochemical heat. (Cabeza et al., 2015) Although, thermochemical energy storage will not be covered in this research.

Sensible heat storage

Sensible heat storage is when the storage material changes temperature as a response to absorbing heat energy. Storage materials such as concrete, water, oil, bedrock, and brick are commonly used. For instance, in architecture, solar walls made with massive concrete can absorb solar radiation during the day and then release the gained heat during the night. (Cabeza et al., 2015) The output of a sensible heat storage system can be determined using equation 1. (Bokel, 2021)

$$Q = \rho \cdot c \cdot \Delta T \cdot d \cdot A \qquad (1)$$

In the case of a sensible heat storage wall, equation 1 is valid if the penetration depth of the wall is greater than the depth of the actual wall. If not the case, then equation 2 applies. (Bokel, 2021)

$$Q = \rho \cdot c \cdot \Delta T \cdot dp \cdot A \quad (2)$$

$$dp = \sqrt{((a \cdot tp)/\pi)} \quad (3)$$

$$\alpha = \lambda/(\rho \cdot c) \quad (4)$$

Latent heat storage

Latent heat storage utilizes the heat energy that is released or absorbed during the phase transition of a material. (Figure 2.3) Most commonly when the material changes from solid to liquid and liquid to solid. During the melting process, chemical bonds are broken apart, an endothermic process occurs, and a large amount of heat is transferred to the material. The opposite occurs during solidification, but the process is exothermic, and a large amount of heat is released into the environment. (Baetens et al., 2010) According to Mavrigiannaki & Ampatzi (2016), latent heat has up to 15 times higher theoretical volumetric storage density than sensible heat systems. Phase change materials utilize latent heat, and the storage capacity Q can be determined using equation 5. (Bokel, 2021)

$$Q = m \cdot c \cdot \Delta T + m \cdot \Delta h \quad (5)$$

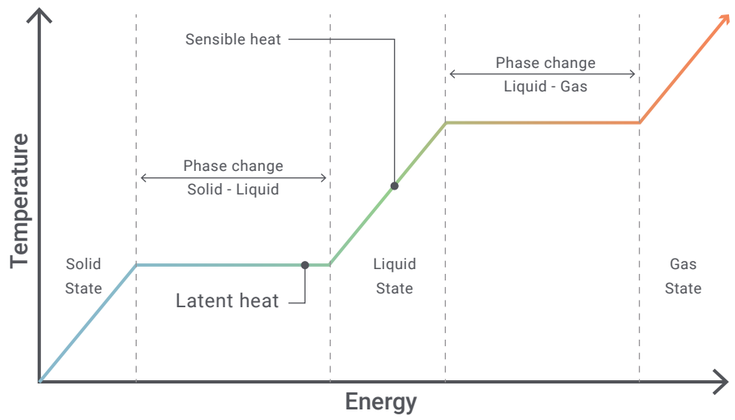

Figure 2.3:
Phase change diagram illustrating sensible and latent heat stages.

Phase Change Material

As mentioned in the previous chapter, phase change materials mainly utilize latent heat as a thermal energy storage system. It can be implemented in various applications, such as food packaging and transportation, military and spacecraft equipment thermal protection, microelectronics, and solar power plants. (Kośny, 2015) Studies have shown that it can be implemented in buildings to lower energy consumption, maintain desired indoor air temperatures for a more significant period, and directly increase occupant comfort levels by up to 32%. (Bland et al., 2017) In passive building applications, the PCM absorbs heat and melts when the ambient temperature rises during the day and then releases the heat once the surrounding air temperature drops below the solidification temperature. In conditions with small temperature fluctuations, the PCM can still operate at high efficiency, assuming that the correct melting temperature of the PCM is chosen. (Ikutegbe & Farid, 2020) Although, PCMs have the benefit of also utilizing sensible heat storage when the temperature of the melted/solidified PCM changes during prominent ambient temperature fluctuations. (Di Bari et al., 2020) As a result, a significant reduction in storage volume can be achieved when using PCMs compared to only a sensible heat-based storage system. Figure 2.4 shows how much latent heat is released/absorbed per kg at a specific temperature of two different organic CrodaTherm PCM products. The graphs illustrate how the latent heat can be distributed on a broader temperature range depending on the chemical composition of the PCM. Notice that there is a difference between melting and crystallization enthalpy distribution.

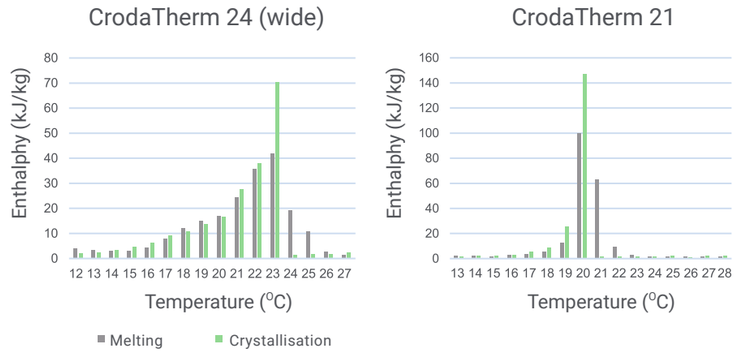

Figure 2.4:
Latent heat of fusion distribution of two types of PCMs from Croda Int. PLC.
(Source: modified from Croda International Plc, 2022)

Desirable characteristics

According to Baetens et al. (2010), the performance of a PCM is determined by certain thermal, physical, chemical, and economic factors. Table 2.2 illustrates the desired characteristics when choosing phase change material.

Desired properties			
Thermal	**Physical**	**Chemical**	**Economical**
High thermal conductivity.	Small volume changes during phase change	Chemically stable.	Abundant and cheap materials.
High latent heat of fusion per unit volume and weight.	Low vapour pressure.	Low corrosion rate.	Commercially viable.
High specific heat.	High density.	Non-toxic, non-explosive and non-inflammable.	Long lifecycle.
Phase change temperature must match the intended application.	No supercooling.	No chemical degradation.	
	No phase segregation.		

Table 2.2: Desired characteristics to look for in a phase change material. (Source: modified from Bland et al., 2017)

Types of PCMs

Three types of phase change materials work within the solid-liquid domain, which is organic, inorganic, and eutectic mixtures. There are subclasses within each of these three PCM types. (Baetens et al., 2010) The advantages and drawbacks of the different types are compiled in Table 2.3.

Organic compounds:
This group can be divided into paraffins and non-paraffins. Organic PCMs are generally chemically stable with limited supercooling and phase segregation. High latent heat of fusion of 120-210 kJ/kg for paraffins and 155-180 kJ/kg for non-paraffins. The drawbacks of organic PCMs are flammability and low thermal conductivity of 0.2 W/m K for paraffins and 0.15-0.17 W/m K for non-paraffins. (Baetens et al., 2010)

Paraffins have a wide range of available melting temperatures between 20-70 °C, low vapor pressure, non-corrosive, and inexpensive. The chemical structure of commercial paraffin wax is CH3(CH2)nCH3. (Baetens et al., 2010) According to Tebaldi et al. (2016), thermal performance is consistent over many thermal cycles, and chemical degradation does not affect performance. Although, significant volumetric changes during phase change can reduce their effectiveness.

Non-paraffins have excellent melting and solidification characteristics, but they are three times more expensive than paraffins. This group includes fatty acids, esters, alcohols, and glycols. Fatty acids have been given the most attention due to their preferable characteristics over other non-paraffins. They are derived from sustainable sources and have characteristics of congruent melting, small volume changes, color stability, non-corrosive and non-toxic. (Tebaldi et al., 2016) According to Baetens et al. (2010), the chemical structure of fatty acid is CH3(CH2)nCOOH. Depending on which type of fatty acid it is, the n in the chemical composition changes.

Inorganic compounds:
Inorganic compounds generally consist of salt hydrates, salt, and metallics. For building applications, salt hydrates are preferred, given the lower phase change temperature. Salt hydrates are typically composed of anhydrous salt and crystal water. The anhydrous salts are extracted in a purification process from raw salt, which is found in the ocean. (Junaid et al., 2021) Inorganic salt hydrates generally have high latent heat of around 240 kJ/kg and relatively high heat conductivity of circa 0.5 W/m K. They are also non-flammable, abundant, and cheap. (Baetens et al., 2010) Although, salt hydrates are corrosive to metals and suffer from phase segregation and supercooling. (Tebaldi et al., 2016) Therefore, all salt hydrates must be encapsulated to prevent unexpected reactions or evaporation into the environment. (Kośny, 2015)

The chemical structure of salt hydrates is typically expressed as AxBy.n(H2O), where n is the number of water molecules while AxBy indicates which base ion the salt hydrate consists of. Usually, it is either acetate, chloride, metal carbonate, nitrite, oxide, phosphate, or sulfite. (Junaid et al., 2021)

Eutectic mixtures:
A eutectic PCM consists of two or more chemicals and can be divided into three groups: organic-organic, organic-inorganic, and inorganic-inorganic. For instance, the eutectic mixture of the fatty acids CH3 (CH2)8COOH and CH3 (CH2)10COOH can form capric-lauric acid with a melting point of 21°C and a latent heat of 143 kJ/kg. (Tebaldi et al., 2016) Depending on the ratio of the chemicals within the mixture, specific properties can be achieved, such as a precise melting temperature. Although, eutectic mixtures are expensive to produce. (Kalnæs & Jelle, 2015)

PCM type			
Paraffins	**Non-paraffins**	**Salt hydrates**	**Eutectic mixtures**
Advantages	**Advantages**	**Advantages**	**Advantages**
High latent heat of fusion (120 - 210 kJ/kg)	High latent heat of fusion (155 – 180 kJ/kg)	High latent heat of fusion (180 - 240 kJ/kg)	Sharp melting points
Chemically stable	Small volume change	Thermal conductivity (Ca. 0.5 W/m K)	Properties can be designed to match specifications
No supercooling	No supercooling	Cheap & abundant	
Non-corrosive and non-toxic		Non-flammable	
Low vapour pressure		Sharp phase change	
Drawbacks	**Drawbacks**	**Drawbacks**	**Drawbacks**
Thermal conductivity (ca. 0.2 W/m K)	Thermal conductivity (ca. 0.15 - 0.17 W/m K)	Supercooling	Expensive
Large volume change during phase change	Expensive	Phase segregation	
Flammable	Flammable	Corrosive to metal	

Table 2.3: Advantages and drawbacks of PCM types. (Source: modified from Baetens et al., 2010 : Kalnaes & Jelle, 2015)

PCM limitations

Depending on the application, specific disadvantageous properties can affect the PCM's performance, feasibility, and longevity. These are supercooling, low thermal conductivity, phase segregation, lifecycle, fire safety, and cost. If the issues are not appropriately addressed, the longevity and effectiveness of the system can be significantly reduced. (Bland et al., 2017)

Supercooling:
Supercooling is a characteristic that affects salt hydrates due to their insufficient nucleating properties leading to crystallization below the usual freezing point. Consequently, the release of latent heat is delayed, and the frequency of supercooling increase the more thermal cycles the salt hydrate goes through. (Figure 2.4) This can permanently change the crystallization temperature. As a result, there is a large gap between the melting and solidification temperature. (Safari et al., 2017) According to Ikutegbe & Farid (2020), the freezing and melting points should be the same so that the PCM can operate during minor temperature fluctuations.

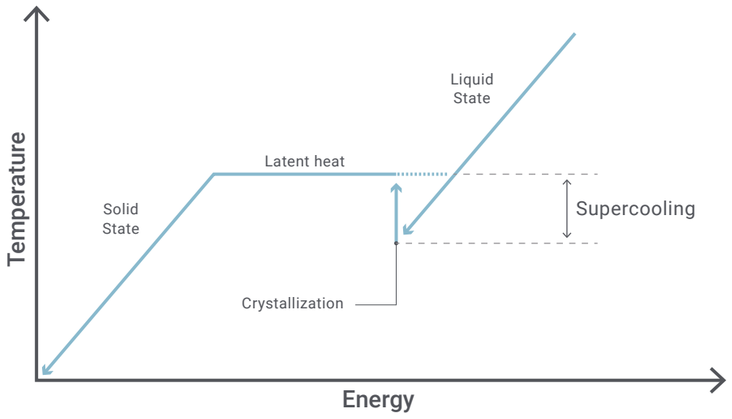

Figure 2.4: Supercooling and how it delays the discharge of latent heat. (Source: modified from Bruno et al., 2015)

Low thermal conductivity & phase change rate:
Low thermal conductivity is a disadvantage that organic PCMs suffer from, influencing how fast they can charge and discharge heat. Many PCMs also demonstrate insulating qualities in the solid state, which can delay the melting cycle. This is an issue because the whole PCM volume might not have time to change phase before environmental temperatures drop again. Drastically reducing the full potential of the system. (Hasnain, 1998)

Veerappan et al. (2009) conducted a study on the solidification rate of different PCMs in a solar energy storage scenario. The PCMs tested were capric/lauric acid, calcium chloride, n-octadecane, n-hexadecane, and n-eicosane. The PCMs were contained in a 4 cm wide sphere capsule, and the results showed that calcium chloride with a latent heat of fusion of 187 kJ/kg solidified the fastest due to the greater thermal conductivity compared to the other organic mixtures materials. See Figure 2.5 for the solidification rate of all the PCMs tested.

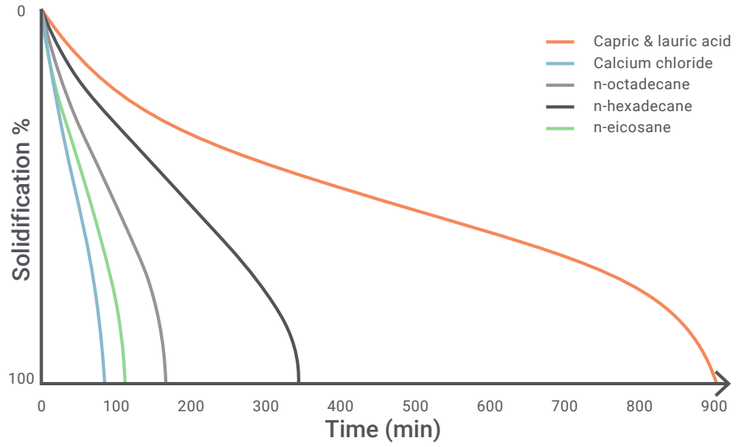

Figure 2.5: The solidification time of different PCMs contained in a 40 mm spherical capsule. (Source: modified from Veerappan et al., 2009)

Phase segregation:
Phase segregation is when the internal chemical structure of the PCM changes phase at different stages. Inhomogeneous chemical compositions such as salt hydrates, non-pristine PCMs, and eutectic compounds are prone to phase segregation. (Ikutegbe & Farid, 2020) For salt hydrates, this happens during incongruent melting, when the water in the compound separates from the salt. As a result, the salt turns into its anhydrous form, which may have a higher density than the salt hydrate compound. Due to gravity, the denser anhydrous salt sinks to the bottom of the encapsulation, rendering it unable to reabsorb the water during the next phase change cycle. Consequently, the total amount of PCM that can undergo phase change has decreased. (Kalnæs & Jelle, 2015)

Thermal cycles:
One of the significant drawbacks of PCMs is the risk of chemical degradation over time. According to Bland et al. (2017), many salt hydrates without additives have an expected lifetime of 1000 thermal cycles. This becomes a significant issue when the PCM is impregnated with building components that are difficult or expensive to replace, such as walls, floors, and ceilings. Another aspect to consider is the maximum service temperature of the PCM. Exceeding the recommended temperatures can lead to chemical degradation and reduce the lifecycle of the PCM. According to Rubitherm Technologies GmbH (2022), the maximum service temperature for their PCMs suitable for building applications are 45°C (salt hydrates) and 50-65 °C (organic).

Cost:
The kilogram price for raw paraffin wax is around $2, and for the salt hydrate calcium chloride without additives, the cost is around $0.20 per kg. For commercially available PCMs that are enhanced with additives, the cost is roughly 25 times more. (Bland et al., 2017) Table 5 shows the cost of different commercial-grade PCMs manufactured by Rubitherm Technologies GmbH, PCM Products Ltd, and PureTemp LLC.

Fire safety:
Many organic PCMs can heat up and turn into vapor if the temperatures are high enough. The vapor can then escape or break the encapsulation and ignite when contacting fire. This becomes a dilemma for gypsum wallboards, typically part of the fire-resisting system. If wallboards are enhanced with organic PCMs, the fire-resisting characteristics are neutralized. (Kośny, 2015)

Commercially available PCMs

Table 2.4 lists a selection of commercially available PCMs in the melting range 21 – 25 °C. The data is derived from the manufacturer's website, and product prices are given through email contact with the manufacturer. Among the listed commercial PCMs, PureTemp products are biobased using 100% renewable sources. It is tested to be chemically stable after 10,000 thermal cycles or 27.4 years of a continuous daily cycle. The material is clear when it is in a liquid state and waxy when being in solid form. It is manufactured in the US and is non-hazardous. (PureTemp LLC, 2022) Croda International is a PCM manufacturer based in Europe. The products are also bio-based from renewable sources and tested to perform over 10,000 thermal cycles without signs of chemical degradation. (Croda International Plc, 2022) Rubitherm Technologies GmbH is a Germany-based company that manufactures high-quality organic and salt-hydrate PCMs. They also offer solutions with micro and macroencapsulations. Their RT-line offer high-capacity PCMs in certain melting temperatures, which have 25 – 30% higher latent heat of fusion and a smaller melting range than typical organic PCMs. Their salt hydrates are also tested to perform over 10,000 thermal cycles with minor degradation. (Rubitherm Technologies GmbH, 2022)

Commercial PCMs

Product	Type	Latent heat (kJ/kg)	Cost (EUR/kg)	Manufacturer
RT 21	Organic	165	6.41	Rubitherm GmbH
RT 21 HC	Organic	190	11.83	Rubitherm GmbH
RT 24 HC	Organic	200	12.76	Rubitherm GmbH
SP24E	Salt-hydrate	180	3.31	Rubitherm GmbH
SP25E	Salt-hydrate	180	3.19	Rubitherm GmbH
PlusICE S21	Salt-hydrate	220	1.6 - 2.3	PCM Products Ltd
PlusICE S23	Salt-hydrate	200	1.6 - 2.3	PCM Products Ltd
PlusICE A21	Organic	160	5 - 7	PCM Products Ltd
PlusICE A23	Organic	155	5 - 7	PCM Products Ltd
PureTemp 23X	Organic	201	2 - 5	PureTemp LLC
PureTemp 25X	Organic	187	2 - 5	PureTemp LLC
CrodaTherm 21	Organic	190		Croda Int. PLC
CrodaTherm 24W	Organic	184		Croda Int. PLC

Table 2.4: Commercially available organic and inorganic PCMs in the melting range of 21-25°C. The table shows PCM type, latent heat of fusion, cost per kg and thermal cycle stability. (Source: email contact with manufacturer and data listed on their websites)

Encapsulation

Encapsulating a PCM in a leakage-proof shell isolates it and prevents undesirable reactions with the environment. It can also overcome PCM drawbacks such as volumetric changes, supercooling, low thermal conductivity, phase segregation, corrosiveness, and flammability. This method broadens the use of PCMs to applications where direct immersion is not suited. (Tebaldi et al., 2016) The most common methods to encapsulate PCMs are microencapsulation, macroencapsulation, and bulk storage. Although, bulk storage is more applicable for active and large-scale thermal storage systems. (Bland et al., 2017)

Microencapsulation:

Microencapsulation is the smallest type of encapsulation with a particle size in the range of 0.01 – 1.00 mm, and it is produced in three different forms: dry powder, wet cake, or slurry. The difference between the three forms is the water-to-solid PCM ratio. When manufacturing dry powder, the encapsulated PCM particles are immersed in water, and then when the water is removed, a dry PCM powder is left. For the wet cake, 30% of the water remains in the mix, and for the PCM slurry, 60% of the water remains. (PureTemp LLC, 2022) Microencapsulation is applied to textiles, latex, PU foams, adhesives, insulation, and even polymers or plastics. (Rubitherm Technologies GmbH, 2022)

Microencapsulation naturally has higher heat transfer rates than other encapsulation methods due to the larger surface area per volume PCM. This can be achieved by mixing it with a high thermal conductive fluid to create a PCM slurry. Although, microencapsulation suffers from lower heat storage capacity per unit volume than macroencapsulation due to the additional encapsulation material. (Kalnæs & Jelle, 2015) In addition, salt hydrates should be avoided in microencapsulation since the capsules are too small to incorporate the nucleating agent needed to mitigate supercooling. (Bland et al., 2017)

Microtek Laboratories Inc. has various microencapsulated PCM products for applications such as building materials, bedding, and consumer textiles. The company offers solutions from brands such as Nextek, Fibratek, Micronal, Vivtek, and MPCM. The PCMs are paraffin based except Vivtech, which is bio methyl ester. The products are sold in either dry powder, cake, or slurry form (Figure 2.6) with particle sizes in the range of 0.015 – 0.3 mm. (Microtek Laboratories Inc., 2022)

Figure 2.6: From left to right: dry powder, wet cake and PCM slurry. (Source: https://www.microteklabs.com/wp-content/uploads/sites/2/2022/11/PCM_Types_Green4.png)

Macroencapsulation:

Macroencapsulations are the most common PCM encapsulation type, with a size usually larger than 1 cm. This encapsulation type offers much flexibility in size and shape depending on application and purpose. For instance, it can be in the form of tubes, spheres, panels, or pouches. (Kalnæs & Jelle, 2015) The ambient air can be used as a heat transfer medium, given the increase in module size compared to microencapsulation. This, combined with the mechanical stability and durability of the shell, makes it convenient to package, transport, and implement in residential applications. (Bland et al., 2017) PCMs in macroencapsulations tend to have uneven melting patterns due to the naturally low thermal conductivity of PCMs. The PCM along the edges melts/solidifies before the centrum causing a slower charge/discharge rate. If the volume is too large, the whole PCM might not go through the thermal cycle leading to a drop in performance. (Kalnæs & Jelle, 2015)

Axiotherm is a company that manufactures macroencapsulations. They have developed HeatSel (Figure 9), a PCM product meant for water-based applications. The shell form is designed to accommodate a large heat storage capacity while ensuring that the whole PCM can quickly charge and discharge. This is solved by providing a large heat transfer area and small layer thickness. (AxioTherm, 2023)

The PCM panel on the right in figure 2.7 is developed by BOCA international limited, a stackable PCM macroencapsulation made with high-density polyethylene. The encapsulation is mechanically robust, and each panel holds 3.8 liters of PCM. The shell is designed so that 160 panels can fit within a cubic meter while maximizing the thermal exchange rate with water. The shell cap is welded using ultrasonic acoustic vibrations to ensure a leakage-proof encapsulation. (Boca PCM, 2023)

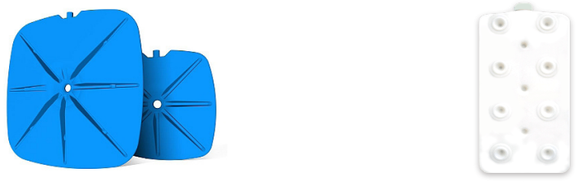

Figure 2.7:
Left: HeatSel macroencapsulation from axiotherm. Right: PCM panel developed by BOCA International LLC.
(Source: https://www.pcm-ral.org/pcm/en/members/axiotherm-gm-bh/ : https://pcm-tes.com/pcm-panel/)

Encapsulation material:

It is recommended to select the shell material after the PCM is chosen. This is because the shell must be compatible with the PCM. Otherwise, unintended issues might occur, such as corrosion. The primary purpose of the shell is to contain the PCM and prevent it from reacting with the environment. Therefore, knowing which materials are compatible with each other narrows down the available options. For instance, salt hydrates do not work well with metallic shells; thus, a polymeric option should be investigated. After the compatibility study, the following properties should be evaluated: nontoxicity, UV-resistance, non-flammability, mechanical strength, thermal stability, availability, and economic feasibility. (Liu et al., 2018) Non-flammable materials can help suppress the fire if the PCM ignites. Mechanical strength is essential to prevent cracking or leakage caused by volumetric changes during thermal cycling. Thermal stability is also essential, so the shell does not degrade over time. High thermal conductivity is preferable to enhance the heat exchange rate between the environment and PCM. The material should also be abundant and economically feasible for large-scale production. (Kalnæs & Jelle, 2015)

According to Liu et al., 2018, common shell materials for organic PCMs include metals such as copper, aluminum, and stainless steel due to their high thermal conductivity and strength. For salt hydrates, the standard options include various polymers, such as PVC, HDPE, and polyolefin, as well as glass and silicon dioxide (SiO2). In addition, shells with antimony oxide, decabromodiphenyl oxide, and octabromophenyl oxide are promising for organic PCMs due to their flame-suppressive characteristics. (Tebaldi et al., 2016) According to Ahangaran et al. (2019), polymethyl methacrylate, or PMMA, is commonly used as encapsulation material due to its transparent, mechanical, chemical, and biological characteristics.

Shell thickness & volume depth:

According to Tebaldi et al. (2016), thicker shells demonstrate higher heat release rates but at the cost of less space for PCM. On the other hand, thinner shells can alter the mechanical strengths and increase the risk of leakage. Thermeleon BV is a startup based in Delft that produces PCM solutions for greenhouses. They have designed a shell solution with thicker edges made with PMMA to even out the melting process of the whole volume.

The depth of the PCM volume is recommended to be up to 15 mm for PCMs that are heated from one direction, such as solar walls. However, 30 mm is feasible for PCMs operating on two sides. According to a simulation performed in Shanghai by Wang & Zhao (2015), a 5 mm thick PCM-filled curtain can reduce heat transfer rates up to 16.2%, while a 10 mm and 15 mm thick layer can reduce it by 23.8% and 30.9%, respectively. Worth mentioning is that Hendriks, Kees Jan (2019) illustrated in his master thesis that if the PCM layer is too thin, the risk of overheating increases, which can cause chemical decomposition in salt-hydrates. Therefore, salt hydrates should be avoided in smaller volumes exposed to solar heat gain. On the other hand, exceeding the recommended depths can lead to an uneven phase change, causing melted PCM to rise to the top. This is because warm liquids are less dense than cold/solid mediums. The encapsulation can be compartmentalized into smaller volumes to achieve an efficient melting process and reduce the impact of vertical flow. Similar results can be achieved by reducing the height and increasing the system's width. It is also essential to incorporate extra space to allow for thermal expansion caused by phase change.

A study on the melting rate of spherical capsules with different diameters was conducted by Veerappan et al. (2009). The capsule sizes studied were between 4 cm and 12 cm in diameter. The PCM tested was calcium chloride with a melting point at 29°C, and the surrounding heat transfer medium was 45°C. Figure 2.8 shows that it took 26 minutes for the PCM in the 4 cm sphere to melt and 94 minutes for the 8cm sphere to melt.

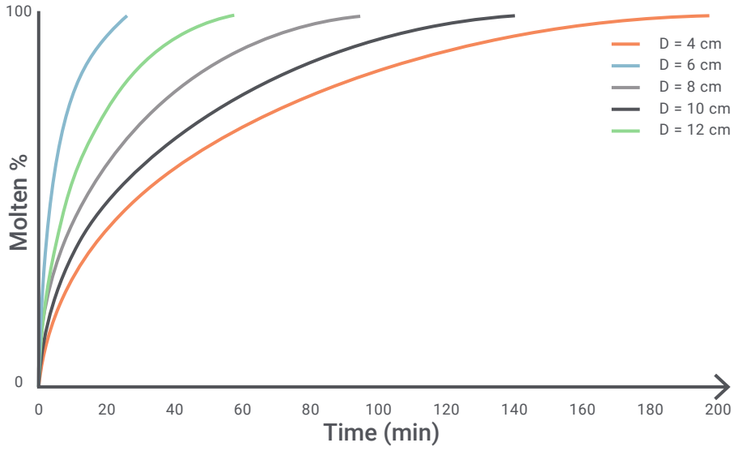

Figure 2.8:
The melting time of calcium chloride contained in different sizes of spherical capsules. (Source: modified from Veerappan et al., 2009)

Shell enhancements:

Heat transfer within the PCM can be increased by implementing additives with high thermal conductivity, such as expanded graphite, copper, or aluminum powder. The heat transfer of the PCM to the environment can also be enhanced by applying either a graphite matrix, aluminum fins, or porous metal foam. Studies analyzed by Liu et al. (2018) show that implementing porous metal foam can increase thermal conductivity by 20-130 times. This method also shows improvement in melting uniformity. Although, enhancing the thermal conductivity by applying additives or increasing the surface area will reduce the total heat storage capacity due to less available space for the PCM. Table 2.5 describes different strategies that can be used to improve thermal conductivity and how efficient it is. Note that metal cannot be used with salt hydrates due to their corrosivity.

PCM enhancement		
Additive	**PCM**	**Thermal conductivity**
Non-metal		
Graphite matrix	Paraffin wax	20 - 130 times
Expanded graphite (2.5 wt%)	$NaC_2H_3O_2 \cdot 3H_2O$	6.1 times
Carbon nanofillers (5 wt%)	Paraffin wax	1.7 times
Metal		
Aluminum fin (rectangular)	Lauric acid	Solidification time reduced by 40%.
Copper powder (47-74%)	Paraffin	17.18 - 156.30 W/m K

Table 2.5:
Heat transfer solutions. (Source: modified from Liu et al., 2018)

Surface shape:

According to Liu et al. (2018), the encapsulation form greatly influences the PCM's melting process. Therefore, the heat exchange rate between the environment and PCM can be controlled locally by manipulating the surface shape. The smoothness of a surface also impacts how good the heat exchange rate is. Simulations and experimentations performed by Cupkova & Promoppatum (2017) on a set of deformed vertical surfaces indicate that the surface smoothness has a significant impact on air movement, which influence the thermal exchange rate. For instance, Surfaces curved in a sinusoidal fashion show higher heat release rates than surfaces with sharp edges. (Figure 2.9) This is due to the effect that sharp edges create jacked crevices which trap the air causing the heat transfer rate to decrease. This effect can be used strategically to delay the heat-reradiation effect. The curves' size, proportion, and orientation also impact heat transfer rates. The experimentation results also concluded that a surface area to volume ratio of 1:12 is ideal for desired thermal behavior. (Cupkova & Promoppatum, 2017) Another study by Tebaldi et al., 2016, show that spherical capsules have more efficient heat release than cylindrical-, plate- and tubular shapes. The study also concluded that the discharge time increase when the distance to the centrum of the capsule increase. As a result, the planar and tubular shapes are disadvantageous in specific applications when rapid thermal cycling is preferred.

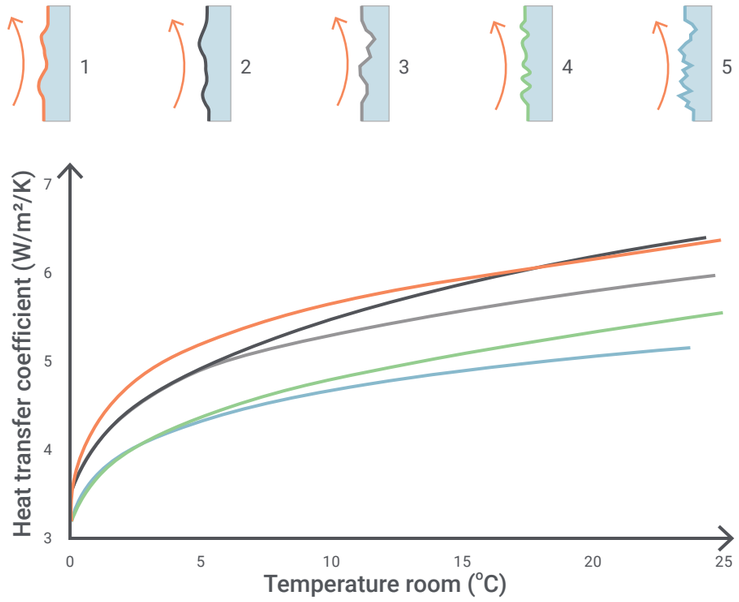

Figure 2.9:
The thermal exchange rate from air to surface can be altered by modifying the surface shape. S1_B has the greatest heat transfer at room temperatures below 20 °C. S2_B and S2_C has greater heat transfer rates above 20°C. (Source: modified from Cupkova & Promoppatum, 2017)

PCM system

Vigna et al. (2018) did a SWOT analysis on PCM-filled interior window shutters to see if it can solve the problem of overheating that traditional shutters are prone to. The analysis concluded that the shutter could not increase in temperature until all the PCM is melted, leading to a lower surface temperature and g-value of the window system. In addition, the thermal inertia is higher, and the insulating properties of PCM can help reduce heat loss in the winter. However, Vigna et al. also saw the weaknesses of PCM leakage, shell degradation due to UV light, limited daylight, and overheating when the melting temperature is too low.

Performance

Phase change temperature & product

As mentioned before, the correct melting temperature must be chosen to achieve a good thermal performance of the system. The optimal melting point depends on seasons and sun exposure. During the summer months, a higher melting temperature is recommended due to higher ambient temperature and more sun exposure, while in the winter, it is the exact opposite. Therefore, a lower melting temperature will lead to better performance. According to simulations by Hendriks, Kees Jan (2019), a melting temperature of 23°C is suitable during heating seasons, while a melting temperature of 26°C is ideal during the cooling season. The simulation also showed that the optimal melting temperature that reduces the energy demand the most annually is 25°C. The simulation was performed on a Trombe wall in a Dutch office exposed to solar radiation and high internal heating loads. Based on those results, the RT 24 HC (organic) and SP24E (salt hydrate) PCM from Rubitherm are suitable for this temperature range. The RT 24 HC has a phase change in the 23 - 26°C, with the peak at 24°C. This temperature is sufficient for a Dutch dwelling with a smaller internal heating load than an office. The PCM is also efficient at slightly lower temperatures, which is beneficial during winter. The SP24E has a phase change between 22 – 24°C, and the peak crystallization and melting points are much sharper than the RT 24 HC. Appendix A shows the latent heat distribution of the two Rubitherm products.

Air gap

The distance between the window and the PCM system can also influence the system's thermal performance. Wang & Zhao (2015) investigated heat transfer rates of the air gap between a window and a 2 mm thick PCM-filled cloth curtain. The air gap distances were 20 mm, 50mm, and 80 mm, and the height and width of the test model were 450x450 mm. The simulation covers 3-5 days during summer conditions in Shanghai. The results show that the heat transfer rates increase during the daytime, with a peak at 11:36 AM. The simulations also show that when natural convection is neglected, the highest heat transfer rates occurred in the 20 mm air gap with a value of 73 W. Although when natural convection was considered, the 80 mm air gap had the highest heat transfer rate of 112 W. It is worth noting that colder air accumulates at the bottom, and the temperature difference between the top and bottom of the air gap can reach up to 51°C. (Figure 2.10) Leading to a less efficient melting process of the PCM. As a result, a PCM curtain system can theoretically perform better if multiple PCMs with slightly different melting temperatures are applied. In other words, natural convection plays a vital role in transferring heat, and adjusting the air gap distance according to the seasonal temperatures, can reduce energy demand even further.

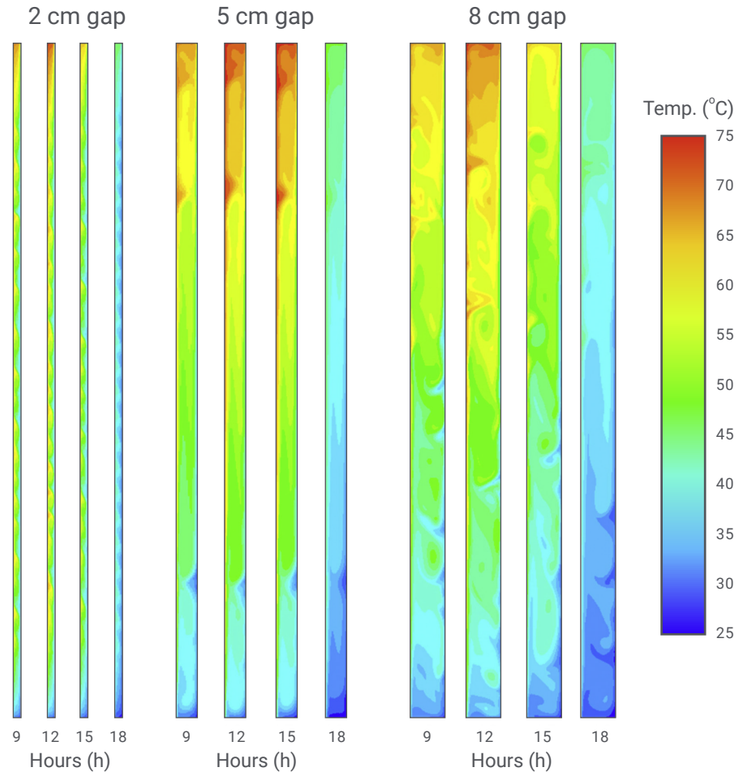

Figure 2.10: Simulation of the temperature range within different air gap thicknesses depending on the time of the day. Left to right: 20, 50, and 80 mm. (Source: modified from Wang & Zhao, 2015)

PCM and insulation combination:

Combining PCM with an insulation layer can help control how the heat flows from the PCM to the environment. The Double face 2.0 research project from TU Delft investigated using PCM and aerogel insulation in an adaptive Trombe wall. The wall's main components consist of a PCM-filled section (≈2.5 x 2 x 80 cm) facing one side and a 1 cm thick aerogel layer facing the opposite side. The aerogel blocks unwanted solar gain and heat loss and ensures that the stored heat is not released on the wrong side of the system. (Figure 2.11) Depending on the season and time of the day, the system rotates to optimize the thermal comfort of the room. Between sunrise and sunset (winter), the PCM faces the window to absorb solar heat gain. The system then rotates to face the room between sunset and sunrise to discharge the stored heat. The Trombe wall system does the opposite in the summer by absorbing heat from internal sources between sunrise and sunset. Then the system rotates to discharge the stored heat

toward the window in the evening. The average result of a range of computational simulations shows that the Double Face 2.0 system could reduce heating demand by 36.1% and cooling demand by 49.9% in a Dutch temperate climate. The PCM was a salt hydrate with a melting temperature of 23 - 25°C. The dimension of the system is 80 cm wide and 240 cm high, and the size of the rooms tested was 20 m2 and 100 m2. (Tenpierik et al., 2020)

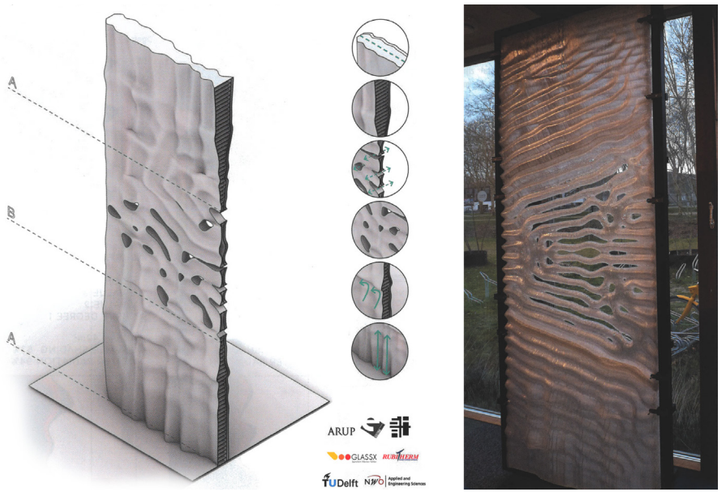

Figure 2.11:
The Double face 2.0 research project by TU Delft and partners.
(Source: Tenpierik et al., 2020)

Visual Comfort

In terms of visual comfort and occupants, psychological well-being: the transparency and shading ability of the system is essential to consider. Vigna et al. (2018) analysis of the PCM-filled interior shutters concluded that the appearance between solid, phase change, and liquid states could drastically affect the visual comfort in a room. According to Kośny (2015), many PCMs are transparent in the liquid state and become milky when solid, reducing the effectiveness of sun shading applications. For instance, when shading is desired during the early afternoon, the PCM is in a transparent liquid state, and when the sun has set, the PCM is in a solid and milky state. Therefore, adding a fabric layer can provide shading and diffuse direct sunlight. According to BBSA (2023), a comfortable indoor light intensity when sitting in front of a computer is around 500 lux. On a sunny day, the sun can generate 100,000 lux; on a cloudy day, it can be as much as 10,000 lux.

Human interaction

According to Bluyssen (2013), humans respond to external stressors, such as thermal and visual discomfort, by altering the production of hormones and cytokines. The body is doing that to try to restore some sense of balance. Personal factors, time, season, and previous experiences also heavily influence this response. Although, long-term exposure to such external stressors without the ability to affect the situation can cause illness and other physiological problems. Therefore, products allowing human interaction and control can significantly mitigate those issues. In this particular case, controlling the amount of daylight and heat gain is relevant. In addition, having an aesthetically pleasing design can also increase visual comfort.

Case study

GlassX AG manufactures the GlassX Crystal, a transparent sunscreen filled with PCM that is useful for buildings with much glazing. It blocks out the solar heat gain, stabilizes indoor temperatures, and simultaneously allows the maximum amount of diffuse sunlight into the room. Performance tests on the GlassX elements show that it can reduce energy demand by 20-40% due to the combination of prismatic reflective glass, phase change material, and three layers of insulating glass. Furthermore, the small footprint of the GlassX system, compared to passive walls in wood construction, can result in up to 0.4 m2 more usable area per system. In addition, the system is designed to be maintenance-free.

In terms of operation, The U-value of the glazing is 0.5 W/m2K. The prismatic glass reflects solar radiation if the incidence angle is above 40 degrees, preventing the PCM from overheating. (Figure 2.12) Solar radiation passes right through when the incidence angle is below 40 degrees, allowing the PCM to melt. Salt hydrate with a melting range of 26-28°C is contained in horizontal polycarbonate compartments. The encapsulation is colored grey to improve thermal absorption. A 6mm safety glass is needed to secure the system on the interior side. The system is a maximum of 3 meters high and 2 meters wide and has a storage capacity of 1185 Wh/m2. (GlassX AG, 2023)

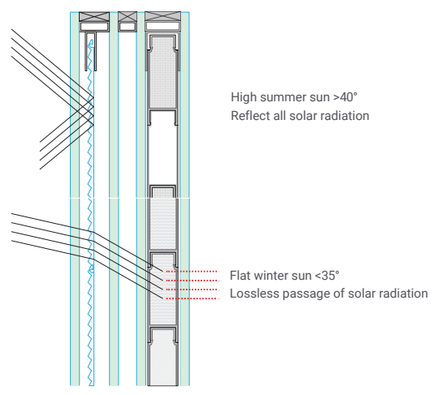

Figure 2.12:
Left: Section of GlassX Crystal illustrating how sun angle influence solar radiation. Right: GlassX Crystal implemented in a retirement home in Domat, Switzerland.
(Source: modified from GlassX AG, 2023)

Conclusion: literature study

To balance between heating and cooling, a dwelling in the Netherlands should have a melting temperature of 23-24°C. To achieve this, two Rubitherm PCM products (RT 24 HC and SP24E) are suitable for this climate zone and application. However, it's important to note that the maximum service temperature for these two products is relatively low, at 56°C and 45°C, respectively. This means there may be a risk of overheating during the summer if the PCM melts too quickly. It's essential to implement design techniques to mitigate overheating to prevent this from happening.

When choosing a PCM, there are pros and cons for both organic PCMs and salt hydrates. Organic PCMs are stable chemically and won't experience issues such as supercooling or phase segregation, but they do have low conductivity, are flammable, and can be expensive. Salt hydrates, on the other hand, have higher thermal conductivity but are prone to chemical degradation and supercooling, and are corrosive. However, by adding certain additives, the limitations of salt hydrates can be mitigated. It's also worth noting that the cost of PCMs varies depending on the manufacturer, performance, and type. Generally, salt hydrates are much cheaper than organic PCMs. For instance, SP24E salt hydrate costs 3.31 EUR/kg, while the organic RT24 HC costs 12.76 EUR/kg. This price difference can have a significant impact on the overall cost and marketability of the PCM system.

To prevent the PCM from reacting with the environment, it will be enclosed in a macroencapsulation. The size and shape of the encapsulation affect its performance, with a thickness of 10-30 mm being ideal for efficient melting. A high surface-to-volume ratio is also beneficial for faster melting and crystallization. Smooth, sinusoidal surfaces are better at exchanging heat than rough, edgy surfaces. See Figure 2.13 for clarification. Spherical volumes have naturally good heat exchange rates. Additionally, adding aluminum fins to the outside of the encapsulation can further improve heat exchange with the environment. Internal fins, metal matrices, and graphite flakes can be implemented to enhance thermal conductivity within the encapsulation.

To ensure even heat distribution, it is recommended to compartmentalize the volumes horizontally and use PCMs with varying melting temperatures for optimal system performance. This also helps prevent overheating. A rotating system that can discharge/absorb heat energy where necessary can provide consistent performance throughout the day and year. Adding an insulating layer to the rotating system can control heat discharge and prevent unwanted solar heat gain and loss. The distance between the window and the PCM system affects the heat transfer rate, with 50-80mm being an adequate distance based on the literature.

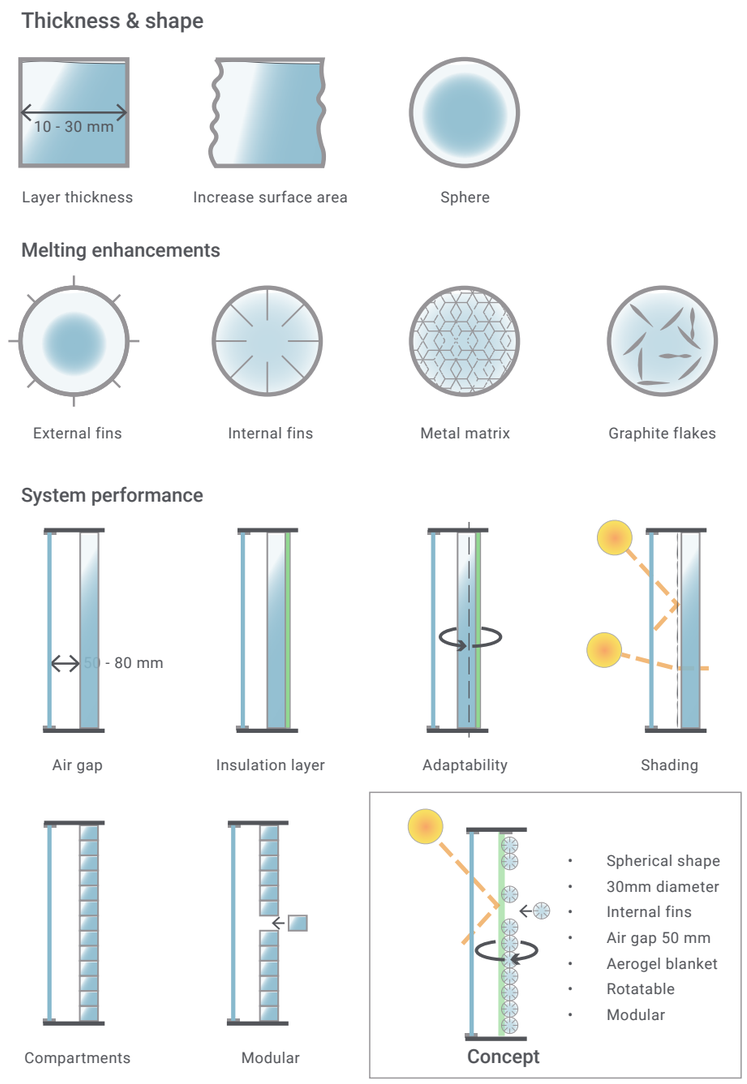

Figure 2.13: Performance enhancement strategies on macroencapsulations and complete PCM system.

3. BACKGROUND RESEARCH

Electromagnetic waves

Galindo (2023) explain that radiation is energy that moves in the form of electromagnetic waves or particles from one place to another. Depending on the wavelength of the electromagnetic wave, it can be low-energy non-ionizing radiation or higher-energy ionizing radiation, which is harmful to organisms and specific materials, see figure 3.1. The wavelength and frequency are inversely proportionate, meaning that the shorter the wavelength, the higher the frequency and the more energy it has. Electromagnetic waves always travel at the speed of light or 299,792 km per second and do not require any medium to propagate. (Bokel, 2021) According to NASA, Science Mission Directorate (2010), the terms radiation, electromagnetic waves, and light refer to electromagnetic energy.

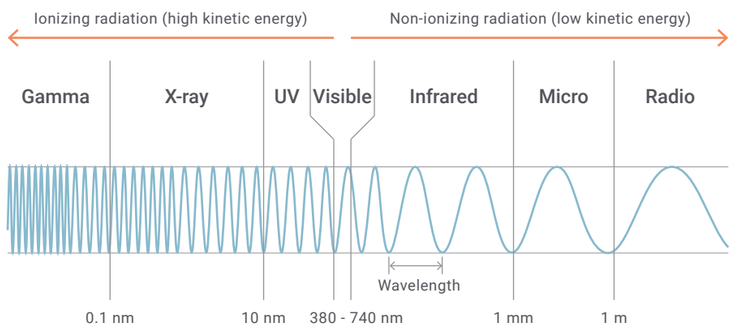

Figure 3.1: Electromagnetic waves and how the spectrum is classified into gamma, X-ray, UV, visible, infrared, micro, and radio waves depending on wavelength.

Electromagnetic wavelengths can be shorter than an atom and longer than the earth's diameter. The shorter the wavelength, the more kinetic energy it has, defined in electron volts. The kinetic energy also influences how radioactive the waves are. For instance, gamma rays, the most radioactive electromagnetic waves, have the shortest wavelengths of less than 0.1 nm. X-rays and Ultraviolet light have slightly longer wavelengths, between 0.1 - 10 nm and 10 - 380 nm, respectively. These waves are harmful to humans and certain materials if exposed for longer durations of time. (NASA, Science Mission Directorate, 2010) Visible light that the human eye can detect falls in wavelengths between 380 - 740 nm. Electromagnetic rays that are longer than 740 nanometers are either infrared waves (740 nm - 1 mm), microwaves (1 mm - 1 m), or radio waves (>1 m). (Van der Linden et al., 2018) The solar radiation reaching the earth's surface has wavelengths from 295 to 2500 nm. (Yousif & Haddad, 2013) According to Science on a Sphere, NOAA (2023), visible light accounts for 43% of all the radiant energy the sun emits, while infrared accounts for 49% of the output. UV-light accounts for 7%, and x-rays, gamma rays, and radio waves account for less than 1%.

The temperature of the specific wavelengths can be determined using Wien's displacement law (6). (Sheldon, 2023)

$$\lambda_{max} = K_w / T \quad (6)$$

For instance, the wavelength that radiates 23°C, can be calculated using equation (6).

$$\lambda = 2{,}897{,}770 \text{ nmK} / 296 \text{ K}$$
$$\lambda = 9790 \text{ nm}$$

Ultraviolet light

Ultraviolet light or UV-light is invisible to the human eye, and this type of light can be subdivided into UV-A (400 - 315 nm), UV-B (315 - 280 nm), UV-C (280 - 100 nm), and extreme ultraviolet (100 - 10 nm) light. (NASA, Science Mission Directorate, 2010) According to Alexander (2019), the atmosphere absorbs almost all UV-C and most UV-B light. These two UV lights are the most harmful to the human organism. 95% of the UV light that makes it to the earth's surface is UV-A light which can also harm the human organism through skin damage. UV radiation, especially UV-B radiation, can alter the mechanical and aesthetical properties of organic materials such as polymers. This is caused by photodegradation which build up free radicals that attack the polymeric chains causing reduced impact and tensile strengths, less molecular weight, discoloring and unpredictable performance. (Andrady et al., 1998) To counteract this degradation, most polymers in applications exposed to UV radiation use certain additives to increase UV resistance.

UV-resistant additives

Several methods can be used to protect polymers from UV degradation. The most common methods include UV absorbers, stabilizers, or quenchers. (Yousif & Haddad, 2013) UV absorbers prevent UV radiation from forming free radicals and instead absorb the UV energy and release it as heat energy. The amount of UV absorber that can be applied is determined by the absorption depth or thickness of the material. Therefore, the protection is limited for thinner polymeric shells, films, or fibers. Other factors that influence how much absorber is needed depend on the compatibility with the selected color/paint and polymer and the mechanical effects of a high concentration of UV absorber. Benzophenones and benzotriazoles are commonly used as UV absorbers for polymers needing transparency. Different types of pigments can also be used. For instance, adding a mass fraction of 3 - 5 % of carbon black to the polymer mixture is recommended for optimal UV protection. In addition, powder metals such as aluminum or titanium dioxide are suitable pigments that reflect UV light. (Yousif & Haddad, 2013)

Stabilizers such as HALS or hindered amine light stabilizers are similar to absorbers. However, instead of absorbing the UV radiation, it reacts with the harmful free radicals that UV radiation form and remove them before they can break down the polymer structure. HALS is one of the most commonly used and effective stabilizing methods since it is usually a regenerative process ideal for long-term use. (Yousif & Haddad, 2013)

Polymers commonly have impurities or contaminants trapped during manufacturing which can absorb UV light and turn into a high-energy state. During this state, the polymers can readily react with the oxygen in the air and start to break down. To prevent this from occurring, quenchers, such as nickel, can be implemented to suppress the impurities from getting into a higher energy state. (Yousif & Haddad, 2013)

Visible light

Visible light is the electromagnetic waves the human eye can detect, which falls in the 380 - 740 nm spectrum. Each color that humans can detect has a unique wavelength. For instance, blue/violet is in the 380 - 500 nm range, green is between 500 - 600 nm, and red is between 600 - 740 nm. The wavelengths radiated from an object can help determine its temperature. As the temperature of an object increases, the wavelengths radiated become shorter. Warmer objects radiate a blueish color, while less warm objects radiate yellow and red. (NASA, Science Mission Directorate, 2010)

Infrared light

Infrared light is invisible to the human eye but can be felt through heat radiation, see figure 3.2. Any object with a temperature above 0 kelvin radiates heat in the form of infrared light. The higher the temperature, the more heat the object radiates. When the object is extremely hot, it emits visible heat, for instance, a hot stovetop. Electromagnetic waves turn into heat when it strikes a surface or object. Thermal cameras can capture infrared radiation to detect heat leakages in buildings. (Van der Linden et al., 2018) The infrared spectrum is divided into near (740 - 3000 nm), mid (3000 - 8000 nm), thermal (8000 - 15000 nm), and far (0.015 - 1.0 mm) infrared. (NASA, Science Mission Directorate, 2010) Bokel (2021) mentioned that when near-infrared waves and visible light pass through a window and come in contact with the interior surfaces, the surfaces start emitting far-infrared wavelengths.

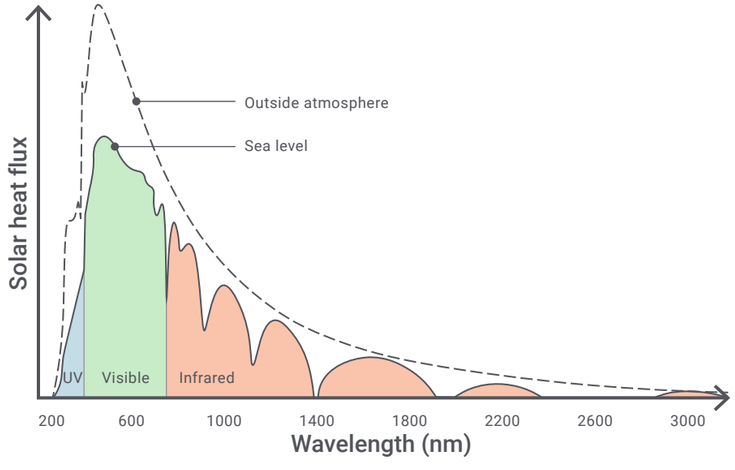

Figure 3.2:
Solar energy spectrum
(Source: modified from Dr. RMJ Bokel, 2021)

Emission & absorption

According to Van der Linden et al. (2018), visible light (photometric) and heat radiation are part of the same electromagnetic radiation family but operate very differently. For instance, a white-painted surface absorbs around 20% of visible light and around 90% of heat radiation. In contrast, a black-painted surface absorbs around 90% of visible light, while the heat absorption stays the same at 90%. In other words, the color of the paint has little impact on heat absorption unless painted with a metallic paint which significantly impacts the emission coefficient. When the emission coefficient ε = 1, the maximum amount of surface radiation is emitted, called a black body radiator, which does not reflect any radiation at a specific wavelength. According to Kirchoff's law, a surface can absorb as much radiation as it emits. Therefore, the emission coefficient is equal to the absorption coefficient a.

Typically, when radiation hits a surface, it is not entirely absorbed. Some of the radiation may be reflected and transmitted. Although, the sum of the absorption coefficient + reflection coefficient + transmittance coefficient is equal to 1. For most building materials, the emission coefficient is around 0.90 to 0.95, meaning that the remaining 0.10 to 0.05 is either transmitted or reflected. The emission coefficient for a smooth blank aluminum surface is around 0.07 to 0.09. (Bokel, 2021)

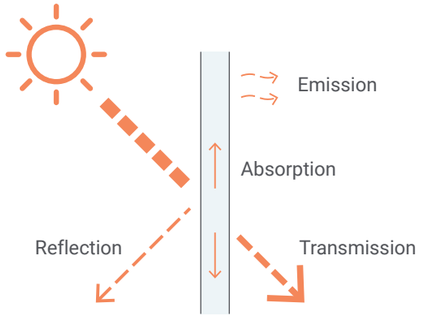

Figure 3.3:
Illustration of how electromagnetic radiation is splitted when it falls on a surface.

Transmittance:

Bokel (2021) mentioned that the percentage of radiation that passes through a layer such as glazing or curtain is called transmittance. It can be broken down into specific types of electromagnetic wavelengths that are transmitted, such as visible light transmittance, UV transmittance, or total solar energy transmittance. Visible light transmittance (VLT) is essential for curtain and glazing products since it determines how effective the product is at letting through daylight, controlling glare and privacy, room temperature, and views to the outside. A higher VLT value means that more light is transmitted. Different coatings, films, and tints can be applied to glass or polymers to block out undesirable wavelengths while letting visible light through. The portion of solar energy that is transmitted through a fenestration system is represented by the solar transmission factor (g). For example, a g-factor of 0.3 indicates that 30% of solar energy is transmitted. (Van der Linden et al., 2018)

Reflectance
According to Bokel (2021), the reflectance of glass and polymers depend on the surface quality, smoothness, additives such as coatings or films, and the angle of incidence of the light. The greater the angle from the surface normal, the more it reflects. For example, for clear glass, solar radiation with a 70-degree angle of incidence reflects >50% of the light.

Absorption
When a material absorbs electromagnetic radiation, it heats up and transfers the heat to the environment via convection. The higher the absorption coefficient, the more effective the convective heat transfer is. The portion of the g-factor transmitted via convection is represented as the convection factor (CF). It is usually not desirable to have a high convection factor since it directly contributes to a rise in air temperature. The absorption factor can be altered by implementing additives such as tints that absorb the visible light, making the material heat up faster. (Bokel, 2021)

Mitigation strategies

There are many strategies to reduce the amount of solar energy that passes through a layer of glass or polymer. The most common methods are Low-E coatings and tints. However, there are also a few different strategies, such as prismatic glass, photochromic coating, and passive daytime radiative cooling coatings which can be used for specific applications. To get a good understanding of what type of method to implement. Knowing the irradiance or how much electromagnetic radiation falls on a given surface or glass can be helpful. Irradiance is expressed in W / m2. A pyranometer or computational simulation tools can be used to measure irradiance. (Brembilla, 2021)

Low-E coating
Low emissivity or Low-E coatings are designed to reflect UV and infrared light while allowing visible light to pass through. Higher-grade Low-E coatings are invisible to the naked eye but can show certain reflective qualities at specific angles and lighting conditions. The coatings are made with highly reflective materials such as silver or other metallic oxides in a layer much thinner than human hair. There are different levels of how much of the electromagnetic spectrum is transmitted. It can be high-transmission, moderate-transmission, or low-transmission Low-E coatings. (Bokel, 2021) Figure 3.4 show the difference between high and moderate transmittance low-E coating on the electromagnetic spectrum. Depending on the application, the Low-E coating can either be magnetron sputter vacuum deposition (soft coat) or pyrolytic (hard coat). (Vitro Architectural Glass, 2023)

Magnetron sputter vacuum deposition or MSVD coatings are applied to the glazing surface in a vacuum chamber during low temperatures. This type of coating is not very durable and, therefore, is primarily used inside double or triple-glazing units to prevent exposure to the environment. The emission coefficient ε of MSVD coating is typically in the range of 0.10 - 0.02. (Bokel, 2021)

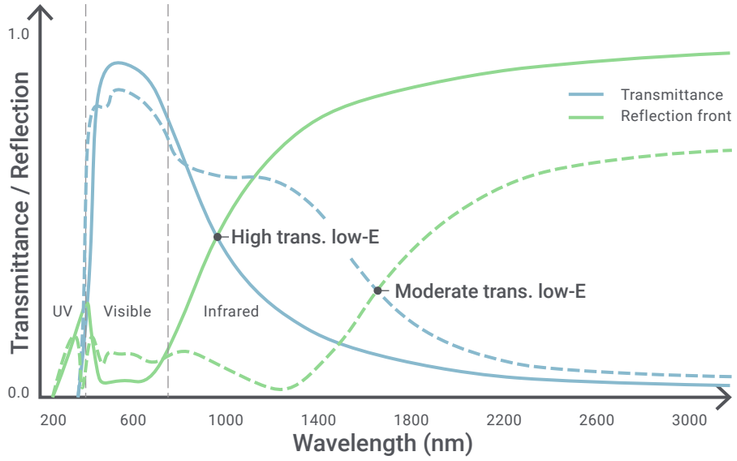

Figure 3.4:
Diagram of the difference between high transmission, and moderate transmission low-E coating in regards to solar radiation. (Source: modified from Dr. RMJ Bokel, 2021)

On the other hand, pyrolytic coatings are much more durable and are applied to the glazing surface while it is hot from manufacturing. As a result, the coating is stuck firmly to the surface. This coating process is not applicable for polymers since the application temperature supersedes most plastics' melting point. The Pyrolytic coatings have an emission coefficient between 0.10 - 0.20. (Bokel, 2021)

Tint
Tints can be used for two different purposes. It can be used aesthetically to color a polymer/glass or for solar heat management. Regarding heat management, tints are used to reduce the amount of solar radiation directly transmitted to the inside. Instead, it absorbs the solar radiation, heats up, and eventually transfers the heat to both the inside and outside via convection. This heat management strategy is less efficient than Low-E coatings but better than glazing with no coating. It can be applied in films and coatings or blended into the chemical composition during manufacturing. (Bokel, 2021)

Additives such as pigments are used to modify the chemical composition to make tinted polymers. Depending on the additive, the color and transparency of the tint can be customized, see Figure 3.5. The specific tint color and type of polymer result in unique transmittance, absorption, and reflection properties. Tints with a light blue or green appearance can be spectrally selective, which absorbs parts of the near-infrared wavelengths while transmitting the visible wavelengths. Spectrally selective tints can reduce heat loss in the winter and heat gain during the summer. (Bokel, 2021)

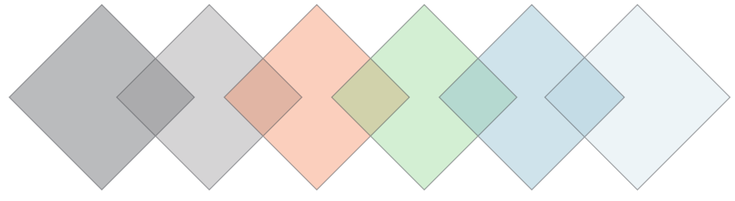

Figure 3.5:
Illustration of what tinted glass can look like.

Photochromic coating

Photochromic coatings contain molecules that react with the intensity of UV light. The coating allows all light to pass through if there is little to no UV radiation striking the coating, for instance, during an overcast day. When there is high-intensity UV light, such as on a clear sunny day, the photochromic coating darkens, preventing most of the light from passing through, see figure 3.6. The molecules that react with UV light are temperature sensitive, meaning that when the molecules are cold, they will take longer to activate than when they are warm. This effect can increase the efficiency of the PCM melting process during the winter. (Transitions Optical Limited, 2023)

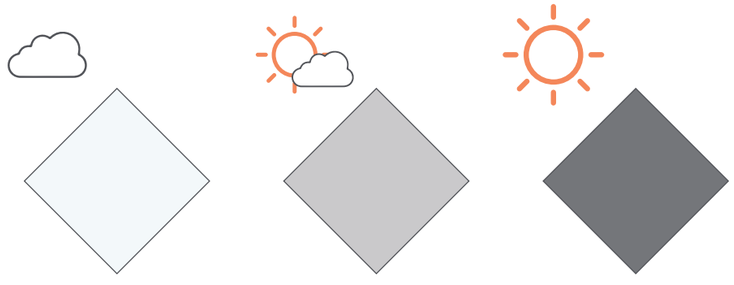

Figure 3.6: Illustration of how photochromic coating look like during the different intensities of UV radiation.

Prismatic glass

Glass or transparent plastics can be cut at precise angles to reflect or refract (bend) light depending on the angle of incidence. This type of glass, called prism, can be used for many applications, from analyzing the light spectrum, controlling heat gain, or correcting double vision. Each wavelength refracts a different amount, making it possible to separate longer wavelengths from shorter ones, see figure 3.7. Understanding how the different angles affect the incident wave makes it possible to design prims in many different forms and geometries to fit the specific application. (Britannica Editors, 2023a)

Prismatic glass is used in the GlassX Crystal project to reflect solar light striking the glass at higher incidence angles during the peak summer season. When the solar incidence angle is smaller, the prismatic glass refracts the light toward the inside. The structure of prismatic glass is made with one smooth side, and the other side is similar to a ridged surface with sharp edges. (GlassX AG, 2023)

Although, for this system to work as intended, the prismatic glass must be fixed at a constant angle. If the glass moves, the angle at which the glass is refracting will shift, causing unpredictable performance.

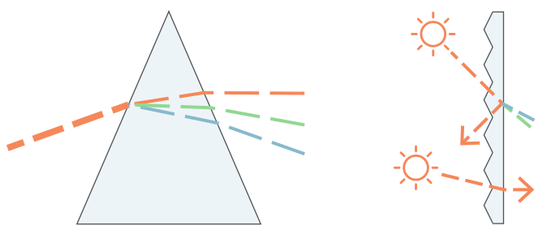

Figure 3.7: Left: Illustration of a prism refracting light differently depending on wavelength. Right: Illustration of how prismatic glass or polymer can be used to refract visible light while reflect infrared light. (Source: modified from Britannica Editors, 2023 : GlassX AG, 2023)

Passive daytime radiative cooling coating

Researchers from Columbia University and MIT have conducted experiments on coatings that reflect solar radiation in the wavelengths 300 to 2500 nanometer and, at the same time, emit heat through the atmosphere's infrared transmission window between 8000 - 13,000 nanometers. This type of coating is a form of passive daytime radiative cooling fabricated using a phase inversion technique to achieve a hierarchically porous polymer coating. Essentially, this process creates air pockets in the coating layer that reflect and scatter most incoming light, see figure 3.8. The results show a hemispherical solar reflectance and far infrared emittance of approximately 0.96 and 0.97, respectively. The primary benefit of this form of coating is that it can be applied to plastic, metal, or wood surfaces at room temperature using practical painting or spraying techniques. (Mandal et al., 2018)

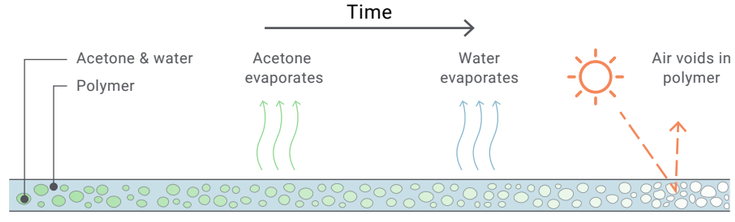

Figure 3.8: Illustration of how the passive daytime radiative cooling coating is fabricated. (Source: modified from Mandal et al., 2018)

Lighting (photometric)

As mentioned, the human eye can detect electromagnetic wavelengths between 380 - 740 nm. According to Van der Linden et al. (2018), the human eye is most sensitive to the wavelength of 555 nm, which is yellow-greenish light. While violet, blue, and red colors are more challenging to see in poor or low-light conditions. That said, it is essential to distinguish that color is not a property of electromagnetic radiation but rather a feature of human perception. Several factors determine how humans perceive light, and providing adequate and evenly distributed indoor lighting is a critical factor in achieving good visual comfort and being able to perform tasks. Therefore, it is essential to understand the factors determining the amount, quality, and relationship between indoor and outdoor light, see figure 3.9 for a summary of important terms regarding visible light.

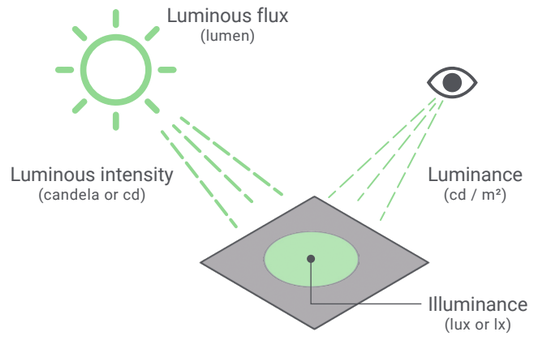

Figure 3.9: Illustration of what the different terms and units of lighting are and how they relate to one another. (Source: modified from https://arendlighting.com/illuminance/?lang=en)

Iluminance

Illuminance E is the amount of light (luminous flux) that falls on a given surface. Equation 7 can be used to calculate the illuminance. (Van der Linden et al., 2018)

$$E = Im / A \quad (7)$$

According to Van der Linden et al. (2018), illuminance is commonly used to determine how much lighting is needed to perform specific tasks. The amount of illuminance can be classified into three segments: orientation lighting, lighting in the workplace, and special work lighting.

Orientation lighting:	50 - 100	lx
Lighting in the workplace:		
Typical living room:	150 - 200	lx
Basic detail work, carpentry:	200	lx
Reading, writing:	400	lx
Fine detail work, drawing:	800	lx
Special work lighting:		
Precision work, watch assembly:	1600	lx
Operating theatre:	>3200	lx.

(Source: Van der Linden et al., 2018 : Engineering ToolBox, 2004)

Surface color reflection

The light will reflect differently depending on the surface finish and material properties. Van der Linden et al. (2018) point out that if the luminance is the same in every direction of a surface, the surface predominantly reflects diffused light. The amount of visible light reflected also depends on the surface's color and brightness. Hence, a higher reflection factor reflects more light.

Surface color	**Reflection factor**
White:	0.70 - 0.80
Yellow:	0.30 - 0.70
Beige:	0.25 - 0.65
Grey:	0.20 - 0.60
Blue:	0.08 - 0.55
Green:	0.12 - 0.50
Red:	0.10 - 0.35
Black:	<0.04

(Source: ir. A. C. Van der Linden et al., 2018)

Daylight factor

The daylight factor is the relationship between indoor illuminance and outdoor illuminance (horizontal surface) at the same time. (Equation 8) It is typically defined using overcast sky conditions to reduce the sun's influence. It is a good indicator to determine the illuminance required throughout the day. (Van der Linden et al., 2018)

$$DF = (E_{inside} / E_{outside}) * 100\% \quad (8)$$

For instance, if the indoor illuminance is 150 lx and the outdoor illuminance is 6000 lx (which is achieved 90% of the time during the hours 08:00 - 16:00), the daylight factor would be (8):

$$DF = (150 lx / 6000 lx) * 100\% = 2.5 \%$$

Multiple factors determine a space's daylight factor, such as the size and number of windows and the properties of the glass. In addition, the type of shading devices, room depth, and light reflection by walls, ceiling, and floor also affect the daylight factor.

The daylight calculation is based on a cloudy sky to mitigate the influence and variations of the sun throughout the year, location, and weather. According to NARM Secretariat (2018), a minimum daylight factor of 1.5% at an elevation of 0.85m above the floor is recommended for domestic living areas such as a living room. Figure 3.10 show an example of a daylight factor simulation of a living room in a dutch terraced house.

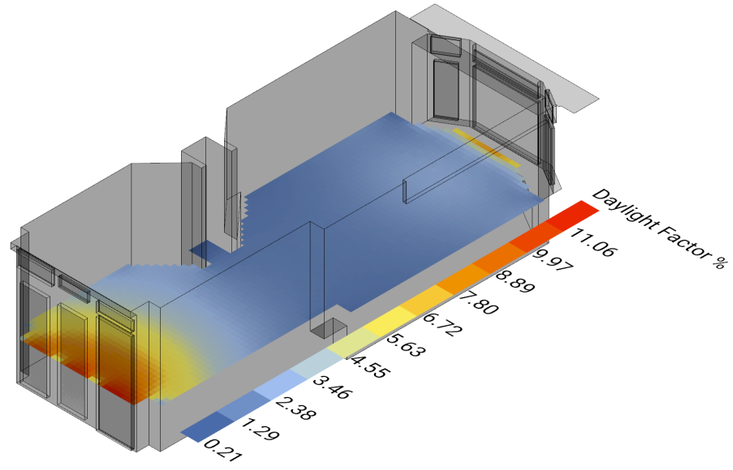

Figure 3.10: Daylight factor simulation performed using Grasshopper and Ladybug.

Shading types

Shading can be implemented on the exterior, between double or triple-glazing panes, or on the interior side of the building envelope. The shading type's effectiveness at blocking solar heat is defined by the shading coefficient (SC), which is expressed in a value between 0 and 1. A lower value means that the shading blocks more solar heat. For instance, exterior shading types are the most efficient, and an SC of 0.15 is not uncommon for louvers and screens, which means that they block out 85% of solar heat. The science behind it is that solar radiation is reflected and absorbed by the shading before it can be transmitted through the building envelope. Resulting in significantly less solar gain, see Figure 3.11. (Van der Linden et al., 2018)

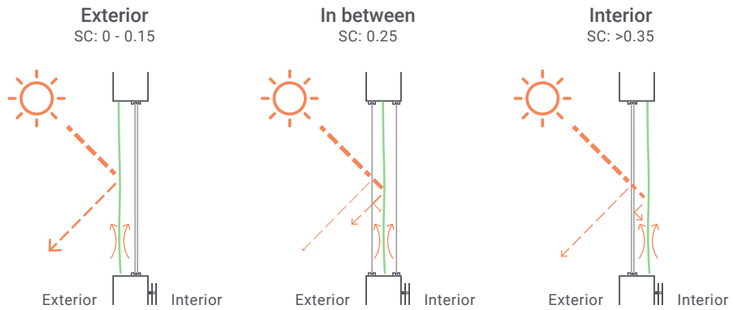

Figure 3.11: Illustrations of sunshading placement and how it affect the shading coefficient.

On the other hand, internal shading can be beneficial in the winter to increase solar heat gain and reduce heating demand. Unlike external shading devices, solar radiation is transmitted through the glazing when it contacts the shading system. The shading reflects some of the radiation, but most of it is absorbed, causing the shading to heat up. The warm shading then emits heat via convection to the indoor air. (Van der Linden et al., 2018)

There are many different ways to provide interior shading. The most widely used options are venetian blinds, roller blinds, vertical blinds, or curtains, commonly made with either polymers, aluminum, wood, or fabric, depending on aesthetical intentions and budget. (BBSA, 2023)

Venetian blinds

Venetian blinds consist of multiple horizontal slats that cover the window, see Figure 3.12. The angle of the slats can be adjusted to control the amount of diffused or direct light that passes through between the slats. Complete privacy can also achieved. The ability to control the light transmittance makes venetian blinds one of the most popular shading options. The blinds can be manufactured in a variety of materials and colors. Wood, aluminum, or plastics are the most commonly used materials. In addition, highly reflective coatings can be applied to reduce solar heat gain. The durability might differ depending on the choice of material, but generally, the system is resistant to everyday wear and tear. Venetian blinds can be operated either manually via cords or remotely by a DC motor. (BBSA, 2023)

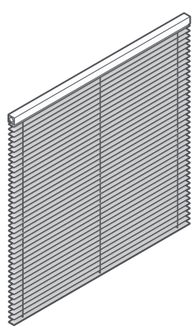

Figure 3.12: Illustrations of a venetian blind.

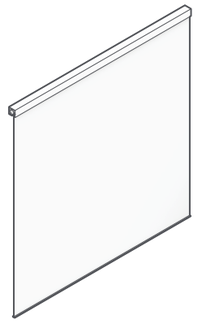

Figure 3.13: Illustrations of a roller blind.

Roller blinds

Roller blinds consist of one screen that provides the shading, limiting the control of how much light is transmitted, see Figure 3.13. Although, the versatility and simplicity of roller blinds make them one of the most popular types of shading solutions. The shading rolls are usually made with either textile, polymer, or vinyl, and can be highly transparent to blackout. Customized patterns can be woven, embroidered, or digitally printed to the roller. Highly reflective fabrics can also be used to improve thermal performance. The mechanism that makes the shading roll up or down can be spring, push/pull, chain, gear, or motor driven. (BBSA, 2023)

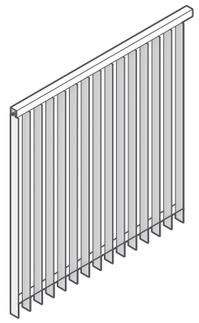

Figure 3.14: Illustrations of a vertical blind.

Vertical blinds

Vertical blinds consist of multiple louvers suspended from a tracking system, see Figure 3.14. The louvers are connected by a chain and cord that control the tilting angle and traversing. A DC motor can also be used to move the louvers. Usually, the louvers are made with stiffened fabric, but other materials such as PVC, aluminum, and wood can also be used. Customized prints and highly reflective coatings are also available options. (BBSA, 2023)

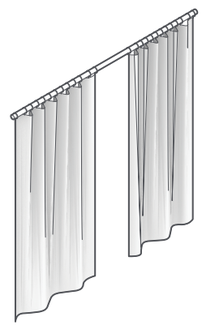

Figure 3.15: Illustrations of a curtain.

Curtain

A curtain is a fabric suspended from a railing system to form a screen against solar radiation, see Figure 3.15. Curtains are usually hung in pairs of two and can move sideways parallel to the window. They offer much freedom in the choice of textile color and pattern, visible light transmittance, and how they are suspended from the railing system. The way the curtain is suspended from the railing system affects the appearance and how it will fold. Several curtain layers with different transmittances can also be implemented to control the shading precisely. Common curtain suspension styles are grommet/eyelet, tabbed top, hidden tab, rod pocket, and different types of pleats. (Terry's Fabrics, 2023) According to Smartblinds.com (2021), tracking systems can also be motorized for automatic closing and opening.

Suspension system

The most common method to suspend a curtain is using a rod, track, or tension wire, see Figure 3.16. Each system has its benefits and limitations. Curtain rods have a simple design with minimal risk of malfunction. Some rods can be extendable to fit different window widths. Curtain rods have an end and starting point determined by the wall fastening brackets. Tracking systems are more complex but offer more design freedom in the shape of the track and the total length since the fastening brackets are not interfering with the track. Curtains are usually suspended to a sliding mechanism using hooks and gliders, which can get stuck if dirt is on the track. Finally, tension wire systems have a thin and minimalistic look. It takes up less wall space and can be shipped in smaller packages than curtain rods and tracks. Although, the wire need to be in a large amount of tension force to be as straight as possible.

The track can be mounted on the wall, window header, or window trimmer. The chosen method depends on aesthetics, function, and accessibility reasons. Inside the track are gliders, which can be in the form of wheels or sliders. The shape of the track also influences the shape of the gliders. For example, the glider should be compact for curvy tracks to handle a small turn radius.

A standard solution to hang the curtain to the gliders is by sewing or stitching pleats or pleating tape to the curtain, which hooks can hold onto. The hooks are then hung on the gliders. There is a large variety of pleating styles that have a considerable impact on the overall look and folding of the curtain. Common styles are pinch, inverted pinch, goblet, and cartridge pleat. Pleating can also be used to hide the track. (Terry's Fabrics, 2023)

Figure 3.16:
Left: curtain rod. Middle: curtain track. Right: curtain tension wire. (Source: author, inspired by IKEA railing systems)

Materials

Textile

The openness factor, thickness, and color determine the visible light transmittance of the textile. Brighter textiles have a higher VLT than darker ones. The openness factor depends on the density of the weave. Less densely woven textiles let more light through, see Figure 3.17. This type of fabric is used in sheer/voile curtains to maintain indoor privacy without compromising daylighting. Thicker fabrics made with more than one layer also reduce the transmittance. The recommended VLT for a shading curtain in highly exposed environments should be up to 5% and between 5 - 10 % for moderately exposed environments. (BBSA, 2023 : Terry's Fabrics, 2023)

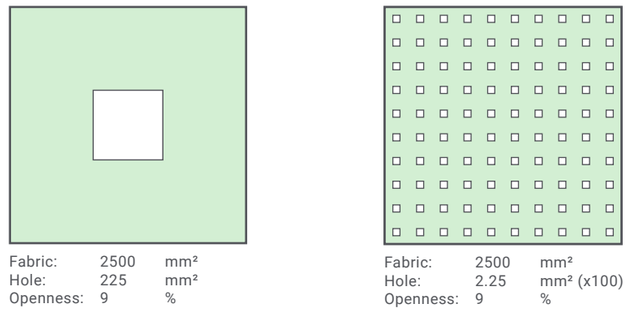

Figure 3.17:
Illustration of openness factor and how it can be distributed over an area.
(Source: modified from BBSA, 2023)

Polyester fiber:

Polyester is a synthetic fiber most commonly made from PET polymer. It is used in sportswear and outdoor applications exposed to sunlight and rain due to its UV and water-repelling characteristics. (Council of Fashion Designers of America, 2016) Polyester requires much less water for manufacturing and washing than many natural fibers. The fabric is non-toxic, recyclable, and looks similar to natural fibers. (Trevira, 2023)

Microscopic aluminum particles can be mixed into the polyester resin during production, leading to a highly reflective layer against heat radiation. For example, Moondream Technology & Comfort (2023) have designed a curtain lining containing 99.99% polyester and 0.01% aluminum, which can lower the temperature of a south-facing room by up to 7^{o}C in the summer as compared to a situation withouth curtain.

Flax (linen) fiber:

According to the Council of Fashion Designers of America (2016), linen is a strong, durable, and sunlight-resistant fiber made from the stem of the flax plant. It is a high-quality and rare fiber, accounting for less than 1% of all textile fibers consumed worldwide. Linen is among the most sustainable fibers available due to the small amount of water and energy needed to grow and harvest the plant. Linen is naturally bright, with colors ranging from beige to grey. It also has good thermal regulating characteristics, giving the sense of warmth in cold weather and the opposite during warm weather. It can be blended with cotton or synthetic yarn to increase versatility and softness and reduce the effect of creasing, which is typical for linen.

Insulation

According to Cambridge Dictionary (2023), insulation slows or prevents heat and sound from transferring from one side to another. This is usually accomplished using porous materials that can trap air, which in itself has a thermal conductivity of ca. 0.025 W/m K at room temperature. (Engineering ToolBox, 2003) Table 3.1 provide data on a few different materials.

Figure 3.18: Illustration of insulation color nuance. Left-Right: Aerogel, natural wool, synthetic.

Aerogel:
Silica aerogel is an extremely low-density (0.001 g/cm3), high specific surface area (500-2000 m2/g) material. Almost the entire material consists of air pockets surrounded by an intertwining structural network of silica. The aerogel composition makes it one of the most effective thermal insulator on the market. (Aerogel Technologies, LLC., 2023)

Natural wool:
Wool is an animal fiber that grows on mammals such as sheep, goats, and camels to protect and insulate them from the environment. It is usually acquired by shearing the hair from living sheep and processing it to remove grease. Wool is naturally a bulky fiber due to its crimp or waviness, which traps air. The more crimp the wool has, the more insulative it is. In addition, wool is self-extinguishing and water-repellant. (Britannica Editors, 2022b)

Synthetic:
Synthetic insulation for clothing is made from polyester fibers and works similarly to natural wool because it can trap air very well. It is also resistant to moisture, and it dries fast. (Outdoor Research, 2022)

Insulation

Type	Thermal conductivity (W/m K)	Thickness (mm)	Cost (EUR/m²)	Reference
Aerogel	0.021	8	117	Aerogel Technologies, 2023
Natural wool	0.039	5	10	Engineering ToolBox, 2003 : Chimney Sheep Ltd., 2023
Polyester	0.050	6	1.56	Engineering ToolBox, 2003 : Rijs Textiles, 2023
Bubble wrap	0.038	5	0.49	Tian et al., 2021 : Profipack.nl, 2023

Table 3.1: Thermal conductivity and price information on commercially available insulation materials.

PCM encapsulation

The properties of the encapsulation material significantly impact the system's thermal performance, durability, and safety. The choice of material can also affect the form-flexibility of the encapsulation. Depending on the application, it could be helpful to consider whether the encapsulation should be rigid or more flexible. As mentioned in the literature study, the material should be nontoxic, UV-resistant, non-flammable, mechanically durable, thermally stable, and economically feasible. The most suitable polymers are PMMA, PC, PET, and LLDPE. See Table 3.2 for a comparison between the four polymers. The complete table of 10 different polymers are listed in appendix B.

Polymethyl methacrylate (PMMA)
PMMA, or acrylic glass, is a transparent, UV-resistant thermoplastic. Its excellent surface finish, hardness, stiffness, and abrasion resistance make it suitable for subsonic aircraft canopies, motorcycle windshields, lenses, and skylights. Fragments upon cracking are much duller than glass shards. Some limitations are high flammability, low service temperature (56°C), poor scratch resistance, and high embodied energy (118 MJ/kg). Additives such as flame retardants and impact modifiers are available. Finally, PMMA is recycled under code 7. (Granta EduPack, 2022)

Polycarbonate (PC)
Polycarbonate is a tough, impact-resistant, and transparent thermoplastic. It is suitable in any color and transparency and maintains durability over a large temperature span (-47 to 116 °C). It is also self-extinguishing and can be UV stabilized to achieve excellent long-term resistance toward solar radiation. It is commonly used in consumer electronics, supersonic aircraft canopies, safety helmets, bulletproof glazing, and kitchenware. Non-hydrolysis-resistant grades of polycarbonate have gradual chemical decomposition if in contact with hot water, which also leads to lower impact strength. Like PMMA, polycarbonates are recycled under code 7 and have a similar embodied energy of 111 MJ/kg. (Granta EduPack, 2022)

Polyethylene Terephthalate (PET)
PET is one of the most widely used polymers due to its surface finish, strength-to-weight ratio, coloring, and transparency characteristics. It is used in clothing (polyester), beverage bottles, packaging films, and industrial straps. PET is a good barrier against water vapor and oxygen, is somewhat UV resistant (without stabilizer), and is cheap (0.61 EUR/kg). It is less brittle and has lower embodied energy than PMMA and PC, with a value of 76.8 MJ/kg. On the other hand, it is highly flammable without fire retardant additives and is susceptible to heat degradation. Recycling PET is well established and can be recycled under code 1. (Granta EduPack, 2022)

Linear Low-Density Polyethylene (LLDPE)
Unlike PMMA, PC, and PET, which are rigid, linear low-density polyethylene, can be processed into a transparent soft form-flexible encapsulation. The characteristics of LLDPE are similar to low-density polyethylene but with higher impact strength and puncture resistance making it more practical for packaging films. It is also a hydrolysis-resistant and cheap polymer with a price of around 0.78 EUR/kg. It can also be easily recycled under code 4. On the other hand, LLDPE is highly flammable, has poor UV resistance, and additives have limited effects in thin films. (Granta EduPack, 2022)

Encapsulation

Property	PET Polyethylene Terephthalate	PMMA Polymethyl methacrylate	PC Polycarbonate	LLDPE Linear low density polyethylene
Material family	Thermoplastic	Thermoplastic	Thermoplastic	Thermoplastic
Impact strength (kJ/m²), Notched	6.2 - 6.8	1.9 - 2.1	10.1 - 83.1	590 - 1000
Transparency	Optical quality	Optical quality	Optical quality	Transparent
Service temp. (°C)	(-58) - 65	(-75) - 56	(-47) - 116	(-79) - 97
UV resistance	Fair	Good	Fair	Poor
Water (Salt)	Excellent	Excellent	Excellent	Excellent
Flammability	Highly flammable	Highly flammable	Slow-burning	Highly flammable
Recycle (#)	Yes (1)	Yes, others (7)	Yes, others (7)	Yes (4)
Density (kg/m³)	1290 - 1390	1170 - 1200	1190 - 1210	918 - 940
Embodied energy (MJ/kg), Typical	68.7 - 76.8	107.0 - 118.0	100.0 - 111.0	69.8 - 77.2
Price (EUR/kg)	0.61 - 1.08	1.59 - 2.22	2.11 - 2.69	0.78 - 0.96

Table 3.2: Properties of four different polymers. Blue rectangle indicate most preferable value while orange indicate the opposite. (Source: Author : Granta EduPack, 2022)

Suspension system

The components that make up the suspension system should preferably be made with the same base material for simplified recycling. It should also have a high modulus of elasticity, low density, be durable against water (salt), easy to manufacture, and have low embodied energy. Aluminum and steel are commonly used in similar applications due to their mechanical properties.

Aluminum is a lightweight metal that can be cast or wrought. It is commonly used in the aerospace industry due to its strength-to-weight ratio. It is also easy to weld and cast and is a good conductor of heat and electricity. Aluminum is generally twice as expensive and has a higher embodied energy than most steels. (Granta EduPack, 2022)

Steel is an iron and carbon alloy with robust mechanical properties used in various applications where strength and reliability are paramount. The properties of steel can be customized to a great extent by applying additives to make carbon, alloy, tool, or stainless steel. For this project, stainless steel is suitable due to the potential exposure to corrosive salt hydrate. Stainless steels are characterized by their high chromium content, giving them a distinguishable shiny look and less maintenance. In addition, it has a much higher Young's modulus and density than aluminum. (Granta EduPack, 2022)

According to Granta EduPack (2022), the specific alloy depend on whether it is cast or wrought processing technique. For wrought metals, the most suitable options are aluminum 6463 (T4) or stainless steel AISI 409 (ferritic), and for casting, it is aluminum 413.0 and stainless steel ASTM CB-30 (ferritic). See table 3.2 for a brief comparison of the different alloys.

Suspension system

Property	Aluminum 6463 (T4)	Stainless Steel AISI 409	Aluminum 413.0	Stainless Steel ASTM CB-30
Processing	Wrought	Wrought	Cast	Cast
Young's modulus (GPa)	72 - 75	195 - 205	69 - 72	196 - 204
Density (kg/m³)	2660 - 2720	7610 - 7820	2630 - 2680	7450 - 7600
Embodied energy (MJ/kg)	113 - 132	22.7 - 26.5	108 - 126	24 - 28
Price (EUR/kg)	1.7 - 2.0	1.0 - 1.3	1.7 - 2.0	1.2 - 1.5
Recyclable	Yes	Yes	Yes	Yes

Table 3.3: Properties of four different alloys. (Source: Author : Granta EduPack, 2022)

Conclusion: background research

Ultraviolet light (10 - 380 nm) harms humans and can alter the mechanical properties of polymers if not UV treated. The most common UV additives are absorbers, stabilizers, and quenchers. The thickness, type, and color of the material influence how good an effect the stabilizer will have. Thinner films can only absorb a little bit and therefore have limited longevity.

Visible light (380 - 740 nm) is measured in electromagnetic heat radiation and photometry. Very hot objects radiate heat in the visible light spectrum. At the same time, the human eye can photometrically detect this heat and perceive it as a unique color. The quality, amount, and contrast of the light significantly impact visual comfort and well-being.

Infrared light (740 nm - 1.0 mm) is invisible to the human eye but felt through heat radiation. Infrared solar radiation transmitted through the building fenestration significantly impacts energy demand and indoor comfort. A material's transmittance, absorptance, and reflectance can be altered by applying a coating, film, or additive. Implementing a spectrally selective pigment is chosen as it can be mixed into the polymer blend during manufacturing to make durable and long-lasting protection compared to applying coatings or films. The spectrally selective pigment should reflect out the far and parts of the near-infrared wavelengths to reduce the risk of the SP24E salt hydrate reaching a temperature above its maximum service temperature of 45oC. The pigment should also transmit visible light to allow daylight into the room and enable the occupant to observe the melting/solidification process.

After conducting research on different shading systems, it has been determined that curtains and roller blinds are the most promising options. Curtains and roller blinds create a continuous barrier with minimal air gaps, helping to trap air between the window and shading layer, providing additional insulation. Venetian and vertical blinds do not provide the same benefits. Additionally, curtains offer more potential for storing PCM than roller blinds, as roller blinds need to be tightly rolled up. Therefore, curtains provide the most promising design flexibility. The ideal fiber for the curtain textile is polyester because it is durable, versatile, and can be woven to match the appearance and feel of natural fibers. Polyester can also be recycled, ensuring the textile gets a new life after use. Polyester is also considered for insulation to make recycling easier.

Rigid and form-flexible polymers were looked into for the PCM encapsulation due to their non-reactive properties toward salt hydrates. The selection criterium is based on embodied energy, durability, safety, cost, ease of recycling, and the ability to absorb energy and prevent cracking/leakage if the encapsulation falls to the floor. The two most suitable options are PET and LLDPE since they are less brittle than PMMA and PC and will most likely survive a fall to the floor.

The curtain suspension system should be stiff, durable, cheap, and recyclable. Therefore aluminum and stainless steel are the two most suitable options. However, the suspension system consists of multiple components that require different processing methods. As a result, two alloys (wrought and cast) of each metal are picked based on an analysis in Granta EduPack (2023). The candidates for further study are aluminum 6463, stainless steel AISI 409, aluminum 413.0, and stainless steel ASTM CB-30.

4. VISION & CONCEPT

Design vision

The design vision of this project is to have an interior sun shading and thermal energy storage curtain system composed of an insulation and heat reflective layer, a shading layer, and a PCM layer that will enhance thermal and visual comfort throughout the day and night. The curtain can be fully closed to trap the air in front of the window to amplify the insulation, or it can be pulled aside when the outdoor view is desired. It can also be rotated to boost thermal performance during all four seasons. The mechanics are durable, simple, replaceable, and can be adjusted to fit many window sizes.

Design concept

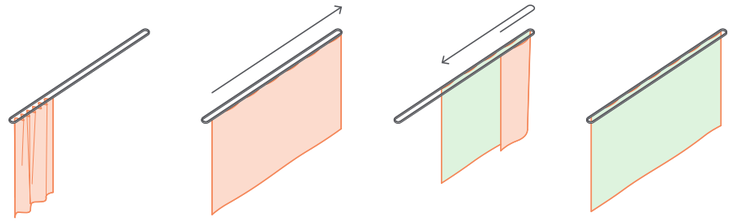

Figure 4.1:
The curtain is attached to a looping tracking system to be able to switch which side faces the indoor and outdoor.

Design strategies

Aesthetics

To have a successful product, it needs to be marketable and stand out among the competition. To achieve that, aesthetics, functionality, and uniqueness are vital parameters. The curtain must fit into different interior designs without making a radical high-tech statement.

Adaptability

The tracking system needs to be adaptable to fit many different window widths. The track length should be manufactured in a few different lengths and can be connected to match the total length needed. Likewise, the curtain should be designed and manufactured in such way that it can simply be cut to fit different window widths and heights. More than one curtain might be needed depending on window size and personal preferences. Custom-made curtain sizes should also be available.

Modularity

The curtain system will be exposed to intensive solar radiation. After prolonged use, there is a risk that the PCM has been degraded and operating at reduced capacity. Therefore, the encapsulation must be simple to remove without any tool. The encapsulation can then be shipped back to the factory for correct recycling or remixed for continued use. A modular design approach can support product families, such as unique encapsulation designs and volumes. Upgrading specific components when breakthrough innovations are available is also an option. Given the standardized dimension, large-scale production, packaging, and transportation are also economically feasible for modular design. Finally, quality control can efficiently be conducted on sample modules.

Human interaction

Besides having encapsulations that can be removed easily, the system should be simple to install, maintain, and clean by the dwelling occupant. The curtain must be simple to pull aside and fold into a tight profile to minimize the obstruction to the outdoor view. The user-curtain interface should also be straightforward to understand so the user knows which curtain side to face in what direction.

Product options

There should be different product options that the customer can choose between. For instance, the PCM volume and user automation may vary depending on the product variant. For example, a basic option is manually operated, while a premium version is fully automatic and can track the weather.

Cost

The material, PCM, and manufacturing costs are important considerations to make it a cost-effective product. Limiting unnecessary material use also guides the design process for both cost and environmental reasons.

Sustainability

Minimizing virgin-grade material and prioritizing recycled materials produced within Europe is essential to reduce the embodied energy for each curtain system. The end-of-life opportunities for the materials are also considered to allow the product to be recycled. The manufacturer must have the facility and machinery to recycle the broken PCM encapsulations to reduce the amount ending up in the landfill.

Light transmittance

Providing enough daylight is essential for indoor visual comfort. Therefore, the system should be equipped with two curtain types. One with PCM attached to it with translucent properties to transmit enough daylight into the room. The other curtain layer should be opaque to block out all visible light.

Safety

The encapsulation must be puncture resistant and durable enough to survive a fall to the ground without cracking. The PCM is corrosive and oily, which can stain and damage furniture. In case of a fire, the materials should have flame-retardant properties that can slow down the fire propagation.

Design criteria

Soft

Aesthetic	**PCM layout:**	Encapsulations should be distributed logically so the curtain folds into a tight profile.
	Daylight:	Diffuse and regulate direct daylight to enhance visual comfort.
	Design:	Have a subtle appearance to blend in with a wide range of interior designs. The encapsulations should look well-integrated and coherent with the curtain.
Functional	**User friendly:**	The system must be straightforward to assemble. Components need to be simple to remove and replace without any tools. The curtain is easy to rotate between day and night. The system must have a simple interface to understand which side needs to face what direction.
Cost & Sustainability	**Material:**	The system is made with abundant, recyclable materials processed in Europe.
	Design:	The shape of the components must be efficient to avoid excessive material use.

Hard

Aesthetic	**Thickness:**	The PCM & insulation layer should be at most 10 mm thick, respectively.
	Size:	The curtain is 1500 mm wide but can be cut at specific widths. The height depends on user preferences.
	Encapsulation:	Edges and corners should be smooth to even out the melting pattern and reduce stress concentrations if fallen to the ground.
Functional	**Performance**	The PCM volume should be as much as possible without compromising the folding of the curtain. Insulation needs to block unwanted heat flow. An aluminum layer will reflect summer heat gain.
	Durable:	The encapsulation must withstand everyday wear and tear, resist UV light and mitigate the risk of PCM overheating. The fabric must be strong enough to hold the weight of the PCM. The tracking system must be robust so the curtain does not fall.

Operational concept

The system will operate similarly to the Double Face 2.0 project by incorporating an insulation layer to control heat flow and provide the ability to change which side the PCM is facing depending on the day and night requirements. For optimal performance during the different times and seasons, see Figures 4.2 - 4.6.

The system needs to consider thermal performance, visual comfort, and the occupant's ability to control both parameter to their best ability. For optimal thermal performance, the PCM curtain should be closed most of the time to reduce heat gain in the summer and heat loss in the winter. Although, if the curtain is closed most of the time, there will not be enough daylight to satisfy the occupant, and the use of artificial light will be increased. Therefore, the curtain should be partially translucent to allow enough daylight to transmit. With that said, if total darkness in the room is desired, the system should also accommodate that.

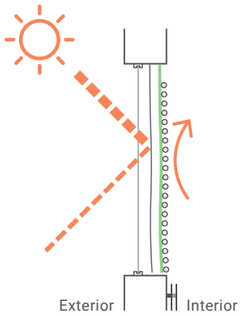

Figure 4.2: Summer - day
The PCM should face toward the room to absorb heat from internal sources to lower the indoor temperature. In addition, the trapped air between the glazing and curtain will help slow down solar heat gain. Finally, for optimal performance, a secondary blackout curtain with a reflective aluminum layer can reflect incoming solar radiation. According to Van der Linden et al. (2018), the g value of a reflective aluminum curtain is approximately 0.35, of which 25% is given off as convective heat.

To reduce the risk of PCM overheating if the occupant forgets to rotate the curtain between day and night. The shell should have a spectrally selective tint that blocks visible and near-infrared lighting, responsible for the most significant portion of heat radiation.

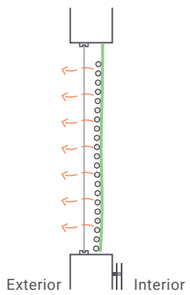

Figure 4.3: Summer - night
The curtain should be rotated during sunset to discharge the stored heat toward the outdoors for optimal operation. The window or ventilation grill should be open to release the stored heat outdoors. The direction where most heat is discharged is controlled by an insulation layer on one side of the PCM.

Individual PCM encapsulations can be removed from the curtain and rinsed with cold water to speed up solidification during warm nights.

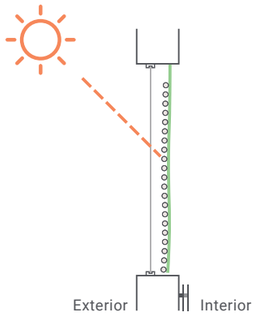

Figure 4.4: Winter - sunny day
During sunny winter days, the PCM should face the exterior to absorb solar radiation. Therefore, the tint on the PCM encapsulation must transmit enough solar radiation to melt the entire PCM volume but not to the degree of risking overheating. In addition, the layer should allow some solar radiation and visible light through for additional heat gain and visual comfort.

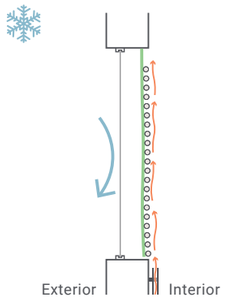

Figure 4.5: Winter - night
The PCM should face the room during nighttime to discharge the heat toward the room. The trapped air between the glazing and curtain will also help reduce heat loss.

Individual PCM encapsulations can be removed and used as heating elements to warm the bed or pillow.

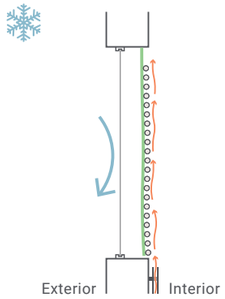

Figure 4.6: Winter - booster mode
When it is overcast, and the solar radiation is not intense enough to melt the PCM, or during freezing times, a typical window radiator commonly found in older Dutch dwellings can be turned on to melt the PCM. The PCM should face the room for maximum efficiency. For cost-effective operation, the radiator can be switched on to melt the PCM when the energy prices are lower at night.

5. PRODUCT DESIGN

Ecapsulation development

Figure 5.1:
Left: sequin fabric. Middle: Ariel detergent pods. Right: 3D printed fabric.
(Source: istockphoto.com : ari-elarabia.com/en : geeetech.com/blog/2018/02/3d-printing-on-fabric-is-easier-than-you-think/)

The design process of the encapsulation started with investigating how liquids can be contained in smaller pouches or shells and potential ways to attach the encapsulation to a curtain. The primary inspiration sources were the sequin fabric pattern, Ariel detergent pods, and 3D printing on fabric, see Figure 5.1. Next, 32 design iterations were generated in Rhinoceros 7 based on sequin fabric and ariel pods. The size of the encapsulations is in the range of 30x30x10 to 50x50x10 mm. See Figure 5.2 for some of the design options investigated.

3D-printing

Rapid prototyping in the form of 3D printing is a great tool used in this project to quickly find out how the encapsulations look in real life without the need to manufacture expensive molds applicable for large-scale manufacturing. Furthermore, the 3D-printed encapsulations were attached to a textile to determine the most suitable options, see Figure 5.3.

The 3D-printed encapsulation also revealed that they make much noise when clanking into each other. The encapsulations hung from a rope are much more prone to clanking compared to the encapsulation directly mounted on a button, which also has a more neat and integrated look. Although, this design option has a significant volume tradeoff to accommodate for the button, and after multiple mounting and demounting, the button started sagging. Therefore, the buttons need to be attached to the textile to maintain tension and reduce the risk of slacking over time.

In addition, an essential factor noticed when mounting the shell onto the textile is that the surface roughness dramatically impacts how well the encapsulation sticks to the textile. The 3D printed models, which had a rougher surface finish, stuck much better to the textile than those with a smoother surface finish. This can significantly affect the functionality and mitigate the risk of encapsulations falling to the floor and cracking.

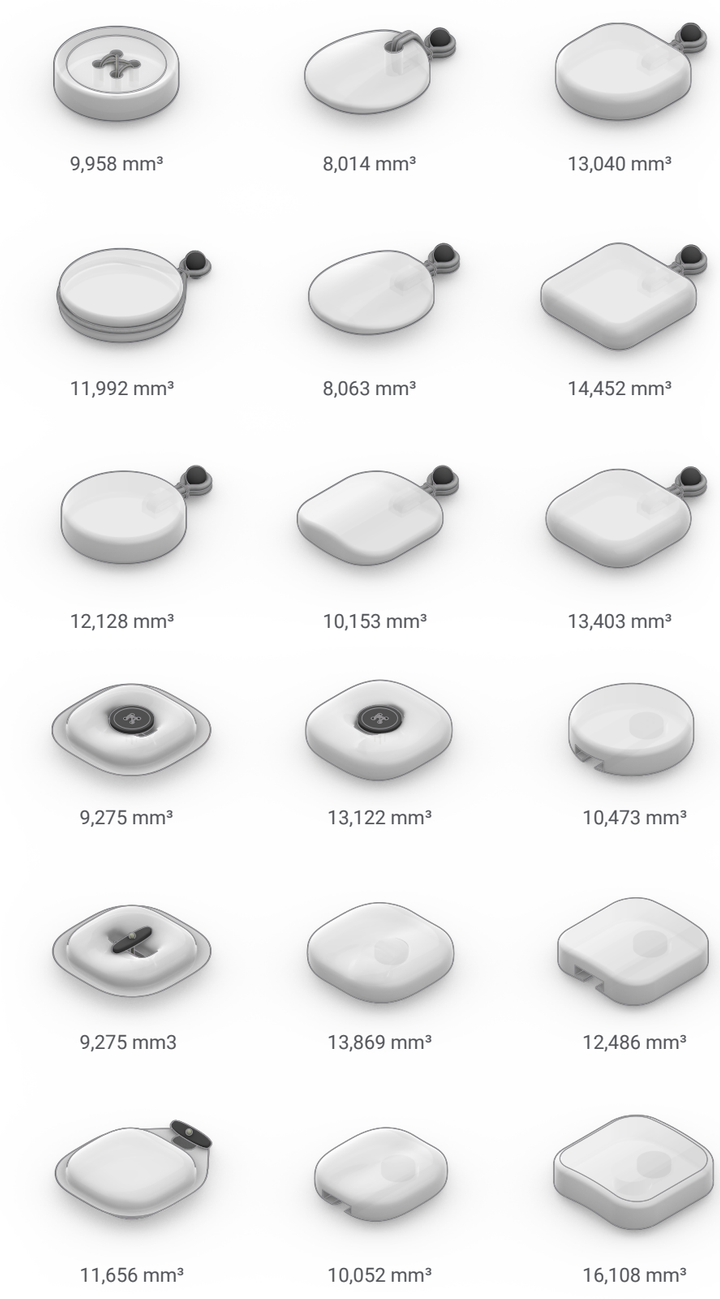

Figure 5.2:
Different encapsulation forms.

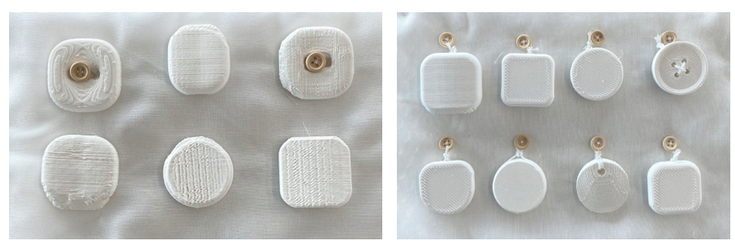

Figure 5.3:
3D printed encapsulations mounted to textile.

Manufacturing

The processing method for the encapsulation needs to be suitable for polymers that are 3D shaped. The tolerances need to be small to ensure the form is consistent and fits the mounting system. In addition, the section thickness should be minimal to allow for more PCM volume per encapsulation and reduce the excessive use of plastics. According to Granta EduPack, (2022), the primary shaping processes that are suitable for 3D shapes in large quantities and work with PET, PMMA, PC, and LLDPE are extrusion blow molding, injection blow molding, and injection molding. See Table 5.1 for a comparison between the three processing methods.

Table 5.1: Comparison between injection molding, injection blow molding, and extrusion blow molding as a primary processing method for the PCM encapsulation. (Source: Author : Granta Edupack, 2023)

Polymer processing			
Property	**Injection molding**	**Injection blow molding**	**Extrusion blow molding**
Processing	Primary, discrete, hollow 3D	Primary, discrete, hollow 3D	Primary, discrete, hollow 3D
Mass range (kg)	0.01 - 25.00	0.001 - 0.250	0.25 - 3.00
Section thickness (mm)	0.4 - 6.3	0.4 - 3.0	0.4 - 6.4
Tolerance (mm)	0.1 - 1.0	0.25 - 1.00	0.25 - 1.00
Economic batch size (units)	10,000 - 1,000,000	100,000 - 10,000,000	10,000 - 1,000,000
Production rate (units/hr)	60 - 3,000 3,210 - 80,300	100 - 2500 4,820 - 16,100	10 - 250 1,610 - 4,820
Tooling cost (EUR)	Extremely varied, containers, knobs, tool handles, housings.	Bottles and containers usually smaller than 0.5L	Small to large bottles and containers.
Typical use			

After a brief discussion with Dr. ir. Fred Veer from TU Delft, Injection molding is the most suitable option to manufacture the shell on a large scale given the complex geometry around the mounting. To manufacture the shell using injection molding, the shape needs to be produced in two separate parts, which can then be sealed together using heat (hot plate or hot gas) or adhesives. Once the seam has cured, secondary machining will be needed to remove excess material from the seam to improve the surface quality. The encapsulation can then be filled with liquid PCM through a small hole in the top. The hole is then plugged and heat-sealed. (Granta Edupack, 2022)

Curtain design and PCM distribution

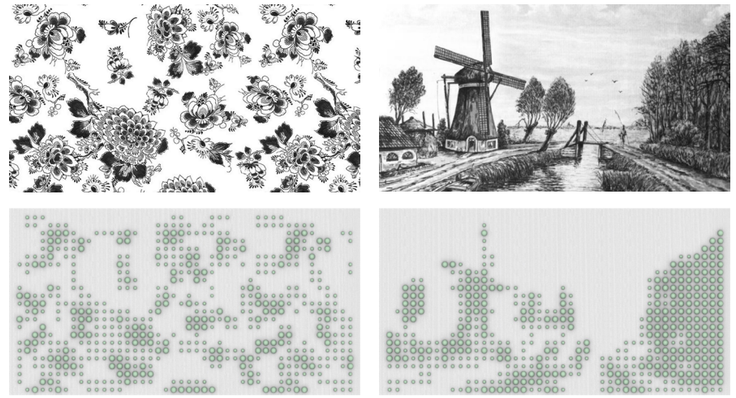

Figure 5.4: Pattern generated in grashopper. Left: Image sampler component of Delfts Bleau floral pattern. Right: Image sampler component of Dutch windmill and canal. (Source: Shutterstock ID:1749513746 : https://www.hollandwinkel.nl/en/postcard-delft-blue-windmill-landscape.html)

The original plan was to utilize both computationally generated and famous artwork-derived patterns to distribute the encapsulations, as shown in Figure 5.4. These patterns were evaluated based on their folding efficiency, and the findings revealed that a pattern that allowed for tight folding without encapsulations colliding was necessary. Therefore, real curtains were studied to identify potential areas where PCM could be applied. The analysis indicated that encapsulations could be added to the lower half of the curtains because of the more distinct turns/folds in that area. It is important to note that adequate space is required between encapsulations for the curtain to fold properly, and the encapsulations should be vertically aligned.

To determine the optimal number of encapsulations and the most suitable scale, various iterations were generated in Grasshopper and Rhinoceros 7. The results revealed that smaller encapsulations (30x30x10) have a more cohesive appearance and natural folding, whereas larger encapsulations (50x50x10) appeared bulky and did not blend well with the curtain, see Figure 5.5. This difference may also be attributed to the number of encapsulations implemented. When using smaller shells, a larger quantity is necessary to have a significant thermal impact.

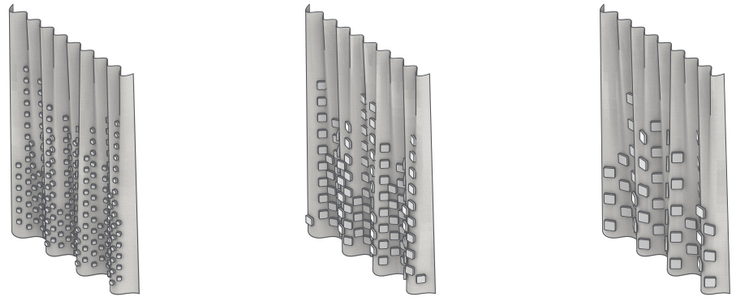

Figure 5.5: Comparison between different encapsulation sizes and how it affect the aesthetics and PCM volume.

30 x 30 x 10 mm
Amount: 228 shells
Volume: 0.86 liter
Coverage: 6.7 %

40 x 40 x 10 mm
Amount: 111 shells
Volume: 1.75 liter
Coverage: 13.5 %

50 x 50 x 10 mm
Amount: 49 shells
Volume: 1.21 liter
Coverage: 9.4 %

To test the viability of the design, a small section of the curtain was constructed in real life using a light-filtering (118 g/m²) 100% PET polyester curtain from IKEA with the product name Hilja. An Insulation layer was sandwiched in between two light-filtering textile layers. However, the results (Figure 5.6, left) were not in line with the computer simulations. The first thing noticed was that encapsulations smaller than 40x40x10 mm are much smaller than what appears in Rhinoceros 7, ultimately rendering them impractical. Secondly, insulation placed only behind the PCM encapsulations significantly affected light transmittance, resulting in a sharp contrast between insulated and uninsulated areas. Further testing was done with different insulation materials, such as polyester insulation (bat, loose stuffing, and sheets) and low-density polyethylene bubble wrap. After analyzing the results, it was concluded that a polyester bat (100 g/m2) is the most suitable option due to its even thickness distribution, cushioning characteristics, and ability to transmit adequate light up to 15 mm thickness.

Figure 5.6:
Left: Physical model of the first design iteration. Right: Physical model of the updated design with ribbons.

With the knowledge gained from previous design studies and insights into the appropriate insulation material, a new design iteration was created as seen in Figure 5.7. The updated design included vertical ribbons with a gap of 2 cm between them, allowing for larger volumes of PCM to be implemented cohesively and functionally, as shown in Figure 5.6 (right). However, it was noted that the gap between ribbons without insulation was quite distinguishable, resulting in a sharp contrast.

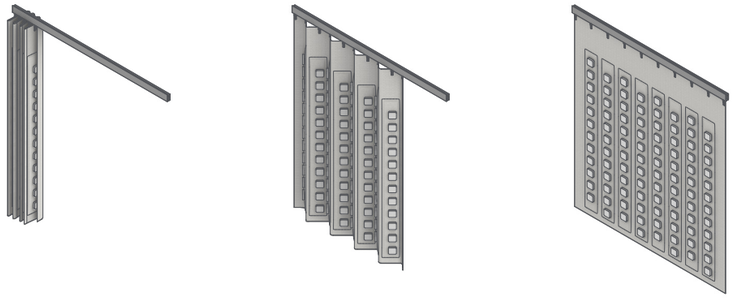

Figure 5.7:
Illustration of how PCM and insulation can dictate the folding pattern of the curtain.

40 x 40 x 10 mm
Amount: 96 shells
Volume: 1.52 liter
Coverage: 11.7 %

A refined design iteration was generated featuring a continuous layer of 10 mm thick insulation across the whole curtain area. The layers are held together by seams every 150 mm, enabling the curtain to fold predictably. This design allows for a more evenly distributed light transmittance and is easier and faster manufacturing. In addition, this design option offers much freedom in the layout of the encapsulations, as shown in Figure 5.8. The most suitable encapsulation size for this design option is 45x45x10 mm, and the maximum amount that could fit is 126 shells per m² without compromising user functionality and folding.

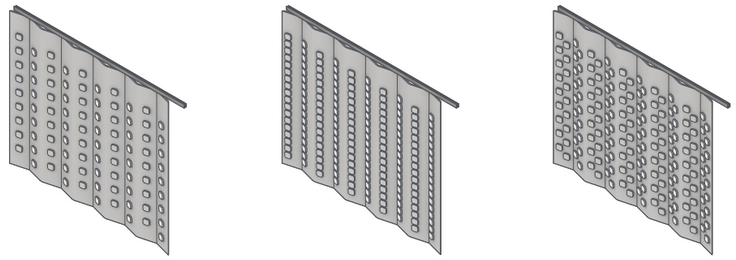

Figure 5.8:
PCM layout options of the refined curtain design featuring a continuous insulation layer.

45 x 45 x 10 mm
Amount: 90 shells
Volume: 1.72 liter
Coverage: 9.6 %

45 x 45 x 10 mm
Amount: 180 shells
Volume: 3.45 liter
Coverage: 19.2 %

45 x 45 x 10 mm
Amount: 180 shells
Volume: 3.45 liter
Coverage: 19.2 %

This design was simulated in MATLAB to get an insight into the system's thermal performance. The results indicated a critical design flaw that neglected the use of winter solar radiation to heat the room. The curtain's current design only enables the winter solar radiation to heat the PCM, while the insulative layer blocks the rest of the solar radiation. This effect causes a dramatic increase in heating energy needed in the winter compared to a simulation without the curtain. The solution would be to mount the PCM encapsulation on a sheer/voile textile with high transmittance and have a separate insulative curtain with highly reflective aluminum fabric that can move to the side when solar radiation is needed.

Manufacturing

Polyester fibers (PET) can be manufactured from recycled plastic bottles or by blending petroleum-based ethylene glycol with terephthalic acid in high pressure and heat. The mix turns into a honey-like consistency, which is then extruded through tiny holes to form long threads. The threads can be woven into textiles of different densities. Other fibers, such as linen or cotton, can also be mixed into the weaving process to change the feel and quality of the textile. Depending on additives and the shape, quality, and diameter of the hole, the strength and durability of the fiber can be altered. (Council of Fashion Designers of America, 2016)

To manufacture polyester insulation, virgin or recycled polyester fibers are sent through a carding machine that aligns the fibers into a nonwoven web-like structure. The fibers are then bonded together either through mechan-

ical needle punching (interlocking fibers), thermal (melting together), or chemical (adhesive) to create a batt. The batt can then be cut into desired shapes and sizes. (Whewell & Abrahart, 2022) The insulation is then sandwiched between two polyester textile layers and sewn with straight lockstitch seams.

PET buttons can be processed using injection molding and secondary machining for a smooth and consistent result. (Granta Edupack, 2022) Buttons can then rapidly be attached to textiles using button sewing machines in a secure lockstitch pattern. The tension of the thread to which the button is attached to can be customized to suit the material, thread, and design intention. (Apparel Resources, 2012) For instance, the thread tension should be tight so the encapsulation does not start sagging after a while.

Suspension system

A thorough analysis of different tracking designs was investigated to find the most suitable option for a track that allows the curtain to change which side faces indoors/outdoors depending on the time of the day. In addition, the solution must be simple, durable, and easy to install. The closed-loop track design concept was established early in the process. The track's section profile is inspired by IKEA's Vidga tracking system but with a more robust profile to handle heavier loads and an additional flange on one side to block airflow, as seen in figure 5.9. In addition, the track profile allows mounting brackets to be attached to the window header without interfering with the sliding system.

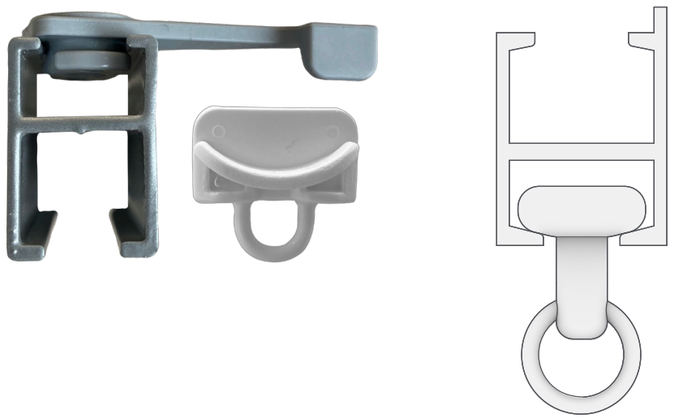

Figure 5.9:
Left: Vidga curtain track and gilder from IKEA. Right: Robust redesign of Vidga curtain system.

Several mounting brackets and track connectors were 3D printed and tested to see if they worked as intended, as shown in Figure 5.10. The results emphasized the importance of accounting for manufacturing tolerances, as the initial versions did not fit into each other. However, after allowing for a tolerance of 0.5 mm on each side, the bracket functioned perfectly. It was observed that the smaller the design tolerances, lead to a more difficult assembly.

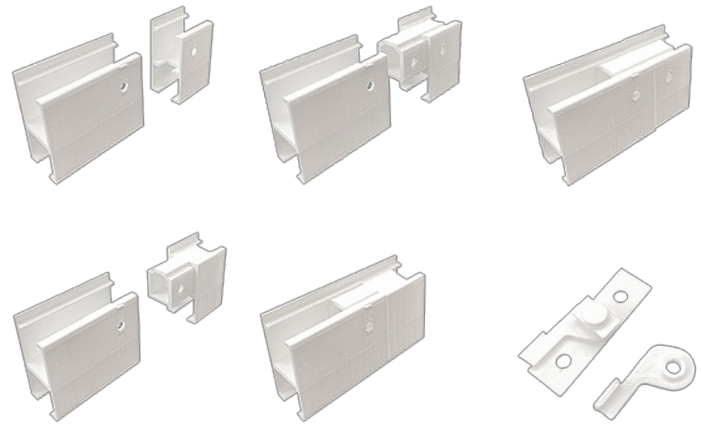

Figure 5.10:
3D printed mounting brackets and track connectors.

The glider's design is inspired by the Vidga gliders from IKEA, as shown in Figure 5.9. The Vidga glider is designed to slide smoothly even if the pulling angle changes, which is essential to consider for a good user experience. For this curtain system, the glider is refined to enable smooth pulling from any direction without the risk of getting stuck. The design has been 3D printed and tested to verify that it functioned as intended, as demonstrated in Figure 5.11, which displays how the various components in the suspension system relate.

Figure 5.11:
Model photo showcasing how the suspension system is assembled.

Manufacturing

According to an analysis in Granta Edupack (2022), hot metal extrusion is the most suitable primary processing method for the track and connector, based on a non-circular prismatic and continuous production. Hot metal extrusion can process section thicknesses of 1 - 100 mm with a 0.5 - 2 mm tolerance. Two suitable alloys for this processing method are aluminum 6463 (T4) and stainless steel AISI 409 (ferritic). The track can be bent with minimal section distortion to form the curve using a profile bending machine. (Borisbang Industrial Technology, 2023)

The mounting bracket and glider are both solid 3D shapes suitable for casting. After considering the mass range, section thickness, tolerance, economic batch size (over 100,000), and production rate, the high-pressure die-casting method is the most suitable option. A secondary machining process will be necessary to drill the hole for the screw. Aluminum 413.0 and ferritic stainless steel ASTM CB-30 are appropriate alloys for this type of processing. (Granta Edupack, 2022)

The pleating hook can be processed using wire drawing equipment and bent into its final shape. However, the alloy needs to be ductile for this process to work. Therefore, aluminum 6463 (T4) or stainless steel AISI 409 (ferritic) suit this component. (Granta Edupack, 2022)

Alloy selection
To determine the alloy for the suspension system, the weight and embodied energy are estimated using a window that is 2750 mm wide. Based on standardized track lengths of 1000, 500, and 250 plus a curve radius of 80 mm, the best fit for this window width is a total track length of 5572 mm. The weight of the mounting bracket, track connectors, gliders, hooks, and screws must also be considered. Given the material properties in Table 3.3, the system's weight is 2.43 kg (aluminum) and 6.66 kg (stainless steel). See Table 5.2 for all the components needed for this system and their respective weight and estimated embodied energy. Parts of the Eco Audit report from Granta Edupack (2022) can be found in Appendix C.

Weight suspension system

Item	Quantity	Volume m³	Aluminum Total weight (kg)	Steel Total weight (kg)
Track				
- 1000 mm	4	1.383e-4	1.493 (6463, T4)	4.259 (AISI 409)
- 500 mm	2	6.903e-5	0.372 (6463, T4)	1.063 (AISI 409)
- Curve	2	3.086e-5	0.167 (6463, T4)	0.475 (AISI 409)
			2.03	5.80
Connector	8	3.832e-6	0.083 (6463, T4)	0.236 (AISI 409)
Mounting bracket	18	8.251e-7	0.039 (413.0)	0.111 (CB-30)
Glider	40	1.085e-6	0.115 (413.0)	0.325 (CB-30)
Hanger	40	9.1e-7	0.098 (6463, T4)	0.280 (AISI 409)
Screws & bolts				
- 60x5 Sencys	18		0.136	0.136
- M3 bolts	16		0.015	0.015
			2.43 kg	6.66 kg
Embodied energy (First life)			293 MJ (21.2 kg CO_2)	195 (17.9 kg CO_2)
Recycling			-202 MJ (-14.1 kg CO_2)	-90.7 MJ (-9.85 kg CO_2)
			91 MJ (7.1 kg CO_2)	104.3 MJ (8.05 kg CO_2)

Table 5.2: Weight and embodied energy of the suspension system based on alloy. (Data from Granta Edupack, 2022)

Conclusion: Product Design

Based on the results of the encapsulation testing, a hard shell is suitable and can be installed in a functional and visually appealing way. As a result, the encapsulations will be made using PET, which is less brittle and prone to cracking than PMMA and PC. Injection molding will be used to form two separate shells that can then be heat-sealed together. The PCM is added through a small hole at the top which can be plugged and heat-sealed. The textile, insulation, and buttons are made of PET material for easy recycling.

To achieve a consistent and compact folding pattern, it is best to stack the encapsulations vertically in a ribbon-like fashion. The ideal size for each encapsulation is around 45x45x10 mm, as it allows for effortless folding and ample storage space. The number of encapsulations and overall storage capacity per curtain will vary depending on the configuration. However, the maximum amount of shells for a 1500 mm wide curtain should be at most 126 per m². In the case of a larger window, multiple curtains may be necessary, resulting in an increased overall storage capacity.

Aluminum has been chosen for the suspension system due to its strong yet lightweight properties and recyclability. The track and connector will be hot metal extruded using wrought alloy 6463 (T4), with a minimum section thickness of 1 mm and a tolerance of 0.5 mm. High-pressure die casting with alloy 413.0 will be used for the glider and mounting bracket, and a tolerance of 0.15 - 0.5 mm can be expected. Lastly, the pleating hook will be produced using a wire drawing machine.

6. DESIGN PROPOSAL

The encapsulations are made with UV-stabilized PET to prevent yellowing and photodegradation caused by solar exposure. Additionally, spectrally selective pigment is implemented to reflect and absorb some of the near-infrared solar radiation and reduce the risk of overheating the SP24E salt hydrate. The pigment simultaneously allows visible light to pass through to brighten up the room but also enables the occupant to observe the melting/solidification process of the PCM. The encapsulation is 45 mm high, 45 mm wide, and 10 mm thick and has a material thickness of 0.5 mm and a storage capacity of 15,455 mm³. (Figure 6.1) It is hung to a sheer curtain using a button, and six protrusions help it stay firmly in place. The sheer curtain allows daylight and solar energy to enter the room.

Additionally, an insulative curtain contains 10mm of polyester insulation and a reflective aluminum layer to reduce heat loss in the winter and solar gain in the summer. (Figure 6.2) The curtains are suspended on a continuous track, and multiple curtain pairs may be required depending on the window width. The track comes in 1000, 500, and 250mm lengths and can be connected via an adapter and two screws.

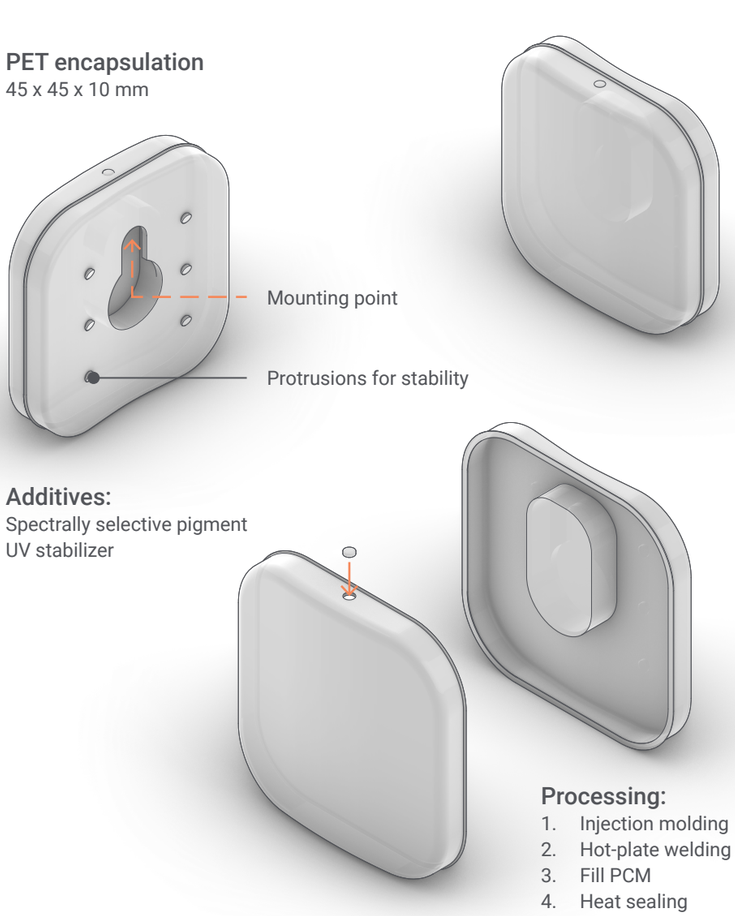

Figure 6.1:
Visual representation of the encapsulation from different angles as well as an exploded view.

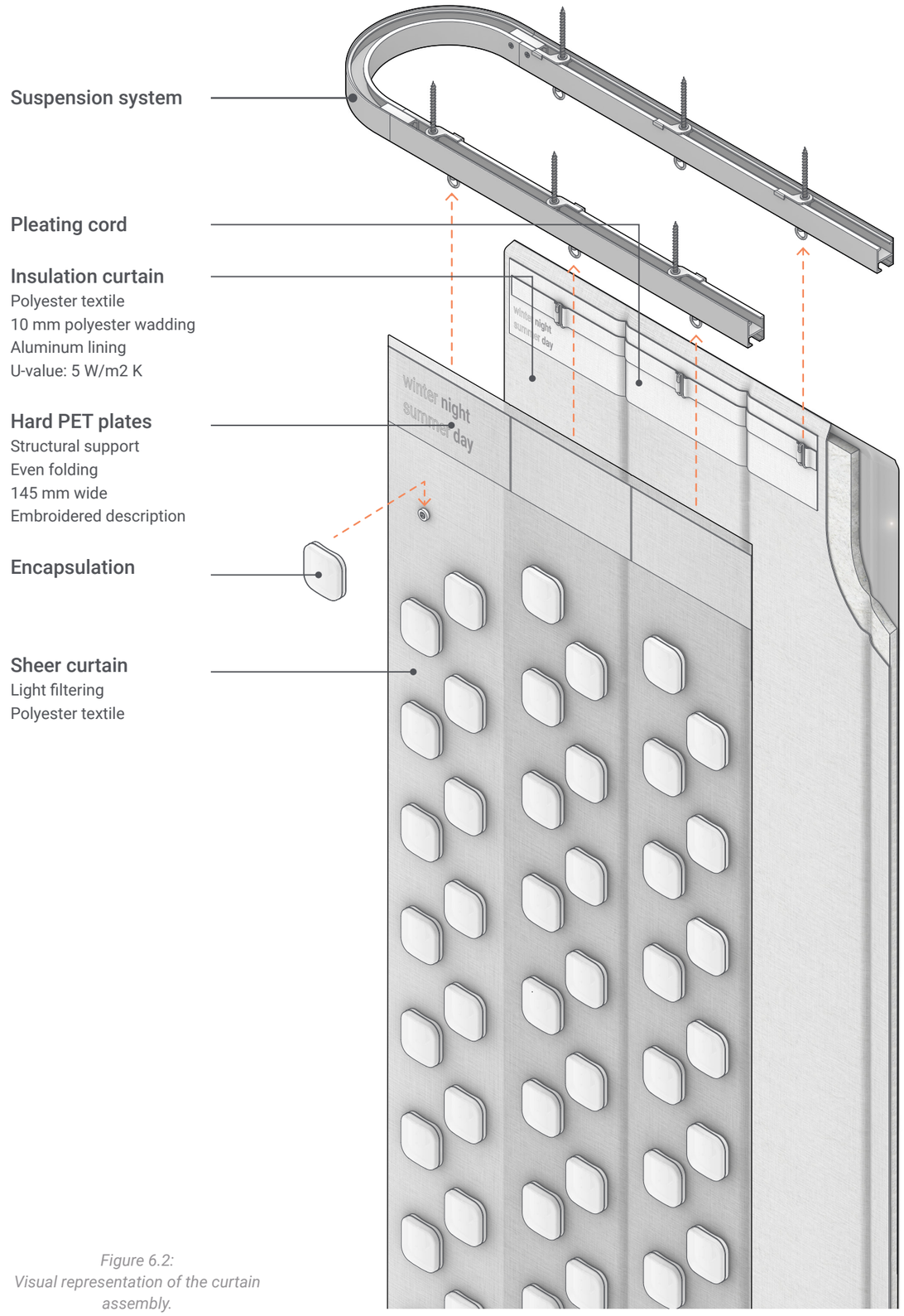

Figure 6.2:
Visual representation of the curtain assembly.

The curtain is available in a width of 1500 mm and comes in three different product variants: basic, standard, and premium. It has two options for PCM volume: 0.97 and 1.95 liter/m², see Figure 6.3 - 6.6. The difference between the product variants is the level of automation. The basic variant is manually operated, the standard variant has a remotely controlled DC motor, and the premium version has an automatic motorized system that tracks the weather. Using the insulative curtain in conjunction with the PCM curtain can enhance the annual thermal performance and visual comfort.

63 encapsulation / m²

0.97 liter / m²

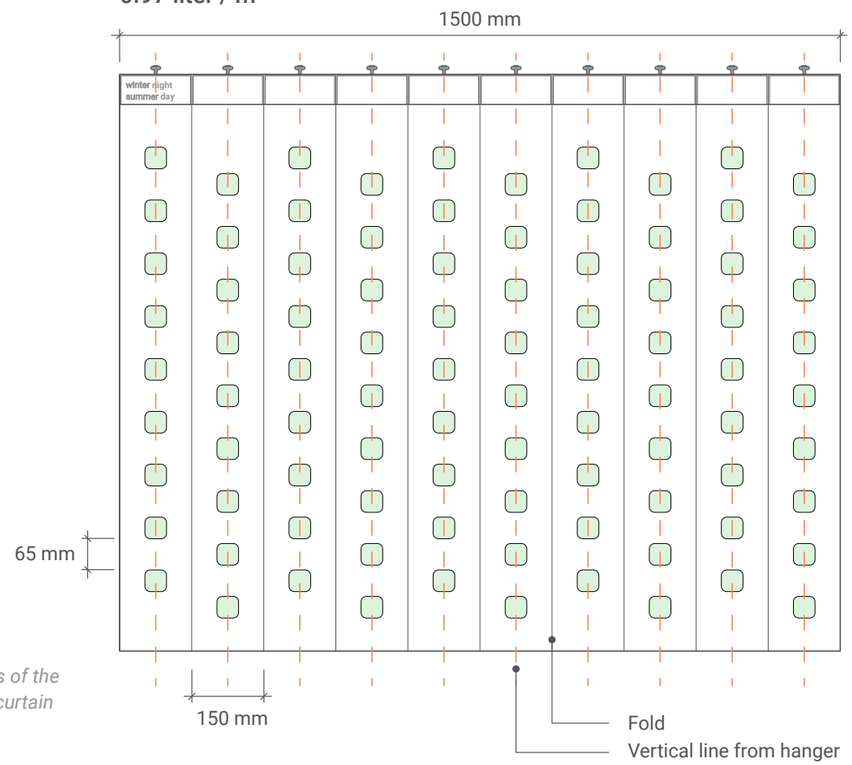

Figure 6.3:
Plan view with dimensions of the 0.97 liter of PCM per m² curtain option.

Figure 6.4:
Visualization of the 0.97 liter/m² option. The window is 2750x1630 mm, and the system holds 8 liters of PCM.

To ensure even folding and proper weight distribution of the PCM, the pleating system at the top of the curtain incorporates 140 mm wide structural PET plates. Consistent folding is also maintained throughout the curtain with the use of 140 mm long aluminum rods fitted into the hem at the bottom.

126 encapsulation / m²

1.95 liter / m²

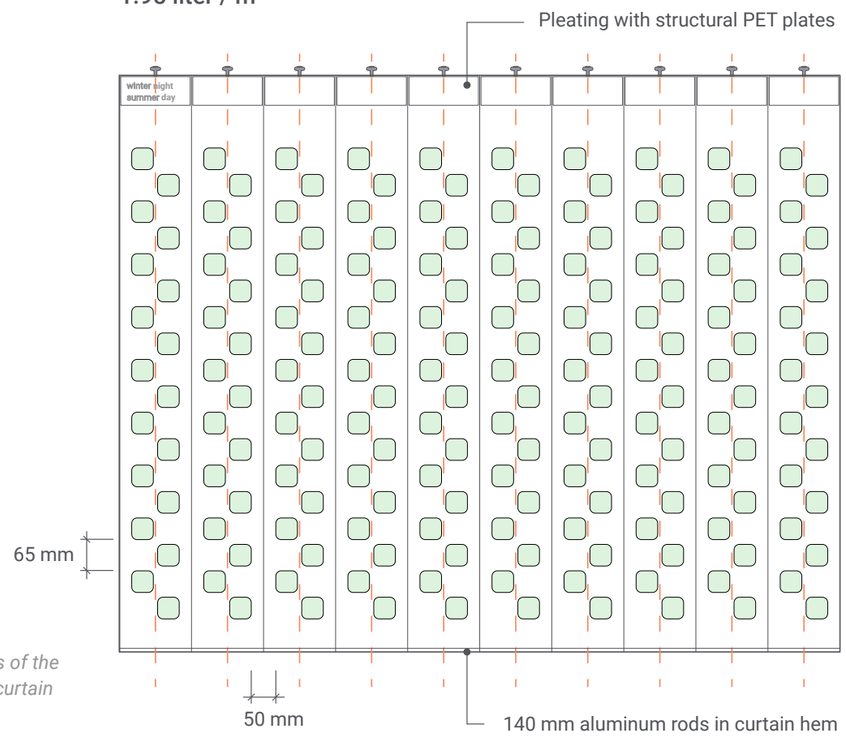

Figure 6.5:
Plan view with dimensions of the 1.95 liter of PCM per m² curtain option.

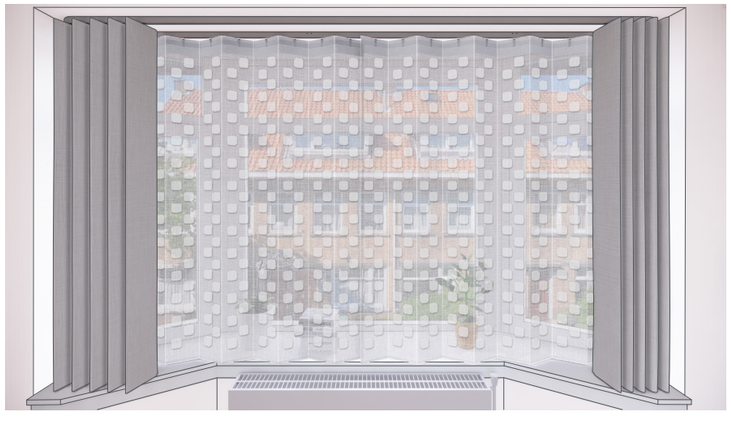

Figure 6.6:
Visualization of the 1.95 liter/m² option. This configuration holds 16 liters of PCM.

System operation

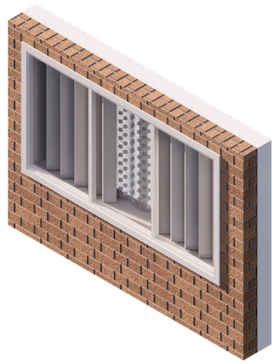

Figure 6.7: Daytime summer
PCM faces the room, and the insulation curtain is partially closed to reflect solar radiation but still lets a small amount of light through.

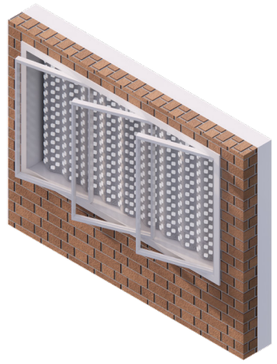

Figure 6.8: Nighttime summer
PCM faces the window (open) to discharge heat to the outdoors, and the insulation curtain is closed to darken the room.

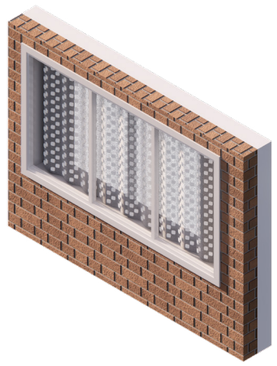

Figure 6.9: Daytime winter
PCM faces the window to absorb solar radiation and simultaneously transmit some solar radiation to the room. The insulation curtain is open.

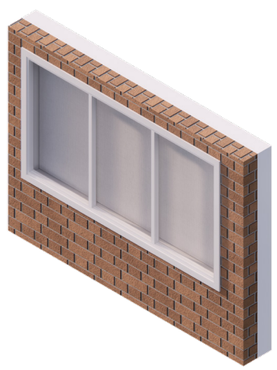

Figure 6.10: Nighttime winter
PCM faces the room, and the insulation curtain is closed to reduce heat loss.

User interface

On the top left corner, on both sides of each curtain, there is a description embroidered onto the fabric, indicating which side should face what direction. If the curtain is in the correct configuration, then the text in Figure 6.11 should face toward the room.

	Sheer (PCM) curtain:	Insulation curtain:
Facing room:	winter **night** summer **day**	**optional**
Facing window:	winter **day** summer **night**	winter **night** summer **day**

Figure 6.11:
Illustration of the embroidered text indicating if the curtain is in the correct position depending on the time of the day and season.

Suspension system

Track connector
Aluminum 6463, T4

Mounting bracket
Aluminum 413.0

Glider
Aluminum 413.0

Track screw
M3 x 10 mm
Stainless steel

Hanger
Aluminum 6463, T4

Bracket screw
60 x 5 mm universal
Stainless steel

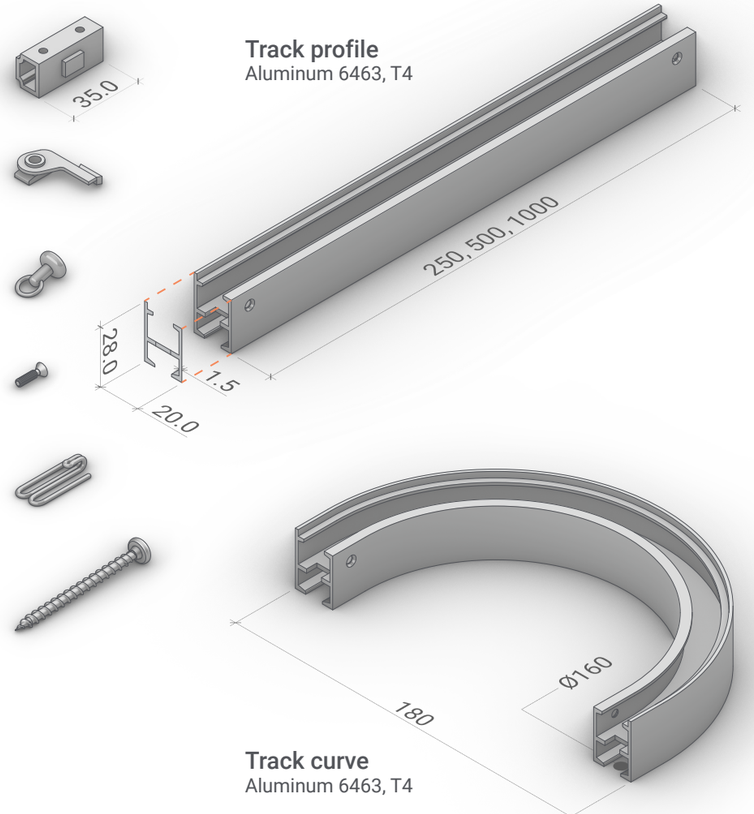

Figure 6.12:
Visualization of the components that make up the suspension system. Dimensions are in mm.

Assembly guide

Figure 6.13:
Insert a 60 x 5 mm screw into the mounting bracket and attach it to the window header.

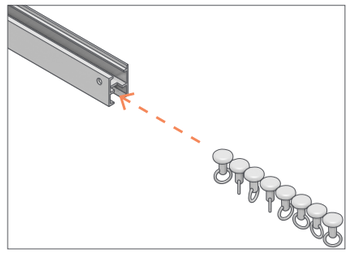

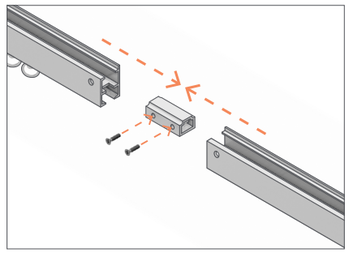

Figure 6.14 (left) & 6.15 (right):
Insert the gliders into the track and connect the track segments.

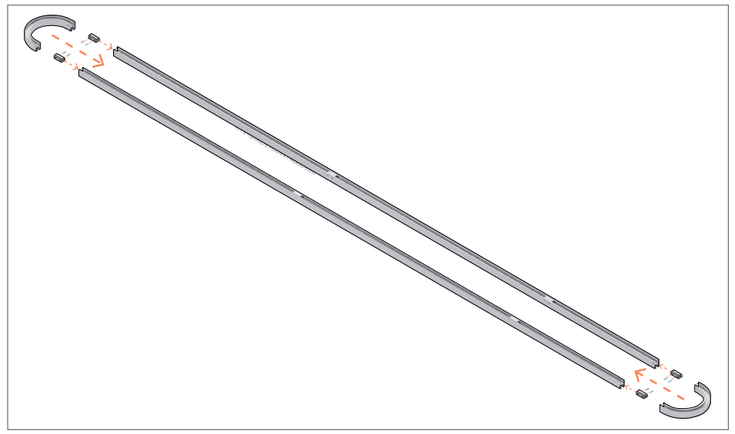

Figure 6.16:
Connect all track segments to complete the loop.

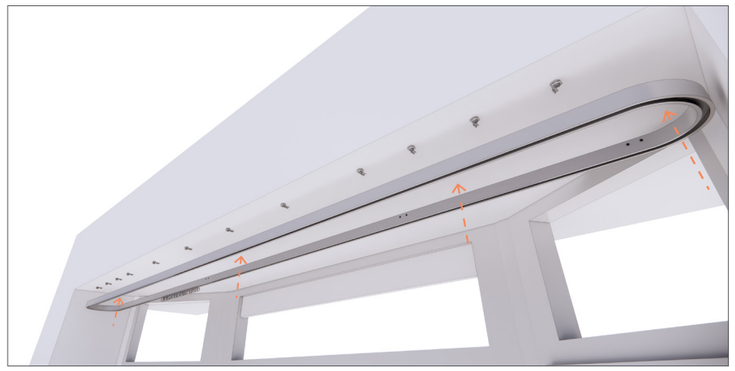

Figure 6.17:
Place the track onto the mounting brackets.

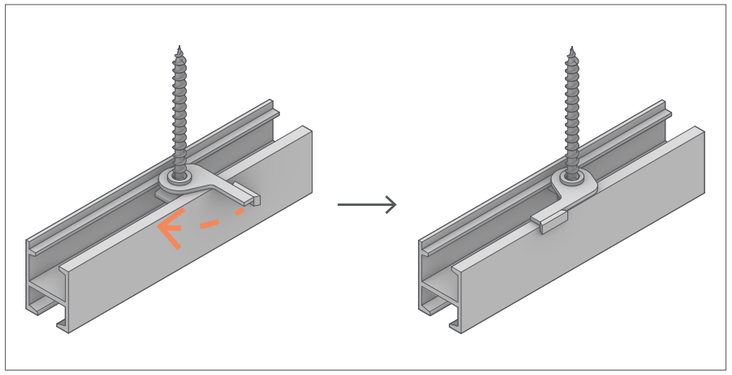

Figure 6.18:
Turn the lever on the mounting bracket counterclockwise to fasten the track and clockwise to release.

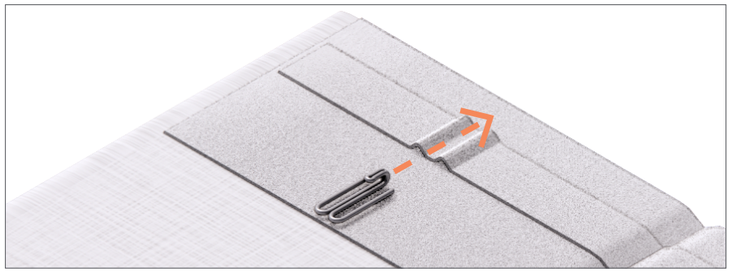

Figure 6.19:
Insert the hangers into the pleating holes.

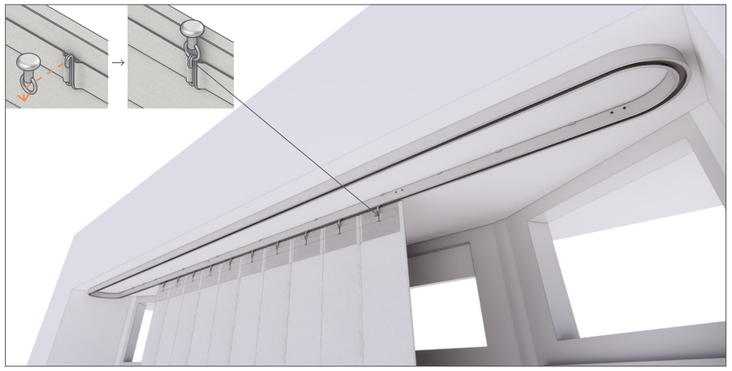

Figure 6.20:
Hang the curtain on the gliders. Make sure that the reflective aluminum lining faces outwards.

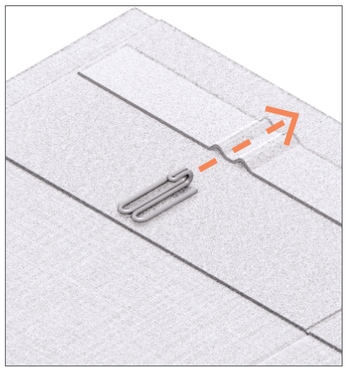

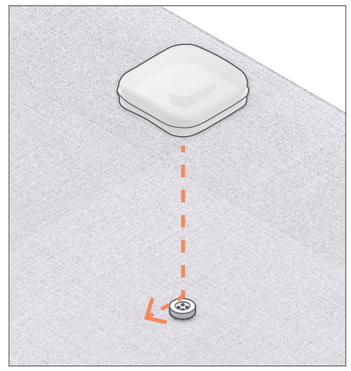

Figures 6.21 (left) & 6.22 (right):
Insert the hangers into the sheer curtain, turn it around, and attach the PCM encapsulations. Then hang the curtain to the gliders. PCM encapsulations must face outwards.

Recycling

The encapsulation will be manufactured from virgin-grade amorphous PET to guarantee it is mechanically strong and contaminant-free. All other components in the curtain system are made from recyclable material. However, to ensure that the curtain system will be recycled at the end of its service life, the whole system should be returned to the manufacturer for a money-back guarantee. The components can then be separated, cleaned, and sorted accordingly. Depending on the condition of the components, they can be reused or recycled at the factory or licensed partner. To simplify recycling, as few material types as possible are used.

PET

According to Weaveable (2020), PET is one of the world's most commonly used consumer plastic. It is readily recyclable through either mechanical or chemical processing. Mechanical processing is the most common method, consisting of cleaning the plastic from contaminants, shredding it, and hot forming it into chips under temperatures of 200 - 300 ^{O}C, which can then be spun into polyester fiber. However, hazardous substances such as volatile organic compounds and phthalates may be released into the air during the hot-forming process without proper measures. Also, polymers containing certain flame retardants should not be recycled in the regular feed due to their toxicity. Furthermore, given the large variety of additives leeched from plastic products during the process, recycled plastics' mechanical properties often differ from the virgin grade. Therefore, recyclates are usually mixed with a virgin-grade polymer to satisfy performance. (Hahladakis et al., 2018)

With that said, chemical processing is another option to recycle plastics by chemically breaking down the polymer structure into its original monomer state, indistinguishable from virgin grade. However, it is more costly and energy-intensive than mechanical processing, and not all plastics suit this process. (Hahladakis et al., 2018) Producing recycled polyester can save up to 59% of energy compared to virgin-grade polyester. (Weavabel, 2020)

Aluminum

Besides the strength-to-weight ratio, the benefit of using recycled aluminum alloy for the suspension system is the reduced embodied energy and CO2 footprint compared to virgin grade. According to Aluminum Association (2021), recycled aluminum can save up to 95% of energy compared to virgin grade. It is practically infinitely recyclable by re-melting and processing into a new product. Although, it is worth noticing that aluminum is listed on the EU assessment of critical raw materials report that was released in March 2023, meaning that it is essential to consider how the material is acquired, used, and disposed of at the end of its lifecycle. It is also a material that is fundamental to the transition to a circular economy. (European Commission, 2023)

Safety

Flame retardants are not used in the encapsulations due to their toxicity and recycling difficulty. Since the salt hydrate is not flammable, the curtain system does not possess a much greater fire hazard than a typical polyester curtain. However, it is essential to note that salt hydrate is corrosive and can cause damage or staining to furniture. To mitigate risks, the encapsulation has been designed with protrusions on its back to decrease the chances of accidental detachment. Additionally, the edges and corners have been smoothed to avoid unnecessary stress concentrations in case of a fall. In addition, PET has been selected as it can absorb impact energy and deform slightly during a reasonable fall before regaining its original form without cracking.

System weight

The total weight and embodied energy of the 8-liter PCM curtain variant are estimated to be 18.8 kg and 285 MJ (17.49 kg CO2) when implementing the system on a living room window in a typical Dutch intermediate terraced home, as seen in Figure 6.4. The width and height of the window is 2750 x 1630 mm. The material and manufacturing data gathered from the Eco Audit tool in Granta Edupack (2022) are shown in Table 6.1 and Appendix C. The weight and embodied energy of the 16-liter variant are estimated to be 30.5 kg and 389 MJ (22.9 kg CO2). As a reference, the carbon footprint to manufacture a pair of jeans is approximately 20 kg. (Eupedia, 2021)

8 liter curtain set

Item	Material	Quantity	Volume (m^3)	Total weight (kg)
Encapulation	PET	520	2.893e-6	2.020
PCM	SP24E	520	1.546e-5	12.000
Insulation	PET (polyester)	4.9 m^2	0.100 kg/m^2	0.490
Textile	PET (polyester)	9.8 m^2	0.118 kg/m^2	1.160
Button	PET	520	1.633e-7	0.114
Reflective lining	0.01% aluminum 99.9% PET	4.9 m^2	0.099 kg/m^2	0.484
				16.37 kg
Embodied energy (First life)				408 MJ (19.7 Kg CO_2)
Recycling				-214 MJ (-9.31 kg CO_2) (excl. PCM)
				194 MJ (10.39 kg CO_2)
Suspension system				+2.43 kg +91 MJ +(7.1 kg CO_2)
				18.80 kg 285 MJ (17.49 kg CO_2)

Table 6.1: Weight and embodied energy of the 8-liter PCM option. (Data from Granta Edupack, 2022)

Air gaps

Minimizing the air gaps between the curtain and wall at the bottom, sides, and top is essential to lower heat loss and solar gain. This requires ensuring that the curtain is the correct length to reduce the gap at the bottom. If the curtain is too long, it can affect its ability to fold smoothly. Air can escape at the top in two places - between the window header and track profile, and between the track profile and curtain (as shown in Figure 6.23). To address this, an additional flange has been added to the track profile to seal the gap. The polyester fabric is also extended and pushed against the track when the curtain is fully closed to seal the gap between the curtain and the track profile. Reducing the gap on the sides of the curtain is more challenging due to the unpredictability of user behavior. However, a primary strategy is to provide a wide enough curtain that covers the entire window opening. While the track will not extend all the way to the wall because space is needed for the curtain to turn around, an extra 75mm of curtain can extend beyond the track by hanging the curtain from the center between each fold, thus reducing the gap.

Flange is extended to be flush against window header.

Curtain is pushing against the track to seal the gap

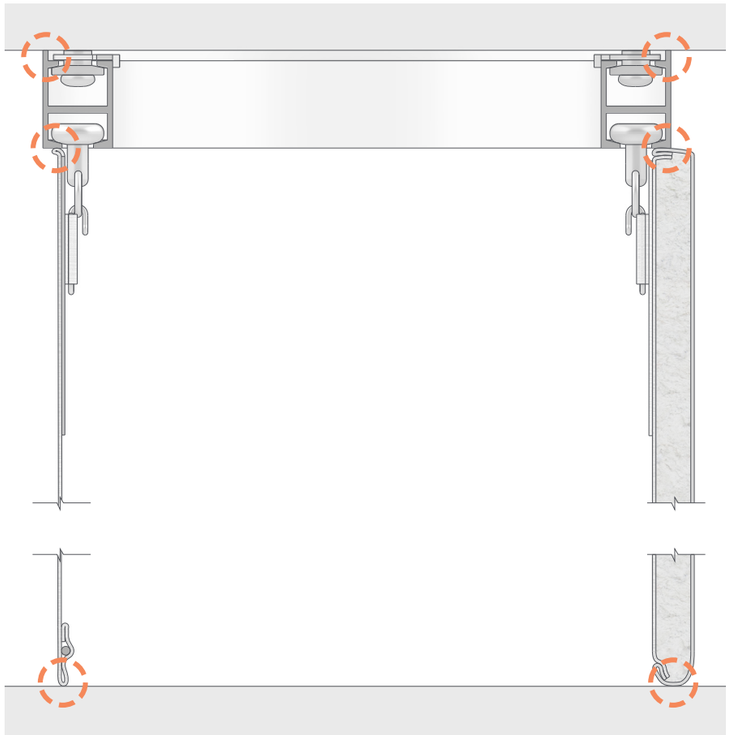

Curtain is long enough to touch the window sill but not long enough to cause extra friction when opening and closing.

Figure 6.23:
Section of the curtain system illustrating how the system addresses air gaps. Orange circles indicate weak spots.

Performance evaluation

The same living room (Figure 6.4) is used to perform a MATLAB simulation to estimate the effectiveness of the PCM curtain system. The MATLAB script is based on a rotatable PCM trombe wall with an insulation layer developed by Van Unen (2019). The living room is 28.8 m² large, and the floor-to-ceiling height is 2700 mm. As mentioned earlier, the window size is 2750 mm wide and 1630 mm high with a surface area of 4.48 m². The room is simulated in four orientations (north, east, south, and west) over a year. The construction is old and has not yet undergone renovation to be on par with today's energy standards. Therefore, the insulation value of the exterior facing walls is 1.7 m² K / W, and the U-value of the fenestration is 2.9 W / m² K. (NEN, 2022) The interior walls, ceiling, and floor are virtually adiabatic for a more accurate study. The large balcony window and door, shown in Figure 6.24, is simulated as a solid wall to give a more precise performance indicator of the PCM curtain.

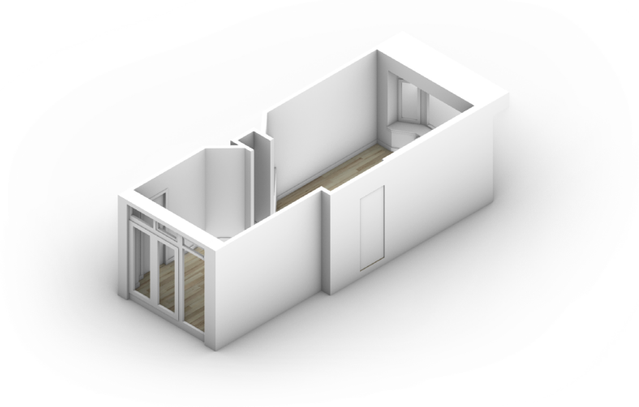

Figure 6.24:
3D model of the living room used for the simulations. The Bay window in the top right is where the PCM is positioned.

The curtain is positioned 80 mm from the window, with a 10 mm air gap underneath and above. Different scenarios were tested, including no curtain, insulation only, and 8 and 16 liters of PCM. The PCM faces the window without insulation applied between 8:00 - 20:00, while during the remaining hours, it faces the room with a 10 mm insulation layer applied. The simulation provides the total heating load in kWh and indoor temperature for a year, and the results are available in Table 6.2, Figure 6.25, and Figure 6.26. The MATLAB input values used in the simulation are given in Appendix D.

Simulation: Heating load

Configuration	North (kWh)	East (kWh)	South (kWh)	West (kWh)
Without curtain:	2583	2030	1971	1978
Curtain without PCM:	2355 (-228)	1868 (-162)	1820 (-151)	1843 (-135)
Curtain with 8 liter PCM:	2352 (-231)	1866 (-164)	1818 (-153)	1843 (-135)
Curtain with 16 liter PCM:	2349 (-234)	1863 (-167)	1813 (-158)	1838 (-140)

Table 6.2:
MATLAB simulation of heating loads in four different orientations and with different curtain configurations.

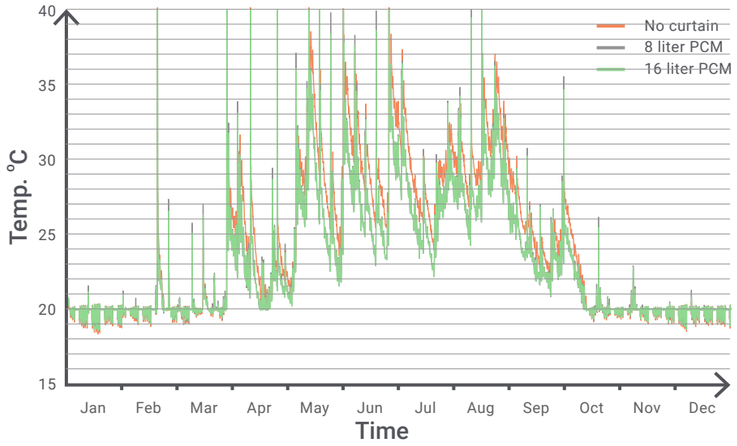

Figure 6.25:
Indoor temperature simulation when the window is facing south. The green color indicates 16 liters of PCM, grey indicates 8 liters, and orange is without any curtain. (derived from MATLAB)

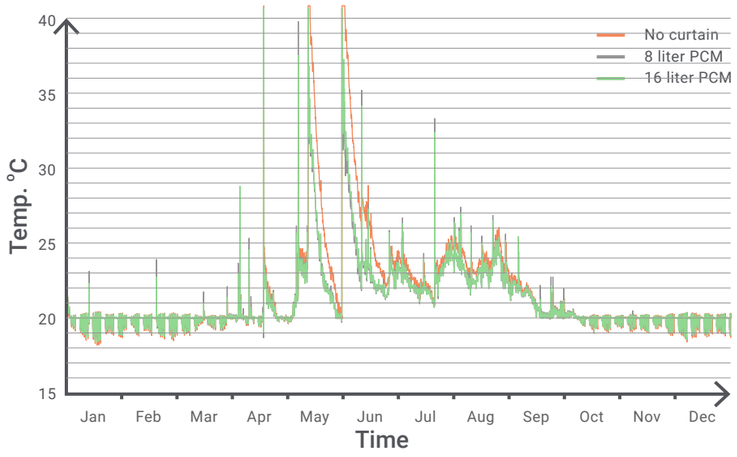

Figure 6.26:
Indoor temperature simulation when the window is facing north. The green color indicates 16 liters of PCM, grey indicates 8 liters, and orange is without any curtain. (derived from MATLAB)

Results

Based on the MATLAB simulation, the curtain system is most effective in saving energy when the window faces north, resulting in a reduction of 228 to 234 kWh annually or 9%, as shown in Table 6.2. Energievergelijk (2023) states on their website that the current price cap per m³ (10.55 kWh) of gas is €1.45 in the Netherlands, which would lead to a cost-saving potential of 31.33 - 32.16 Euro for the living room. However, it is essential to note that north-facing windows have higher heating loads than east, south, and west orientations. Therefore, the lowest heating load can be achieved when the window is oriented towards the south, which receives more solar radiation. By implementing a 16-liter PCM curtain on this orientation, the energy can be reduced by 151 - 158 kWh or 8.7% per year, saving 20.75 - 21.7 euros on the energy bill. The PCM account for 7 kWh of that energy saving. Conversely, the west-facing window shows the lowest effect of 140 kWh or 7%.

However, this data only considers heating loads, as most older Dutch dwellings do not have mechanical cooling. To estimate the cooling effect of the PCM throughout the year, refer to Figure 6.25 for a south-facing window and Figure 6.26 for a north-facing window. These graphs show that implementing PCM lowers average indoor temperatures during summer. It is essential to mention that the simulations were tested in a winter configuration without the insulative curtain blocking daytime solar heat gain.

Hand calculation comparison

The latent heat capacity of the SP24E salt hydrate is 180 kJ/kg. However, this energy is distributed over the 16 - 31 °C temperature range with a sharp solidification peak at 22 - 23 °C and melting peak at 24 °C, refer to Appendix A. The average indoor temperatures for a South-facing window fluctuate between 19-20 degrees Celsius from mid-October to the end of March, which is approximately 157 days, as shown in Figure 6.25. The SP24E can discharge around 9 kJ of heat in this temperature range. Therefore, the theoretical phase change potential of 16 liters (24 kg) PCM is estimated using equation 3:

$$Q = m \cdot \Delta h \qquad (3)$$

$$Q = 24 \cdot 9$$

$$Q = 216 \text{ kJ}$$

This equal 216 kJ / 3600 s = 60 Wh per heating cycle, and the theoretical heating effect of the PCM for the heating-dominated season is:

$$60 \text{ Wh} \cdot 157 = 9.42 \text{ kWh}$$

A Ladybug simulation was conducted to better comprehend the difference between the MATLAB simulation and the hand calculation to assess the solar radiation the PCM shells receive, illustrated in Figure 6.27. The 4.48 m2 exposure area consists of 1040 encapsulations which account for a coverage of 41%. The average exposure is estimated at around 85 kWh/m2. The total kWh that is striking the shells are, therefore:

$$0.41 \cdot 4.48 \cdot 85 = 156.1 \text{ kWh}$$

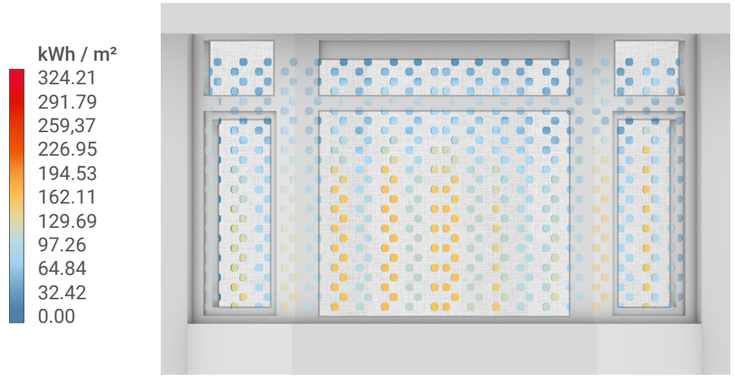

Figure 6.27:
Ladybug analysis of solar radiation (kWh/m2) that strikes the encapsulation between October to end of Mars.

Cost analysis

The cost of the curtain system is determined by the total expenses of material, tooling, energy, labor, administration, and transportation, divided by the number of units produced. This means rapidly producing large volumes leads to a lower cost per unit. Additionally, most of the curtain system's components are designed for easy processing, allowing for traditional and high-speed processing methods like injection molding, hot metal extrusion, and high-pressure die casting. Table 6.3 estimates the production cost for an 8-liter curtain system to be in the range of 156.31 - 212.95 EUR, with manufacturing costs including tooling and overhead. If upgrading to the 16-liter configuration would cost a total of approximately 272.10 - 378.92 EUR. The data is from the cost estimator in Granta Edupack (2022).

8 liter set cost estimation

Item	Quantity	Material (EUR / kg)	Manufacturing (EUR / unit)	Total Cost (EUR)
Track	5 m	1.71 - 1.97	0.9570	1.64 - 1.89
Connector	8	1.71 - 1.97	0.0670	0.92 - 1.06
Mounting bracket	18	1.73 - 2.04	0.2206	6.87 - 8.10
Glider	40	1.73 - 2.04	0.2396	16.58 - 19.56
Hanger	40	1.71 - 1.97	0.0014	0.10 - 0.11
Screws & bolts				*3
Encapsulation	520	0.614 - 1.08	0.1150	36.72 - 64.58
PCM	12 kg	3.31		39.72
Textile	1.160 kg	*1.12 - 1.46		1.30 - 1.69
Insulation	0.49 kg	**3.00		1.47
Button	520	0.614 - 1.08	0.0507	16.19 - 28.47
Reflective lining	0.484 kg	*1.12 - 1.46		0.54 - 0.71
				125.05 - 170.36
Assembly + Additional expenses (25%)				31.26 - 42.59
				156.31 - 212.95

*Material and manufacturing cost per kg
**Rough estimation based on market analysis

Table 6.3: Cost estimation of a curtain set containing 8 liter of PCM. Expected cost is approximately 156.31 - 212.95 EUR

Payback time

The estimated payback time for the 16-liter PCM system is 8.5 years on the north-facing side and 12.5 years on the south. For the 8-liter system, the payback time would be reduced to 5 and 7.5 years, respectively. Without PCM, the payback time would be 2.5 years on the north and 3.8 years on the south.

Discussion

It is important to note that the MATLAB simulation's reliability may be partially accurate, as it was designed based on a solid panel/trombe wall configuration and may not account for the distinct features of this curtain system. However, the results from the hand calculation were similar, indicating that the simulation provided a reasonable estimate of the heat load. The Ladybug simulation revealed that the upper portions of the curtain might not receive enough solar radiation to significantly contribute to the system's performance, which could explain some discrepancies between the simulation and hand calculation results. It is worth noting that the system's performance will depend heavily on user behavior and their understanding of thermodynamics. For example, the system's energy-saving benefits may be significantly reduced if the curtains are frequently left open as the trapped air between the window and curtain contribute to the insulation effect, which is noticeable in the simulation given that the insulation curtain itself has a poor U-value of 5 W/m² K. In addition, the spectrally selective pigment to prevent overheating will lead to a higher reflectance, reducing the melting performance during the winter.

While the SP24E and PET encapsulations are expensive and add complexity to the manufacturing process, they can still be utilized as a marketing tool to promote the use of PCM in building applications. The distinctive appearance of the mounted encapsulations and the ability to observe when the PCM changes phase sets this product apart from other curtains, which is a great selling point. The encapsulations are mobile and can be taken off the curtain and heated up by waste heat sources or brought along when road-tripping. It can add thermal mass to various applications, especially smaller rooms or spaces. Additionally, customers looking to purchase curtains to control shading may be interested in a product that can also improve thermal comfort.

7. CONCLUSION

This research aimed to tackle the high energy costs that old and inadequately insulated lightweight homes in the Netherlands suffer from. Which causing occupants to turn off the heating and live in discomfort. In addition, the research looks into potential methods to implement a passive energy storage system that is easy to install by the homeowner and does not require a building renovation. The main research question that addresses this issue is, therefore:

How can phase change material be incorporated into a cost-effective product to increase the thermal inertia of lightweight dwellings in a Cfb climate to enhance passive cooling and heating throughout the year?

An initial literature study and research gained valuable insights into critical considerations when designing a PCM system. These considerations include selecting a PCM with an appropriate melting temperature for the desired application, optimizing the encapsulation size for maximum efficiency, and determining the optimal location for implementation in a building in a Cfb climate zone. Additionally, the research provided a better understanding of solar radiation, including the specific wavelengths that can melt the PCM and those that can cause polymer photodegradation. Various stabilizing methods were also retained to ensure long-term durability and optimal performance.

The research resulted in a new curtain system using PCM technology, which contains two different types of curtains suspended on a continuous and adaptable looping track. The main curtain has high solar transmittance and is equipped with PCM macroencapsulations, while the secondary curtain has a 10 mm thick polyester insulation and a highly reflective aluminum lining. The curtains have a standard width of 1500mm but can be cut every 150 mm without affecting the system's operability. In addition, the looping tracking system allows the curtain to change which side faces what direction to optimize thermal performance throughout the year.

The PCM volume is encapsulated in 45x45x10 mm transparent PET shells that are UV stabilized and have spectrally selective tint and fire retardant additives. The shells are distributed in up to 126 units per m² curtain, which equals about 1.95 liters or 2.9 kg of Rubitherm SP24E salt hydrate. The encapsulation size and distribution are carefully balanced between storage capacity and attaining a tight folding profile.

The curtain system has several product options that allow for different storage capacities and levels of system automation. The basic option is entirely manual, while the standard option includes a remote controllable DC motor, and the premium version has a fully automated motor that tracks the weather. To reduce costs, the price of each material has been considered, and the system is manufactured on a large scale using techniques such as injection molding, hot metal extrusion, and high-pressure die casting. This results in a drastic reduction in the price per unit. Additionally, the homeowner can transport and install the system, which saves labor fees.

For a typical Dutch intermediate home with a living room window measuring 2750x1630 mm, an 8 or 16-liter PCM curtain can be implemented with an estimated manufacturing cost between 156-213 and 272-379 EUR, respectively. The carbon footprint of producing the 16-liter PCM curtain is estimated to be 22.9 kg of CO2, including end-of-life potential, which is equivalent to manufacturing a pair of jeans.

In order to assess the cost-effectiveness of a product, the annual energy consumption of a room must be reduced, and the payback time should be short. To test this, the 16-liter PCM configuration was simulated using MATLAB and Simulink in a 28.8 m² living room. The results showed that the system reduced annual heat load by 7-9%, depending on window orientation. However, the impact of the 16 liters of PCM was only 5-7 kWh, making the relevance of PCM questionable. The insulation layer had a more significant impact on reducing heat loss. It is worth noting that the peak phase change of the SP24E is sharp between 22-24 °C, which is higher than the average indoor temperature and heating setpoint of 20 °C in the winter. This suggests that the heating effect of the PCM is minimal. On the other hand, the MATLAB temperature simulation indicates that the PCM absorbs heat and buffers indoor temperatures in the summer when the insulation layer and the reflective aluminum lining is not applied during the daytime. Since most older dwellings do not have an active cooling system, it is difficult to determine how much energy saving the PCM would account for.

That said, indoor thermal comfort can be enhanced using the PCM curtain system without requiring expensive and extensive building interventions, substantial upfront investments, or installation costs. It runs without electricity, has no operational fees, and requires minimal maintenance other than changing which side faces what direction. Additionally, it is an aesthetically pleasing product that can add value and comfort to a room. The effect might not be as noticeable as a powerful heating system, but it can reduce the annual energy bill for one room by up to 32.16 euros based on the €1.45 per m³ gas price cap. The estimated payback time is 5 - 8.5 years, depending on PCM storage capacity. Although, less PCM volume leads to shorter payback time, without any PCM applied, it can be reduced to 2.5 years. Therefore, from a heat load reduction, the system is cost-effective.

Limitations

The simulations done through MATLAB have limitations as they do not account for the human factor, which includes variables like how often the curtain is switched, at what time of the day, and how often the insulation curtain is opened for daylight. Moreover, the occupant's attention to detail in minimizing the gap between the curtain and window side wall and opening the window during summer nights to release stored heat outside are essential factors. Additionally, the track profile is sold in standard lengths, making it difficult to fit all window widths correctly, leading to variable gap sizes for each window.

Furthermore, the simulations do not consider the reflective aluminum layer and assume that the insulation layer and sheer/PCM curtain are interdependent. Lastly, the simulations were carried out using only one type of PCM, which may not have been the best option to achieve optimal heat load reduction. The PCM and melting temperature are based on annual energy savings in an office building with more internal heat load than typical dwellings. As a result, there may be more suitable PCMs for this product and application than the chosen one.

Recommendations

To assess the design and functionality of this system, it would be beneficial to create a few prototypes, install monitoring devices, and observe how occupants use it. Then, based on the feedback received, adjustments can be made to better align the system's design with user behavior.

The gap between the curtain and the window side wall can potentially be reduced by implementing a flap on the curtain that can fold out and connect to the window wall. However, it is essential to conduct further research and testing to determine the feasibility of this design and whether the occupant would use this additional function frequently.

Further research is recommended to assess the effectiveness of the PCM encapsulation on the higher regions of curtains in terms of heating. Current simulations suggest that these encapsulations may not be necessary or have inadequate phase change temperatures. Relocating them to areas that receive more solar radiation could also be beneficial. Additionally, another type of PCM with a melting range below the heating setpoint should be simulated and tested to find out if the winter performance can be further improved.

The project has addressed the durability of the encapsulations and suspension system, but it is essential to consider the strength of the light-filtering curtain. Conducting physical tests to verify that the system can hold up to 24 kg of PCM will ensure it functions as intended. Additionally, further testing is needed to determine the durability and tension of the buttons, as it needs to be clarified how much wear and tear they can withstand before they start sagging.

8. BIBLIOGRAPHY

Aluminum Association. (2021) *Aluminum's Sustainability. Retrieved 6-5-2023, from https://www.aluminum.org/sustainability*

Aerogel Technologies, LLC. (2023). *Aerogel Insulation Blankets.* Retrieved 4-1-2023, from http://www.aerogeltechnologies.com/classic-aerogels/classic-aerogel-products/

Ahangaran, F., Navarchian, A. H., & Picchioni, F. (2019). Material encapsulation in poly(methyl methacrylate) shell: A review. *Journal of Applied Polymer Science, 136*(41), 48039. https://doi.org/10.1002/app.48039

Andrady, A. L., Hamid, S. H., Hu, X., & Torikai, A. (1998). Effects of increased solar ultraviolet radiation on materials. *Journal of Photochemistry and Photobiology B: Biology, 46*(1–3), 96–103. https://doi.org/10.1016/S1011-1344(98)00188-2

Apparel Resources. (2012, January 11). Button Sewing and Button Holing Technology Options. Https://Apparelresources.Com/. https://apparelresources.com/technology-news/manufacturing-tech/button-sewing-button-holing-technology-options-2/

AxioTherm. (2023). *HeatSel® – Energy Storage Solutions for water-based applications.* Retrieved 7-1-2023, from https://www.pcm-ral.org/pcm/en/members/axiotherm-gmbh/

Baetens, R., Jelle, B. P., & Gustavsen, A. (2010). Phase change materials for building applications: A state-of-the-art review. *Energy and Buildings, 42*(9), 1361–1368. https://doi.org/10.1016/j.enbuild.2010.03.026

Baggs, D., & Mortensen, N. (2006). Thermal Mass in Building Design. *Royal Australian Institute of Architects, Des 4*. https://www.jstor.org/stable/10.2307/26148285

BBSA. (2023). *Internal.* Retrieved 1-2-2023, from https://bbsa.org.uk/types-of-blinds-shutters/residential/internal/

Bland, A., Khzouz, M., Statheros, T., & Gkanas, E. (2017). PCMs for Residential Building Applications: A Short Review Focused on Disadvantages and Proposals for Future Development. *Buildings, 7*(3), 78. https://doi.org/10.3390/buildings7030078

Bluyssen, P. M. (2013). The Healthy Indoor Environment: How to Assess Occupants' Wellbeing in Buildings. *CRC Press LLC.* http://ebookcentral.proquest.com/lib/delft/detail.action?docID=1524232

Boca PCM. (2023). *PCM Panel: The art of stacking.* Retrieved 7-1-2023, from https://pcm-tes.com/pcm-panel/

Bonvoisin, J., Halstenberg, F., Buchert, T., & Stark, R. (2016). A systematic literature review on modular product design. *Journal of Engineering Design, 27*(7), 488–514. https://doi.org/10.1080/09544828.2016.1166482

Borisbang Industrial Technology. (2023). *Bending process.* Retrieved 3-5-2023, from https://www.angleroller.com/bending-process.html

Britannica Editors. (2022b). Wool | animal fibre. *Encyclopedia Britannica.* Retrieved 14-4-2023, from https://www.britannica.com/topic/wool

Britannica Editors. (2022). Slum. *Encyclopedia Britannica*. Retrieved 15-12-2022, from https://www.britannica.com/topic/slum

Britannica Editors. (2023a). Prism | Optics. *Encyclopedia Britannica. Retrieved 4-4-2023, from* https://www.britannica.com/technology/prism-optics

F. Bruno, M. Belusko, M Liu, N.H.S. Tay. (2015) 9 - Using solid-liquid phase change materials (PCMs) in thermal energy storage systems, *Energy, Advances in Thermal Energy Storage Systems.* Woodhead Publishing. (pp. 201-246). https://doi.org/10.1533/9781782420965.2.201.

Cabeza, L. F., Martorell, I., Miró, L., Fernández, A. I., & Barreneche, C. (2015). Introduction to thermal energy storage (TES) systems. *Advances in Thermal Energy Storage Systems, Elsevier,* 1–28. https://doi.org/10.1533/9781782420965.1

Cambridge Dictionary. (2023). Insulation. *Cambridge University Press & Assessment*. Retrieved 5-1-2023, from https://dictionary.cambridge.org/dictionary/english/insulation

Charles S. Whewell & Edward Noah Abrahart. (2022). Textile. *Encyclopedia Britannica.* Retrieved 14-4-2023, from https://www.britannica.com/topic/textile

Chimney Sheep Ltd. (2023). *Fine Wool Wadding – 75GSM.* Retrieved 15-4-2023, from https://www.chimneysheep.co.uk/product/fine-wool-wadding/

Climate Consultant 6.0. (2021). *Energy Design Tools.* [Computer software]

Council of Fashion Designers of America, Inc. (2016). *Polyester.* Retrieved 6-3-2023, from https://cfda.com/resources/materials/detail/polyester

Croda International Plc. (2022). *Product Finder.* Retrieved 1-2-2023, from https://www.crodaindustrialspecialties.com/en-gb/product-finder?functions=90&currentPage=1&pageSize=20&sortBy=recommended&lang=en-gb

Cupkova, D., & Promoppatum, P. (2017). Modulating Thermal Mass Behavior Through Surface Figuration. *ACADIA 2017: Disciplines and Disruption,* 202–211. https://doi.org/10.52842/conf.acadia.2017.202

Di Bari, R., Horn, R., Nienborg, B., Klinker, F., Kieseritzky, E., & Pawelz, F. (2020). The Environmental Potential of Phase Change Materials in Building Applications. *A Multiple Case Investigation Based on Life Cycle Assessment and Building Simulation. Energies, 13*(12), 3045. https://doi.org/10.3390/en13123045

Dr E. Brembilla. (2021). *Bucky Lab Engineering, AR1B021.* [Lecture]. TU Delft.

Dr. ir. F. Veer. (2023). *Material Science professor.* [Email]. TU Delft

Dr. RMJ Bokel. (2021). *Bucky Lab Engineering, AR1B021.* [Lecture]. TU Delft.

Dusseldorp, A., van Bruggen, M., & Douwes, J. (2007). *Health-based guideline values for the indoor environment* (RIVM report No. 609021044*).*

Energiegids. (2019). *NTA 8800 rekenmethode energieprestatie gebouwen.* Retrieved 28-11-2022, from https://www.nieman.nl/specialismen/energie-en-duurzaamheid/beng-eis-vanaf-01-01-2021/

Energievergelijk. (2023). *Price cap for energy. Retrieved 14/5/2022, from* https://www.energievergelijk.nl/english/price-cap-energy

Engineering ToolBox. (2003). *Solids, Liquids and Gases—Thermal Conductivities.* Retrieved 12-20-22, from https://www.engineeringtoolbox.com/thermal-conductivity-d_429.html

Engineering ToolBox. (2004). *Illuminance—Recommended Light Level.* Retrieved 12-20-22, from https://www.engineeringtoolbox.com/thermal-conductivity-d_429.html

Eupedia. (2021). *Carbon footprint of common consumer products.* Retrieved 15-5-2023, from https://www.eupedia.com/ecology/carbon_footprint_consumer_products.shtml

European Commission. (2022). *Energy performance of buildings directive.* Retrieved 12-15-22, from https://energy.ec.europa.eu/topics/energy-efficiency/energy-efficient-buildings/energy-performance-buildings-directive_en

European Commission. (2023). *Study on the Critical Raw Materials for the EU 2023 - Final Report.* doi: 10.2873/725585

Frontczak, M., & Wargocki, P. (2011). Literature survey on how different factors influence human comfort in indoor environments. *Building and Environment, 46*(4), 922–937. https://doi.org/10.1016/j.buildenv.2010.10.021

Galindo, A. (2023). What is Radiation? *International Atomic Energy Agency; IAEA.* Retrieved 02-28-2023, from https://www.iaea.org/newscenter/news/what-is-radiation

Giovannini, L., Goia, F., Lo Verso, V. R. M., & Serra, V. (2018). A Comparative Analysis of the Visual Comfort Performance between a PCM Glazing and a Conventional Selective Double Glazed Unit. *Sustainability, 10*(10). https://doi.org/10.3390/su10103579

GlassX AG. (2023). *GLASSX®crystal: Das Glas, das speichert, wärmt und kühlt* [Brochure]. Retrieved 13-1-2023, from https://www.glassx.ch/de/produkte/glassx-crystal/

Granta EduPack. (2022). *ANSYS, Inc.* [Computer software].

Hahladakis, J. N., Velis, C. A., Weber, R., Iacovidou, E., & Purnell, P. (2018). An overview of chemical additives present in plastics: Migration, release, fate and environmental impact during their use, disposal and recycling. *Journal of Hazardous Materials, 344*, 179–199. https://doi.org/10.1016/j.jhazmat.2017.10.014

Hasnain, S. M. (1998). Review on sustainable thermal energy storage technologies, Part I: Heat storage materials and techniques. *Energy Conversion and Management, 39*(11), 1127–1138. https://doi.org/10.1016/S0196-8904(98)00025-9

Hendriks, Kees Jan. (2019). *A change of state.* [Master's thesis, Delft University of Technology]. http://resolver.tudelft.nl/uuid:40d4af95-16b1-4b3f-9182-ac96929e2525

Ikutegbe, C. A., & Farid, M. M. (2020). Application of phase change material foam composites in the built environment: A critical review. *Renewable and Sustainable Energy Reviews, 131*, 110008. https://doi.org/10.1016/j.rser.2020.110008

ir. A. C. Van der Linden, ir. I. M. Kuijpers-Van Gaalen, & ir. A. Zeegers. (2018). *Building Physics* (2nd ed.). ThiemeMeulenhoff.

Junaid, M. F., Rehman, Z. ur, Čekon, M., Čurpek, J., Farooq, R., Cui, H., & Khan, I. (2021). Inorganic phase change materials in thermal energy storage: A review on perspectives and technological advances in building applications. *Energy and Buildings, 252,* 111443. https://doi.org/10.1016/j.enbuild.2021.111443

Kalnæs, S. E., & Jelle, B. P. (2015). Phase change materials and products for building applications: A state-of-the-art review and future research opportunities. *Energy and Buildings, 94*, 150–176. https://doi.org/10.1016/j.enbuild.2015.02.023

Kośny, J. (2015). *PCM-Enhanced Building Components.* Springer International Publishing. https://doi.org/10.1007/978-3-319-14286-9

Kvadrat. (2023). *Accent by Kinnasand.* Retrieved 14-2-2023, from https://www.kvadrat.dk/en/products/curtains/6839-accent?id=6839:::0002:

Liu, Z., Yu, Z. (Jerry), Yang, T., Qin, D., Li, S., Zhang, G., Haghighat, F., & Joybari, M. M. (2018). A review on macro-encapsulated phase change material for building envelope applications. *Building and Environment, 144*, 281–294. https://doi.org/10.1016/j.buildenv.2018.08.030

Mandal, J., Fu, Y., Overvig, A. C., Jia, M., Sun, K., Shi, N. N., Zhou, H., Xiao, X., Yu, N., & Yang, Y. (2018). Hierarchically porous polymer coatings for highly efficient passive daytime radiative cooling. *Science, 362*(6412), 315–319. https://doi.org/10.1126/science.aat9513

Mavrigiannaki, A., & Ampatzi, E. (2016). Latent heat storage in building elements: A systematic review on properties and contextual performance factors. *Renewable and Sustainable Energy Reviews, 60,* 852–866. https://doi.org/10.1016/j.rser.2016.01.115

Microtek Laboratories Inc. (2022). *Microencapsulation solutions.* Retrieved 12-1-2023, from https://www.microteklabs.com/microencapsulation-solutions/

Ministerie van Algemene Zaken. (2022, October 30). *Cabinet plans price cap for gas and electricity—Energy crisis.* Retrieved 1-12-2022, from https://www.government.nl/topics/energy-crisis/cabinet-plans-price-cap-for-gas-and-electricity

Moondream technology & comfort. (2023). *Silver Summer Metallized Thermal Lining MC0001*. Retrieved 13-4-2023, from https://www.moondreamwebstore.co.uk/thermal-curtain/silver-summer-metallized-thermal-lining-mc0001-141-145.html

NARM Secretariat. (2018). *NTD12 Daylight in domestic properties* [Brochure]. https://www.narm.org.uk/downloads/daylight-design/

NASA, Science Mission Directorate. (2010). *Anatomy of an Electromagnetic Wave.* Retrieved 27-2-2023, from http://science.nasa.gov/ems/02_anatomy

NEN. (2022). *NTA 8800:2022* (ICS 91.120.10; 91.140.30). Stichting Koninklijk Nederlands Normalisatie Instituut.

Outdoor Research. (2022). *Down vs. Synthetic Insulation: What's the difference?. Retrieved 5-3-2023, from* https://www.outdoorresearch.com/blog/down-vs.-synthetic-whats-the-difference-between-down-and-synthetic-insulati#:~:text=It's%20made%20with%20polyester%20fibers,air%20pockets%2C%20providing%20great%20warmth%E2%80%A6

Peel, M. C., Finlayson, B. L., & McMahon, T. A. (2007). Updated world map of the Ko¨ppen-Geiger climate classification. *Hydrology and Earth System Sciences., 11, 1633–1644. https://doi.org/10.5194/hess-11-1633-2007*

Peterson, K., Torcellini, P., & Grant, R. (2015). A Common Definition for Zero Energy Buildings. *U.S. Department of Energy.* https://www.energy.gov/sites/prod/files/2015/09/f26/A%20Common%20Definition%20for%20Zero%20Energy%20Buildings.pdf

Profipack.nl. (2023). *Noppenfolie—100cm x 25m x 80my.* Retrieved 15-4-2023, from https://www.profipack.nl/noppenfolie-100cm-25m-80my?gclid=Cj0KCQjwlumhBhClARIsABO6p-zsDPOnnE5g4mqRt7PcqnmwZBnrKZqN5VjLeS_OW5gBPo3f41Pkat0aAjOmEALw_wcB

PureTemp LLC. (2022). *PureTemp Phase Change Material*. Retrieved 27-12-2022, from https://puretemp.com/?page_id=173

Rathakrishnan, E. (2012). *Elements of Heat Transfer*. Taylor & Francis Group. http://ebookcentral.proquest.com/lib/delft/detail.action?docID=1689410

Rijs Textiles. (2023). *Polyester Wadding 60 gram (per meter)*. Retrieved 15-4-2023, from https://www.rijstextiles.com/en/haberdashery/polyester-wadding-pillow-stuffing/polyester-wadding-60-gram-per-meter.html

Rubitherm Technologies GmbH. (2022). *What Is PCM.* Retrieved 10-12-2022, from https://www.rubitherm.eu/pcm.html

Sadineni, S. B., Madala, S., & Boehm, R. F. (2011). Passive building energy savings: A review of building envelope components. *Renewable and Sustainable Energy Reviews, 15*(8), 3617–3631. https://doi.org/10.1016/j.rser.2011.07.014

Safari, A., Saidur, R., Sulaiman, F. A., Xu, Y., & Dong, J. (2017). A review on supercooling of Phase Change Materials in thermal energy storage systems. *Renewable and Sustainable Energy Reviews, 70*, 905–919. https://doi.org/10.1016/j.rser.2016.11.272

Science on a Sphere, NOAA. (2023). *ClimateBits: Solar Radiation.* Retrieved 28-2-2023, from https://sos.noaa.gov/catalog/datasets/climatebits-solar-radiation/#description-data-source

Sheldon, R. (2023). *Wien's constant.* Retrieved 4-4-2023, from https://www.techtarget.com/whatis/definition/Wiens-constant#:~:text=Wien's%20constant%20is%20typically%20represented,%E2%8B%85%2010%2D3.

Smartblinds. (2021). *Electric curtain tracks.* Retrieved 10-3-2023, from https://www.smartblinds.com/electric-curtain-tracks/

Tebaldi, M. L., Belardi, R. M., & Montoro, S. R. (2016). Chapter 8 - Polymers with Nano-Encapsulated Functional Polymers: Encapsulated Phase Change Materials. In S. Thomas, R. Shanks, & S. Chandrasekharakurup (Eds.), *Design and Applications of Nanostructured Polymer Blends and Nanocomposite Systems* (pp. 155–169). William Andrew Publishing. https://doi.org/10.1016/B978-0-323-39408-6.00019-4

Tenpierik, M. J., Turrin, M., Wattez, Y. C. M., Cosmatu, T., Tsafou, S. E., Farrugia, E. G., & van Unen, J. A. (2020). Double Face 2.0: An adjustable, translucent, PCM-based Trombe wall. *Bouwfysica, 31*(2). https://repository.tudelft.nl/islandora/object/uuid%3A401c9403-2560-481b-9d77-a57fd939b226

Terry's Fabrics. (2023). *Glossary Of Curtain Fabrics.* Retrieved 14-2-2023, from https://www.terrysfabrics.co.uk/blogs/curtain-fabric-buying-guide/glossary-of-curtain-fabrics

Tian, Y., Liu, X., Chen, F., & Zheng, Y. (2021). A facile approach to achieve subambient radiative cooling through aluminum foils and polyethylene bubble wrap. *Solar Energy Materials and Solar Cells, 230*, 111286. https://doi.org/10.1016/j.solmat.2021.111286

Transitions Optical Limited. (2023). *How do photocromics work?.* Retrieved 4-4-2023, from https://www.transitions.com/en-us/why-transitions/the-technology/photochromic-tech/

Trevira. (2023). *Trevira CS: Fibre-deep flame retardancy.* Retrieved 14-2-2023, from https://www.trevira.de/en/trevira-cs/flame-retardant-textiles

van den Brom, P. I., Camarasa, C., Catenazzi, G., Goatman, D., Jakob, M., Meijer, A., Nägeli, C., Ostermeyer, Y., Palacios, A., & Sainz de Baranda, E. (2018). *Building Market Brief The Netherlands.* CUES Foundation.

van Unen, Jeroen. (2019). *The energy and Comfort Performance of a Lightweight Translucent Adaptable Trombe Wall in Different Buildings and Climates: A numerical study.* [Master's thesis, Delft University of Technology]. http://resolver.tudelft.nl/uuid:2f619b08-4bd4-4d20-98ef-091f2bd1e136

Veerappan, M., Kalaiselvam, S., Iniyan, S., & Goic, R. (2009). Phase change characteristic study of spherical PCMs in solar energy storage. *Solar Energy, 83*(8), 1245–1252. https://doi.org/10.1016/j.solener.2009.02.006

Vigna, I., Bianco, L., Goia, F., & Serra, V. (2018). Phase Change Materials in Transparent Building Envelopes: A Strengths, Weakness, Opportunities and Threats (SWOT) Analysis. *Energies, 11*(1), 111. https://doi.org/10.3390/en11010111

Vitro Architectural Glass. (2023). *How Low-e Glass Works*. Retrieved 6-3-2023, from https://glassed.vitroglazings.com/topics/how-low-e-glass-works#:~:text=Low%2DE%20coatings%20have%20been,radiated%20by%20the%20glass%20surface.

Wang, Q., & Zhao, C. Y. (2015). Parametric investigations of using a PCM curtain for energy efficient buildings. *Energy and Buildings, 94*, 33–42. https://doi.org/10.1016/j.enbuild.2015.02.024

Weavabel. (2020). *What are pros and cons of recycled polyester?*. Retrieved 3-5-2023, from https://www.weavabel.com/blog/what-are-the-pros-and-cons-of-recycled-polyester#:~:text=Recycled%20polyester%20is%20obtained%20by,it%20into%20new%20polyester%20fibre.

Yousif, E., & Haddad, R. (2013). Photodegradation and photostabilization of polymers, especially polystyrene: Review. *SpringerPlus, 2*, 398. https://doi.org/10.1186/2193-1801-2-398

Zhai, Z. (John), & Previtali, J. M. (2010). Ancient vernacular architecture: Characteristics categorization and energy performance evaluation. *Energy and Buildings, 42*(3), 357–365. https://doi.org/10.1016/j.enbuild.2009.10.002

9. APPENDICES

Data Sheet

RUBITHERM Phase Change Material

SP24E

The creation of the latent heat material RUBITHERM® SP has led to a new and innovative class of low flammability PCM. RUBITHERM® SP consists of a unique composition of inorganic components.
RUBITHERM® SP is used as macroencapsulated material. Densities of 1,0 kg/l and more can be achieved. This and all properties mentioned below make RUBITHERM® SP to the preferred PCM used in the construction industry. Both passive and active cooling can easily be realized e.g. air conditioners.
We look forward to discussing your particular questions, needs and interests with you.

Properties:
- **stable performance throughout the phase change cycles**
- **high thermal storage capacity per volume**
- **limited supercooling (2-3K depenndig on volume and cooling rate),**
- **low flammability, non toxic**
- **different melting temperatures between -50°C und 70°C are available**
- **encapsulation necessary, minimum volume: 50ml**

The most important data:	Typical Values	
Melting area	**24-25** main peak: 24	[°C]
Congealing area	**23-21** main peak: 22	[°C]
Heat storage capacity ± 7,5% Combination of sensible and latent heat in a temperatur range of 15 °C to 30°C.	**180**	[kJ/kg]
	50	[Wh/kg]*
Specific heat capacity	**2**	[kJ/kg·K]*
Density solid at 15°C	**1,6**	[kg/l]
Density liquid at 35°C	**1,5**	[kg/l]
Volume expansion	**~6**	[%]
Heat conductivity	**~0,5**	[W/(m·K)]
Max. operation temperature	**45**	[°C]
Corrosion	corrosive effect on metals	

The product must be initialized (melt, homogenize and cool to 0 ° C) once before use to achieve the specified properties.
SP-products may absorb release water if stored improperly. This can result in a change of the physical properties given. Storing in closed containers mandatory.

Beispiel / example: SP24E Teilenthalpie / Partial enthalpy distribution*

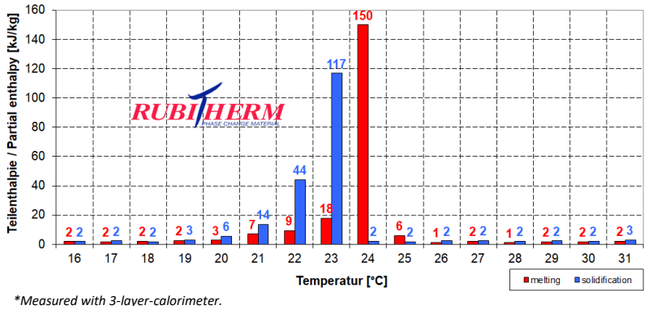

Rubitherm Technologies GmbH
Imhoffweg 6
D-12307 Berlin
phone: +49 (30) 7109622-0
E-Mail: info@rubitherm.com
Web: www.rubitherm.com

The product information given is a non-binding planning aid, subject to technical changes without notice. Version: 12.07.2022

*Measured with 3-layer-calorimeter.

Data sheet

RUBITHERM Phase Change Material

RT24HC

RUBITHERM® RT is a pure PCM, this heat storage material utilising the processes of phase change between solid and liquid (melting and congealing) to store and release large quantities of thermal energy at nearly constant temperature.
The RUBITHERM® phase change materials (PCM's) provide a very effective means for storing heat and cold, even when limited volumes and low differences in operating temperature are applicable.

Properties for RT-line:
- **high thermal energy storage capacity**
- **heat storage and release take place at relatively constant temperatures**
- **no supercooling effect, chemically inert**
- **long life product, with stable performance through the phase change cycles**
- **melting temperature range between -9 °C and 100 °C available**

The most important data:	Typical Values	
Melting area	**23-26** main peak: 24	[°C]
Congealing area	**24-22** main peak: 24	[°C]
Heat storage capacity ± 7,5% Combination of latent and sensible heat in a temperatur range of 16°C to 31°C.	**200**	[kJ/kg]*
	56	[Wh/kg]*
Specific heat capacity	**2**	[kJ/kg·K]
Density solid at 20°C	**0,8**	[kg/l]
Density liquid at 28°C	**0,7**	[kg/l]
Heat conductivity (both phases)	**0,2**	[W/(m·K)]
Volume expansion	**12**	[%]
Flash point	**150**	[°C]
Max. operation temperature	**56**	[°C]

Beispiel / example: RT24HC Teilenthalpie / Partial enthalpy distribution*

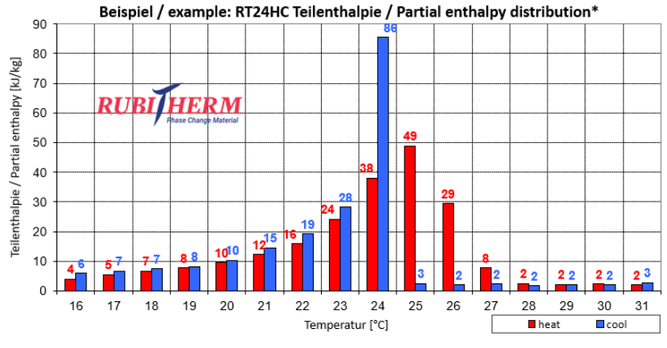

Rubitherm Technologies GmbH
Imhoffweg 6
D-12307 Berlin
phone: +49 (30) 7109622-0
E-Mail: info@rubitherm.com
Web: www.rubitherm.com

The product information given is a non-binding planning aid, subject to technical changes without notice.
Version: 18.11.2022

*Measured with 3-layer-calorimeter.

Appendix B

Rigid shell

Property	PET Polyethylene Terephthalate	PVC Polyvinyl chloride	HDPE High density Polyethylene	PP Polypropylene	PMMA Polymethyl methacrylate	PC Polycarbonate
Material family	Thermoplastic	Thermoplastic	Thermoplastic	Thermoplastic	Thermoplastic	Thermoplastic
Impact strength (kJ/m²) Notched, 23°C	6.2 - 6.8	3.8 - 5.4	6.1 - 18.6	2.5 - 3.4	1.9 - 2.1	10.1 - 83.1
Transparency	Optical quality	Transparent	Translucent	Transparent	Optical quality	Optical quality
Service temp. (°C)	(-58) - 65	(-10) - 66	(-82) - 129	(-17) - 99	(-75) - 56	(-47) - 116
UV resistance	Fair	Fair	Fair	Poor	Good	Fair
Water (Salt)	Excellent	Excellent	Excellent	Excellent	Excellent	Excellent
Flammability	Highly flammable	Self-extinguishing	Highly flammable	Highly flammable	Highly flammable	Slow-burning
Recycle (#)	Yes (1)	Yes, but rarely (3)	Yes (2)	Yes (5)	Yes, others (7)	Yes, others (7)
Processing Injection molding	Acceptable	Acceptable	Excellent	Excellent	Acceptable	Acceptable
Embodied energy (MJ/kg) Typical grade	68.7 - 76.8	52.8 - 58.3	71.2 - 79.0	67.2 - 74.3	107.0 - 118.0	100.0 - 111.0
Price (EUR/kg)	0.61 - 1.08	0.95 - 1.07	0.96 - 0.98	1.90 - 2.43	1.59 - 2.22	2.11 - 2.69

Soft pouch

Property	LDPE Low Density Polyethylene	LLDPE Linear low density polyethylene	POE Propylene-based elastomer A80	PA11 Polyamide 11 (nylon)
Material family	Thermoplastic	Thermoplastic	Thermoplastic	Thermoplastic
Impact strength (kJ/m²) Notched, 23°C	590 - 1000	590 - 1000	590 - 1000	590 - 1000
Transparency	Transparent	Transparent	Transparent	Translucent
Service temp. (°C)	(-68) - 95	(-79) - 97	(-25) - 80	(-60) - 105
UV resistance	Poor	Poor	Good	Fair
Water (Salt)	Excellent	Excellent	Excellent	Excellent
Flammability	Highly flammable	Highly flammable	Highly flammable	Slow-burning
Recycle (#)	Yes (4)	Yes (4)	Yes (5)	Yes (7)
Processing Injection molding	Excellent	Excellent	Acceptable	Excellent
Embodied energy (J/kg) Typical grade	75.9 - 83.9	69.8 - 77.2	111.0 - 123.0	209.0 - 231.0
Price (EUR/kg)	0.93 - 1.36	0.78 - 0.96	1.40 - 1.47	8.69 - 11.90

Appendix C

Eco Audit Report

Product name	Curtain suspension system Aluminum
Country of use	Netherlands
Product life (years)	10

Summary:

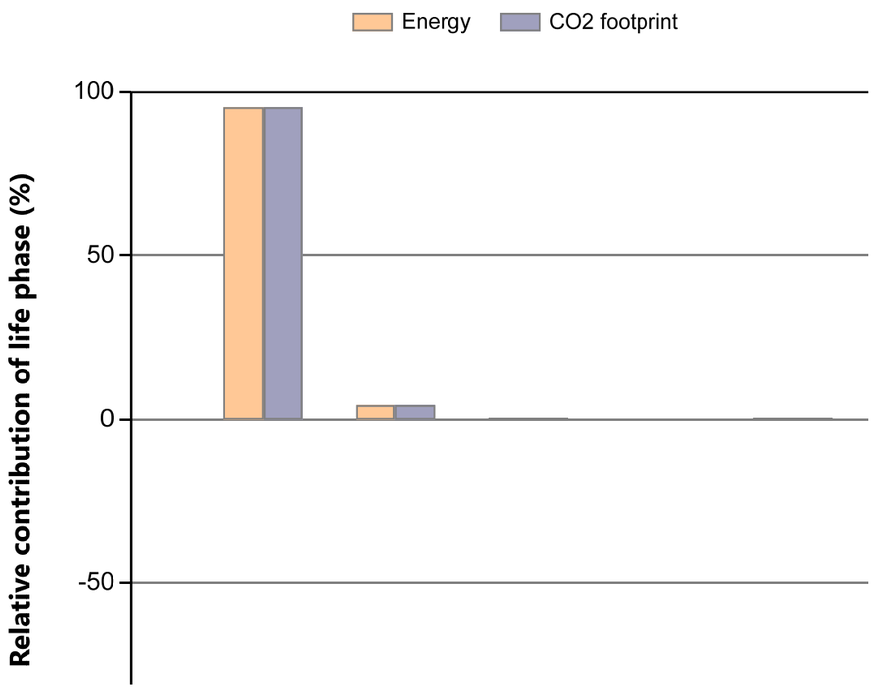

Energy details CO2 footprint details

Phase	Energy (MJ)	Energy (%)	CO2 footprint (kg)	CO2 footprint (%)
Material	279	95.2	20.1	95.2
Manufacture	12.3	4.2	0.898	4.2
Transport	0.2	0.1	0.0144	0.1
Use	0	0.0	0	0.0
Disposal	1.6	0.5	0.112	0.5
Total (for first life)	**293**	**100**	**21.2**	**100**
End of life potential	-202		-14.1	

Eco Audit Report

Product name	Curtain suspension system Stainless steel
Country of use	Netherlands
Product life (years)	10

Summary:

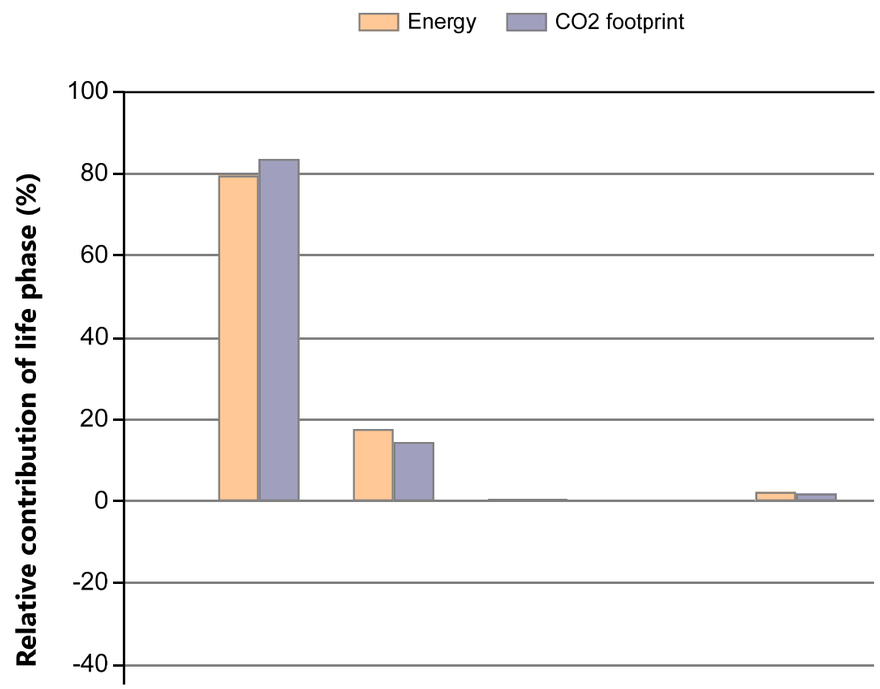

Energy details CO2 footprint details

Phase	Energy (MJ)	Energy (%)	CO2 footprint (kg)	CO2 footprint (%)
Material	155	79.6	14.9	83.5
Manufacture	34.6	17.7	2.6	14.5
Transport	0.568	0.3	0.0409	0.2
Use	0	0.0	0	0.0
Disposal	4.54	2.3	0.318	1.8
Total (for first life)	**195**	**100**	**17.9**	**100**
End of life potential	-90.7		-9.85	

Eco Audit Report

Product name	Curtain 16 liter
Country of use	Europe
Product life (years)	10

Summary:

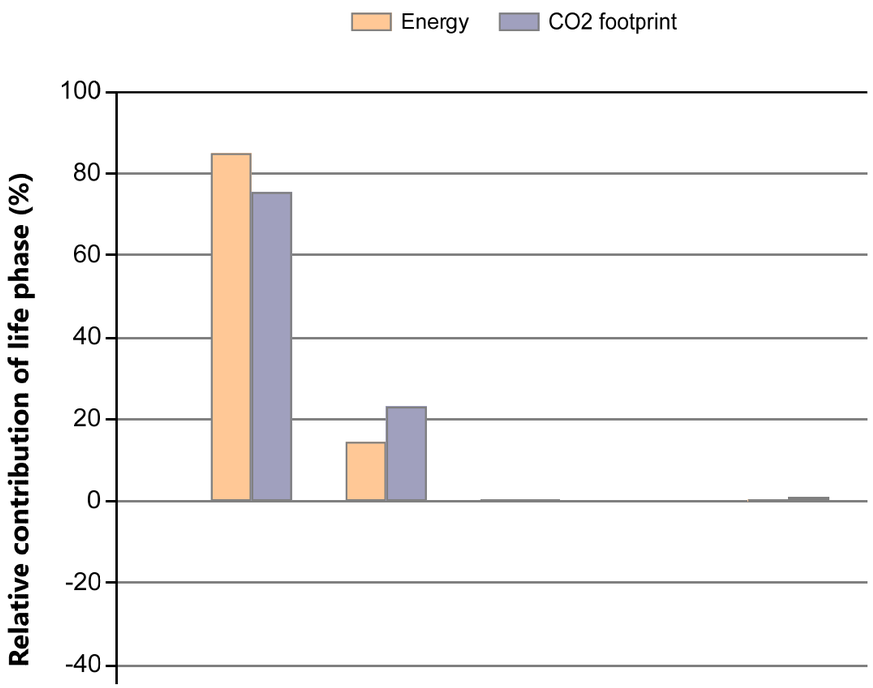

Energy details CO2 footprint details

Phase	Energy (MJ)	Energy (%)	CO2 footprint (kg)	CO2 footprint (%)
Material	534	85.0	22.1	75.7
Manufacture	90	14.3	6.78	23.2
Transport	0.112	0.0	0.00806	0.0
Use	0	0.0	0	0.0
Disposal	4.38	0.7	0.306	1.0
Total (for first life)	**628**	**100**	**29.2**	**100**
End of life potential	-330		-13.4	

Eco Audit Report

Product name	Curtain 8 liter
Country of use	Europe
Product life (years)	10

Summary:

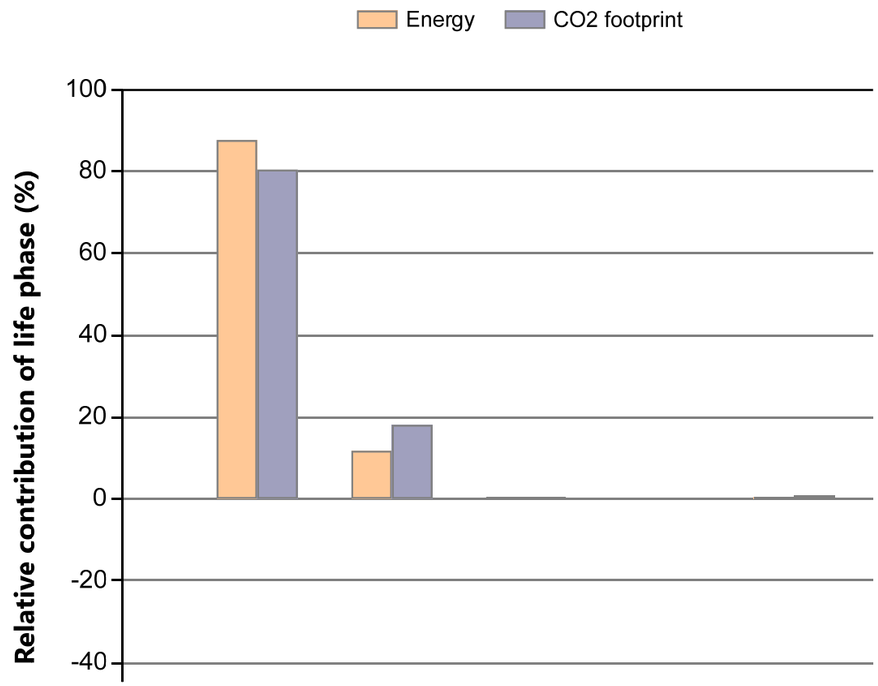

Energy details CO2 footprint details

Phase	Energy (MJ)	Energy (%)	CO2 footprint (kg)	CO2 footprint (%)
Material	357	87.6	15.9	80.6
Manufacture	47.8	11.7	3.61	18.3
Transport	0.0746	0.0	0.00537	0.0
Use	0	0.0	0	0.0
Disposal	2.89	0.7	0.202	1.0
Total (for first life)	**408**	**100**	**19.7**	**100**
End of life potential	-214		-9.31	

Appendix D

```
start_time = 0*86400; % start time of the simulation
stop_time  = 365*86400; % stop time of the simulation

% Glazing data for calculation of transmission of direct solar as function of incidence angle. S
glazing_transmission_data = [
1.470E-02    1.486E+00  -3.852E+00  3.355E+00   -1.474E-03
5.546E-01    3.563E-02  -2.416E+00  2.831E+00   -2.037E-03
7.709E-01   -6.383E-01  -1.576E+00  2.448E+00   -2.042E-03
3.462E-01    3.963E-01  -2.582E+00  2.845E+00   -2.804E-04
2.883E+00   -5.873E+00  2.489E+00   1.510E+00   -2.577E-03
3.025E+00   -6.366E+00  3.137E+00   1.213E+00   -1.367E-03
3.229E+00   -6.844E+00  3.535E+00   1.088E+00   -2.891E-03
3.334E+00   -7.131E+00  3.829E+00   9.766E-01   -2.952E-03
3.146E+00   -6.855E+00  3.931E+00   7.860E-01   -2.934E-03
3.744E+00   -8.836E+00  6.018E+00   8.407E-02    4.825E-04];

TinIC = 23;             % initial temperature in all nodes (23 is average of heating and cooling

orientation =  180;   % in degrees. 0   degrees means that facade with orien1 = north, orien2 =
                    %            90  degrees means that facade with orien1 = east,  orien2 = so

                    % PCM panel is always located at facade with orientation orien1, so...

room.depth  = 8.67;          % in this case in orien1-orien3 direction. In all cases a room with
room.width  = 3.325;    % in this case in orien2-orien4 direction
room.height = 2.7;           % 2.7 in every simulation
room.volume = room.depth*room.width*room.height;    % air volume room, depth x width x height [m
room.area   = room.depth*room.width;

A_gl_orien1 = 4.46;   % surface area glass with PCM panel behind glass orien1 facade (m^2).
A_gl_orien2 = 0;                          % surface area glass orien2 facade (m^2)
A_gl_orien3 = 0;                          % surface area glass orien3 facade (m^2)
A_gl_orien4 = 0;                          % surface area glass orien4 facade (m^2)

% window U values (glazing + frame)
U_gl = 2.9;         % U-value of all glazing must be the same.

U_gl_orien1 = U_gl; % don't change this
U_gl_orien2 = U_gl; % don't change this
U_gl_orien3 = U_gl; % don't change this
U_gl_orien4 = U_gl; % don't change this

% Solar heat gain coefficient glass without sunblinds
SHGC_orien1 = 0.7;
SHGC_orien2 = SHGC_orien1;
SHGC_orien3 = SHGC_orien1;
SHGC_orien4 = SHGC_orien1;

% Solar heat gain coefficient glass with sunblinds
SHGC_orien1_SB = SHGC_orien1*0.25;
SHGC_orien2_SB = SHGC_orien2*0.25;
SHGC_orien3_SB = SHGC_orien4*0.25;
SHGC_orien4_SB = SHGC_orien4*0.25;

% Define glazing transmission type for calculation of transmission of direct solar as ...
glazing_transmission_type =  5;
                            % 1 =   A- 3mm clear
                            % 2 =   B- 3mm bronze
                            % 3 =   C- 6mm bronze
                            % 4 =   D-Single Coated
                            % 5 =   E-Double clear 3mm
                            % 6 =   F-Double coated 3mm clear
                            % 7 =   G-Double 3mm tinted 3 mm clear
                            % 8 =   H-Double glazing: coated - 6mm clear
                            % 9 =   I-Double Glazing:6mm tinted - 6mm clear
                            % 10=   J-Triple-Coated-3mm clear- coated

glazing_transmission_coef = glazing_transmission_data(glazing_transmission_type,:);

ThresholdSBoff  = 97;          % Operative room temperature below which the sunblinds are never us
ThresholdSBon   = 99;          % Operative room temperature above which the sunblinds are in use,
ThresholdSBIsol= 100;          % incoming solar radiative power below which the sunblinds are neve

CFsol  = 0.2;                   % convection factor solar radiation entering the room. The fractio

working_days = 5;               % number of (consecutive) 'working days' in a week, must be >=0 an

p_i_wd =  6;                    % total sensible internal heat production in W/m2, only applies on

p_i_nwd = 6;                    % total sensible internal heat production in W/m2, only applies on
```

```
hour_people_present_wd  = [18,8]; % between these hours on a 'working day'     (0 <= hour <= 24), p

hour_people_present_nwd = [0,24]; % between these hours on a 'non-working day' (0 <= hour <= 24), p

ThresholdWindowOpen    = 25;    % Room air temperatuer above which the windows are opened (can only
ThresholdWindowClosed  = 24;    % Room air temperature below which the windows are closed (a relay
VentRateOpenWindow     = 2/3600;% Additional ventilation rate with windows open [per hour]. Simple

ventilation_rate     = 1.2/3600;% mechanical ventilation rate of the room (s-1).
hour_vent_flow_wd    = [18,8];  % between these hours on a 'working day'     (0 <= hour <= 24), mec

hour_vent_flow_nwd   = [0,24];  % between these hours on a 'non-working day' (0 <= hour <= 24), mec
WTW_efficiency       = 0;     % heat recovery efficiency of mechanical ventilation air.

infiltration_rate = 0.5/3600;   %infiltration rate (s-1) expressed in ACH/3600.

Threshold_Toper_night_ventilation_on  = 24; % Threshold operative room temperaure above which mecha
Threshold_Toper_night_ventilation_off = 23; % Threshold operative room temperaure below which mecha
                                            % night ventilation period is defined as the period whe
Threshold_Toper_bypass_on = 23;             % Threshold operative room temperaure above which WTW i
Threshold_Toper_bypass_off = 22;            % Threshold operative room temperaure below which WTW i

% the ventilation flow (m3/s) between the cavity and the outside air occurs through two ventilation
% height. The solely driving force is the stack effect. Parameters determining the ventilation flow
% difference between these two. The resistance to air flow in the cavity is assumed to be negligibl
% inviscid (i.e. the orifice equation applies).
Q_oc.A1    = 2.7*0.01;   %surface area of vent opening 1 (m2).
Q_oc.A2    = 2.7*0.01;   %surface area of vent opening 2 (m2)
Q_oc.dH    = 1.63;                          %height difference of the two vent openings (m)
Q_oc.Cd    = 0.8;                           %discharge coefficient (see orifice equation) (-)
%control settings for opening/closing of the cavity vents:
ThresholdCavVentOpen    = 23;     % Room operative temperature above which the vents of the cavity ar
ThresholdCavVentClosed  = 22;     % Room operative temperature below which the vents of the cavity ar
hour_cav_vent           = [18,8]; % Only between these hours of a day, the vents of the cavity may be

% thermostat setpoint and heating control
heating_setpoint        = 20;      % setpoint temperature (oC), only applies when people are present
heating_proportional    = 2000;    % proportional part of PI-controller (W/K)
heating_integral        = 0.1;     % integral part of PI-controller (W/Ks)
heating_max_power       = 5000;   % maximum power heating (W)
cooling_setpoint        = 99;      % setpoint temperature, only applies when people are present
cooling_proportional    = 2000;    % proportional part of PI-controller (W/K)
cooling_integral        = 0.1;     % integral part of PI-controller (W/Ks)
cooling_max_power       = 0000;   % maximum power heating (W)
% orien1, external construction 1 layer 1.
% Rc=1.7 m2K/W, old construction, heavy-weight, not adiabatic
e1_constr(1).d   = 0.10;        % thickness, inside layer (sand-lime brick)
e1_constr(1).rho = 2000;        % density
e1_constr(1).c   = 840;         % spec. heat capacity
e1_constr(1).la  = 1.0;         % heat conduction coefficient
% external construction 1 layer 2
e1_constr(2).d   = 0.04;        % thickness, middle layer (insulation)
e1_constr(2).rho = 35;          % density
e1_constr(2).c   = 1470;        % spec. heat capacity
e1_constr(2).la  = 0.027;       % heat conduction coefficient
% external construction 1 layer 3
e1_constr(3).d   = 0.1;         % thickness, outside layer (brickwork)
e1_constr(3).rho = 2100;        % density
e1_constr(3).c   = 840;         % spec. heat capacity
e1_constr(3).la  = 0.8;         % heat conduction coefficient
% surface area external construction 1
e1_constr_A      = room.width*room.height-A_gl_orien1;   % surface area external construction 1

% orien2, external construction 2 layer 1.
% 15 cm concrete, virtually adiabatic (set in heat transfer part)
e2_constr(1).d   = 0.05;        % thickness, inside layer
e2_constr(1).rho = 2400;        % density
e2_constr(1).c   = 840;         % spec. heat capacity
e2_constr(1).la  = 1.7;         % heat conduction coefficient
% external construction 1 layer 2
e2_constr(2).d   = 0.05;        % thickness, middle layer
e2_constr(2).rho = 2400;        % density
e2_constr(2).c   = 840;         % spec. heat capacity
e2_constr(2).la  = 1.7;         % heat conduction coefficient
% external construction 1 layer 3
e2_constr(3).d   = 0.05;        % thickness, outside layer
e2_constr(3).rho = 2400;        % density
e2_constr(3).c   = 840;         % spec. heat capacity
e2_constr(3).la  = 1.7;         % heat conduction coefficient
% surface area external construction 2
e2_constr_A      = room.depth*room.height-A_gl_orien2;   % surface area external construction 2
```

```
% orien3, SAME AS ORIEN1, external construction 3 layer 1
% Rc=1.7 m2K/W, old construction, heavy-weight, not adiabatic
e3_constr(1).d   = e1_constr(1).d;          % thickness, inside layer
e3_constr(1).rho = e1_constr(1).rho;        % density
e3_constr(1).c   = e1_constr(1).c;          % spec. heat capacity
e3_constr(1).la  = e1_constr(1).la;         % heat conduction coefficient
% external construction 1 layer 2
e3_constr(2).d   = e1_constr(2).d;          % thickness, middle layer
e3_constr(2).rho = e1_constr(2).rho;        % density
e3_constr(2).c   = e1_constr(2).c;          % spec. heat capacity
e3_constr(2).la  = e1_constr(2).la;         % heat conduction coefficient
% external construction 1 layer 3
e3_constr(3).d   = e1_constr(3).d;          % thickness, outside layer
e3_constr(3).rho = e1_constr(3).rho;        % density
e3_constr(3).c   = e1_constr(3).c;          % spec. heat capacity
e3_constr(3).la  = e1_constr(3).la;         % heat conduction coefficient
% surface area external construction 3
e3_constr_A      = room.depth*room.height-A_gl_orien3;   % surface area external construction 3

% orien4, external construction 4 layer 1
% 15 cm concrete, virtually adiabatic (set in heat transfer part)
e4_constr(1).d   = e2_constr(1).d;          % thickness, inside layer
e4_constr(1).rho = e2_constr(1).rho;        % density
e4_constr(1).c   = e2_constr(1).c;          % spec. heat capacity
e4_constr(1).la  = e2_constr(1).la;         % heat conduction coefficient
% external construction 1 layer 2
e4_constr(2).d   = e2_constr(2).d;          % thickness, middle layer
e4_constr(2).rho = e2_constr(2).rho;        % density
e4_constr(2).c   = e2_constr(2).c;          % spec. heat capacity
e4_constr(2).la  = e2_constr(2).la;         % heat conduction coefficient
% external construction 1 layer 3
e4_constr(3).d   = e2_constr(3).d;          % thickness, outside layer
e4_constr(3).rho = e2_constr(3).rho;        % density
e4_constr(3).c   = e2_constr(3).c;          % spec. heat capacity
e4_constr(3).la  = e2_constr(3).la;         % heat conduction coefficient
% surface area external construction 4
e4_constr_A      = room.depth*room.height-A_gl_orien4;   % surface area external constructio

% ROOF, external construction 5 layer 1
% 15 cm concrete, virtually adiabatic
e5_constr(1).d   = e2_constr(1).d;          % thickness, inside layer
e5_constr(1).rho = e2_constr(1).rho;        % density
e5_constr(1).c   = e2_constr(1).c;          % spec. heat capacity
e5_constr(1).la  = e2_constr(1).la;         % heat conduction coefficient
% external construction 1 layer 2
e5_constr(2).d   = e2_constr(2).d;          % thickness, middle layer
e5_constr(2).rho = e2_constr(2).rho;        % density
e5_constr(2).c   = e2_constr(2).c;          % spec. heat capacity
e5_constr(2).la  = e2_constr(2).la;         % heat conduction coefficient
% external construction 1 layer 3
e5_constr(3).d   = e2_constr(3).d;          % thickness, outside layer
e5_constr(3).rho = e2_constr(3).rho;        % density
e5_constr(3).c   = e2_constr(3).c;          % spec. heat capacity
e5_constr(3).la  = e2_constr(3).la;         % heat conduction coefficient
% % surface area external construction 5
e5_constr_A      = room.width*room.depth;   % surface area external construction 5 = ROOF ARE

% FLOOR, external construction 6 layer 1
% 15 cm concrete, virtually adiabatic
e6_constr(1).d   = e2_constr(1).d;          % thickness, inside layer
e6_constr(1).rho = e2_constr(1).rho;        % density
e6_constr(1).c   = e2_constr(1).c;          % spec. heat capacity
e6_constr(1).la  = e2_constr(1).la;         % heat conduction coefficient
% external construction 5 layer 2
e6_constr(2).d   = e2_constr(2).d;          % thickness, middle layer
e6_constr(2).rho = e2_constr(2).rho;        % density
e6_constr(2).c   = e2_constr(2).c;          % spec. heat capacity
e6_constr(2).la  = e2_constr(2).la;         % heat conduction coefficient
% external construction 5 layer 3
e6_constr(3).d   = e2_constr(3).d;          % thickness, outside layer
e6_constr(3).rho = e2_constr(3).rho;        % density
e6_constr(3).c   = e2_constr(3).c;          % spec. heat capacity
e6_constr(3).la  = e2_constr(3).la;         % heat conduction coefficient
% surface area external construction 6
e6_constr_A      = room.width*room.depth;   % surface area external construction 6 = FLOOR AR
e1_alpha_i     = 2.7;       % convective surface heat transfer coefficient inside construct
e2_alpha_i     = 2.7;       % convective surface heat transfer coefficient inside construct
e3_alpha_i     = 2.7;       % convective surface heat transfer coefficient inside construct
e4_alpha_i     = 2.7;       % convective surface heat transfer coefficient inside construct
e5_alpha_i     = 2.7;       % convective surface heat transfer coefficient inside construct
e6_alpha_i     = 2.7;       % convective surface heat transfer coefficient inside construct

e1_alpha_e       = 25;      % total surface heat transfer coefficient outside construction
e2_alpha_e       = 0;       % total surface heat transfer coefficient outside construction
```



```
e3_alpha_e       = 0;       % total surface heat transfer coefficient outside cons
e4_alpha_e       = 0;       % total surface heat transfer coefficient outside cons
e5_alpha_e       = 0;       % total surface heat transfer coefficient outside cons
e6_alpha_e       = 0;       % total surface heat transfer coefficient outside cons

e1_sol_abs       = 0.9;     % solar absorption coefficient outside surface constru
e2_sol_abs       = 0;       % solar absorption coefficient outside surface constru
e3_sol_abs       = 0;       % solar absorption coefficient outside surface constru
e4_sol_abs       = 0;       % solar absorption coefficient outside surface constru
e5_sol_abs       = 0;       % solar absorption coefficient outside surface constru

% ---- PCM panel and cavity---%

panel_present = 0;          % 1 = yes, 0 = no
nl_pcm      = 10;           % number of PCM control volume layers, minimum = 1
nl_ins      = 3;            % number of insulation control volume layers, minimum = 1

Ts_pcm      = 21;           % temperature below which PCM is solid  [C]
Tl_pcm      = 25;           % temperature above which PCM is liquid [C]

a_sol1_pcm_s  = 0.1*0.97;  % part of incident solar energy on panel absorbed by the PCM
a_sol1_pcm_l  = 0.1*0.63;  % part of incident solar energy on panel absorbed by the PCM
a_sol1_ins_s  = 0.9;       % part of incident solar energy on panel absorbed by the ins
a_sol1_ins_l  = 0.9;       % part of incident solar energy on panel absorbed by the ins
                           % linear interpolation between solid and liquid state based

a_sol2_pcm_s  = 0.97;      % part of incident solar energy on panel absorbed by the PC
a_sol2_pcm_l  = 0.63;      % part of incident solar energy on panel absorbed by the PC
a_sol2_ins_s  = 0.0;  % part of incident solar energy on panel absorbed by the insulati
a_sol2_ins_l  = 0.0;  % part of incident solar energy on panel absorbed by the insulati
                           % linear interpolation between solid and liquid state based

dead_band_pcm = 2.0;       % PCM dead band due to hysteresis [K]

panel_A_fac = 1.0;         % fraction of the panel surface area not consisting of hole

panel_pcm.d = 0.001793;       % thickness of PCM layer
panel_ins.d = 0.01;        % thickness of insulation layer

panel_pcm.c   = 2000;      % sensible specific heat capacity of PCM [J/(kg K)], assume
panel_pcm.rho = 1500;      % mass density of PCM [kg/m3]
panel_pcm.la  = 0.5;       % heat conduction coefficient of PCM [W/(m K)], assumed eq
panel_pcm.h   = 1.8e5;     % latent heat of PCM (J/kg)

panel_ins.c   = 1250;      % sensible specific heat capacity of insulation [J/(kg K]
panel_ins.rho = 16;        % mass density of insulation [kg/m3]
panel_ins.la  = 0.05;     % heat conduction coefficient of insulation [W/(m K)]

hour_pcm_roomside = [20,8]; % between these hours of the day (0 <= hour <= 24), the PC
%NOT OPERATIONAL, the PCM faces the cavity after sunrise, and faces the room after sun

% the ventilation flow (m3/s) between the cavity and the room is modelled using the fo
% where delta_T is the (absolute) temperature difference between the cavity air and ro
% definition of the coefficients C_0, C_1 and C_n:
Q_room_cavity.C_0 = 0;       % constant part
Q_room_cavity.C_1 = 0.0669;  % flow coefficient
Q_room_cavity.C_n = 0.4627;  % exponent

p_alpha_i     = 2.7;       % convective surface heat transfer coefficient room side c
p_alpha_cav   = 2.7;       % convective surface heat transfer coefficient cavity side

% ------END OF INPUT ------------------------------------------------------------------
```